APPROXIMATE THEORIES FOR THE FLEXURAL VIBRATION OF UNIFORM BEAMS AND THEIR DERIVATION FROM THE GENERAL ELASTIC EQUATIONS

Thesis presented for the Degree of
Doctor of Philosophy
of the
University of Edinburgh.

by

Allan D. S. Barr, B.Sc.

oooOooo

May, 1956.

ACKNOWLEDGEMENTS.

The author wishes to express his indebtedness to Professor R.N. Arnold for providing facilities for carrying out this research; and to Dr. J. D. Robson and Professor Arnold for continual assistance and enlightening discussion.

.....

SYNOPSIS

The approximate theories of flexural vibration dealt with in the thesis are those in which the problem is reduced to the solution of a differential equation with one dependent variable (the transverse displacement of the neutral line of the beam) by a process of making reasonable assumptions during the derivation of the equation. In order to facilitate comparisons of the effects of the various assumptions made in the different theories, the differential equations are derived from the general elastic equilibrium equations written in terms of the stress components.

Particular attention is given to the equation which includes the effects of rotatory inertia and transverse shear (usually referred to as the Timoshenko equation) because of its interesting prediction for a finite beam of the possible existence of more than one natural frequency with the same number of nodes (i.e. a second spectrum of frequencies). This qualitative effect is shown to be a consequence of considering a longitudinal motion independent of the transverse motion. The boundary conditions for the Timoshenko equation are derived from the general elastic equations, and the frequency equation for the symmetric modes of a Timoshenko beam on elastic end supports is given. From this the frequency equations for the free-end and pinned-end conditions are obtained and discussed.

By a logical continuation the theory is then

extended to include in addition the effect of an independent lateral motion, the differential equation and boundary conditions again being derived from the general elastic equations. It is found that solutions of this new equation include the Timoshenko solution exactly, but also contain a third solution which defines a third spectrum of natural frequencies for a beam. The equation also defines three branches to the dispersion curve for flexural waves on an infinite beam.

Experimental work on three deep rectangular sectioned beams is described and it is found that the predictions of the Timoshenko theory are closely followed, including the second spectrum frequencies. Third spectrum frequencies are detected very faintly for only one of the three beams, this is probably because lateral inertia is relatively unimportant for a cross-section of deep rectangular form. However, some experiments on an H-sectioned beam give two distinct spectra of natural frequencies and it is shown that the higher of these sets of frequencies is probably of the third spectrum type. Thus these higher mode frequencies may be important for "open" sections, for which a high lateral inertia obtains without undue transverse stiffness.

CONTENTS

1. INTRODUCTION.

The problem of the flexural vibration of beams has received much consideration since the original setting up of the "classical" differential equation for this type of motion by Daniel Bernoulli in 1735. This equation has been widely used in problems associated with flexure. Its use has generally been restricted to examination of the vibration characteristics of slender beams vibrating in the fundamental mode or in a low order harmonic, the increasing inaccuracy of this equation for flexural wavelengths approaching the order of the radius of gyration of the bar being well appreciated.

Several more precise differential equations have been proposed by various authors (see section 2). Each of these equations includes the effect of some factor which is neglected in the derivation of the classical equation, and gives improved results for the higher modes of vibration.

The most important of these equations is that usually known as the Timoshenko equation (see section 3.5), which includes the effects of the rotatory inertia of the cross-sections and the shearing action between them. The use of this equation is necessary if reasonably accurate values for the frequencies of higher modes are desired. In impact problems on beams where the contribution of the higher modes may be important, the use of the Timoshenko equation may again be necessary.

However, beyond the added accuracy of frequency prediction obtainable with the Timoshenko equation, there arises a new qualitative phenomenon. When the Bernoulli equation is considered for the propagation of flexural waves in an infinite bar, the propagation velocity is found to be a single valued function of the wavelength. This is not so however, for the Timoshenko equation which predicts two possible values of wave velocity for a given wavelength. Or, in terms of a pin-ended beam of finite length the equation predicts that for any chosen number of nodes on the length of the beam there are two distinct possible natural frequencies.

It seems pertinent to ask what consideration is included in the derivation of the Timoshenko equation to introduce this new effect, and also to ask whether the introduction of further corrections beyond those contained in the Timoshenko equation might lead to the prediction of further such effects.

To examine these questions it was felt that recourse should be made to the general elastic equations as a starting point. From these equations the assumptions behind the various approximate theories can be seen and a method for including yet further corrections to the equations may be suggested. Indeed the usual method of setting up these differential equations by physical arguments of the "strength of materials" type becomes increasingly difficult as more refinements are involved. Under these circum-

stances the use of the general elastic equations in conjunction with plausible simplifications will probably be the most straightforward method of approach.

From these features arose the scope of the present work. The primary objects are, firstly, to examine briefly the assumptions implicit in the approximate flexural theories by deriving the differential equations from the general elastic equations, and hence to determine the characteristic which leads to a dual-valued dispersion curve for the Timoshenko equation. Secondly to inspect the possibility of extending the theory to include the three-dimensional motion of the typical particle and to examine any resulting differential equation. Finally, to conduct experimental tests on beams to see whether there might be any evidence for the existence of branches to the flexure frequency curves, and if so, to compare them with the theoretical predictions. For these purposes it was felt to be sufficient to restrict attention to the symmetric modes.

2. HISTORICAL

2.1. The Approximate Differential Equations of Flexure.

The first differential equation for the flexural motion of beams was found in 1735 by Daniel Bernoulli. This equation is the well-known "classical" or elementary equation which is used for the majority of beam problems being unsatisfactory only for foreshortened beams or short wavelengths comparable with the radius of gyration of the beam.

To provide a theory which would be physically satisfactory at short wavelengths various corrections have been suggested for inclusion in the derivation of the differential equation.

A correction suggested by Bresse (1859)* and independently by Rayleigh (1877) allows for the inertia possessed by cross-sections of the beam by virtue of their rotation about the neutral axis during vibration, - the so-called correction for rotatory inertia of cross-sections. This equation is physically more satisfactory in that it does not lead to infinite group velocities for very short wavelengths, but its accuracy for frequency prediction in the higher modes of vibration still leaves much to be desired.

Timoshenko (1921) showed, however, that correction for the shearing motion of cross-sections is as important as the rotatory inertia correction, and proposed a revised differential equation (hereafter referred to as the Timoshenko equation, see section 3.5).

---

* A Bibliography is presented at the end of the thesis.

Numerical results from this equation are in very good agreement with those calculated from the general elastic equations for a circular cylinder (section 2.3). It is of interest to note that this correction for shear was also proposed by Bresse (1859).

Other less important corrections have been suggested. Love (1927) by an energy method made allowance for the inertia of the motion whereby cross-sections are distorted in their own planes. Arnold (1951) proposed a method to allow for the fact that cross-sections which are plane when unstrained, become curved surfaces during the motion. Volterra (1955) suggests a slightly modified form of the Timoshenko equation.

2.2. Plane Strain and Plane Stress Solutions.

The problem of the propagation of flexural waves on an infinite beam where the assumption of plane strain or plane stress can be made, was solved by Lamb (1917), Timoshenko (1922) and Prescott (1942). The solutions are generally too complicated to be of much use, as they contain all the possible flexural modes including those in which the beam has several nodal planes in its depth. Prescott, however, shows that in the first mode at high frequencies, the stresses tend to a maximum near the surface of the beam. This demonstrates the inaccuracy involved in determining the Timoshenko shear coefficient (see Section 3.5) from an assumed static shear stress

distribution. This theory also predicts that at very short wavelengths the propagation velocity approaches the Rayleigh surface wave velocity in the medium.

2.3. The Exact Solution.

Pochhammer (1876) and independently Chree (1889) solved the general elastic equations for the propagation of waves along a circular cylinder whose length is very great compared with its diameter. This solution includes the flexural modes.

The frequency equation for flexural waves is given in determinantal form by Bancroft (1941) and Hudson (1943) has carried out the necessary computations for the first branch and has obtained values which show how the phase velocity of flexural waves depends on the ratio between their wavelength and the radius of the cylinder. Davies (1948) found that values calculated from the Timoshenko differential equation are in remarkably good agreement with those obtained by Hudson. The results are also discussed by Kolsky (1953).

2.4. Notes on the Timoshenko Equation.

There have been numerous recent papers on the Timoshenko equation mainly referring to its use in impact problems. Few of these papers make specific mention of the equation's prediction of a double frequency spectrum for a pin-ended beam.

This double frequency spectrum was probably first noticed by Arnold (1951) who obtained the frequency

equation by substitution of a sinusoidal shape function which fits the end conditions.

Traill-Nash and Collar (1953) have solved the Timoshenko equation and set up frequency equations for the standard end conditions. They observed the existence of two spectra of frequencies for the pin-ended beam. For the free-beam they discuss briefly a numerical example for which in certain isolated instances they obtained two frequencies with the same number of nodes. However, their results do not seem to agree quite with the calculations of section 6.1, and it is felt that there may be errors in their computation.

The double frequency spectrum for the pinned beam is also noted by Anderson (1953), and Volterra (1955) notices that the dispersion curve of the Timoshenko equation has two branches, but he ignores the higher roots considering them to be without physical significance - a remark discussed in section 7.4.

Sutherland and Goodman (1951) derive the Timoshenko equation from the two dimensional equations of elasticity. Mindlin (1951) gives a solution for the Timoshenko free-beam frequency equation by a method of successive approximations.

Several other papers on the vibration of Timoshenko beams have been published but none of these appears to make specific mention of the two frequency spectra or to discuss their characteristics. They are thus felt not to be important from the point of view

of this work, although publications by Mindlin and Deresiewicz (1954) and Goodman (1954) have general bearing on the selection of the Timoshenko shear coefficient η .

There has been no previous experimental work to investigate the existence of higher spectra of flexural vibration.

3. THEORIES OF FLEXURAL VIBRATION.

3.1. The General Elastic Problem.

The general problem of the vibrations of an elastic solid can be stated in the following way.

Determine values for the components of stress (σ_x , σ_y , σ_z , τ_{xy} , τ_{xz} , τ_{yz}) and for the displacements (u, v, w), which, in the region occupied by the beam, satisfy the set of nine equations

$$\left.\begin{aligned} \frac{\partial \sigma_x}{\partial x} + \frac{\partial \tau_{xy}}{\partial y} + \frac{\partial \tau_{xz}}{\partial z} &= \rho \frac{\partial^2 u}{\partial t^2} \\ \frac{\partial \sigma_y}{\partial y} + \frac{\partial \tau_{xy}}{\partial x} + \frac{\partial \tau_{yz}}{\partial z} &= \rho \frac{\partial^2 v}{\partial t^2} \\ \frac{\partial \sigma_z}{\partial z} + \frac{\partial \tau_{xz}}{\partial x} + \frac{\partial \tau_{yz}}{\partial y} &= \rho \frac{\partial^2 w}{\partial t^2} \end{aligned}\right\} \quad \ldots(3.1)$$

and

$$E\frac{\partial u}{\partial x} = \left[\sigma_x - \nu(\sigma_y + \sigma_z)\right] \; ; \; E\frac{\partial v}{\partial y} = \left[\sigma_y - \nu(\sigma_x + \sigma_z)\right] ; \; E\frac{\partial w}{\partial z} = \left[\sigma_z - \nu(\sigma_x + \sigma_y)\right]$$

$$G\left(\frac{\partial u}{\partial y} + \frac{\partial v}{\partial x}\right) = \tau_{xy} \; ; \; G\left(\frac{\partial v}{\partial z} + \frac{\partial w}{\partial y}\right) = \tau_{yz} \; ; \; G\left(\frac{\partial u}{\partial z} + \frac{\partial w}{\partial x}\right) = \tau_{xz} \quad \ldots(3.2)$$

The first set of equations (3.1), are the equilibrium equations for a small element and in the form quoted body forces over and above the acceleration terms are assumed zero.

In addition the components must satisfy the boundary conditions over the whole external surface of the body and the stress components must satisfy the Beltrami-Michell compatibility equations in order that deformation without discontinuities should be obtained.

The complete dynamic problem will also include initial conditions with respect to time, but for present purposes steady state free oscillation will be assumed

so that the displacement components are in phase and sinusoidal with respect to time.

The boundary conditions at any point on the surface of the body, where $\bar{X}$, $\bar{Y}$, $\bar{Z}$ are the components of the surface forces per unit area at this point, are

$$\left.\begin{aligned} \bar{X} &= \sigma_x \cos(n,x) + \tau_{xy}\cos(n,y) + \tau_{xz}\cos(n,z) \\ \bar{Y} &= \sigma_y \cos(n,y) + \tau_{yz}\cos(n,z) + \tau_{xy}\cos(n,x) \\ \bar{Z} &= \sigma_z \cos(n,z) + \tau_{xz}\cos(n,x) + \tau_{yz}\cos(n,y) \end{aligned}\right\} \quad \ldots(3.3)$$

in which $\cos\left(n, \begin{matrix} x \\ y \\ z \end{matrix}\right)$ are the direction cosines of the external normal to the surface at the point.

(The problem as postulated above is that solved by L. Pochhammer (1876) - with transformation to cylindrical co-ordinates - for the case of a circular cylinder of infinite length).

The solution of the above set of equations for even the most simple shape of body presents formidable complications, and for obtaining solutions suitable for practical purposes the equations are artificially simplified and plausible assumptions are made.

In the sections which follow, it will be seen that the "classical" theory of bending vibration makes the most sweeping assumptions while the more exact theories make fewer simplifications and so more nearly approach an accurate solution.

What is desired, and what is actually carried out in the various approximate solutions, is not to provide a complete solution to some simplified form

of the equations (3.1) to (3.3)*; but to eliminate dependent and independent variables in a reasonable manner so that the problem is reduced to the solution of one partial differential equation in one dependent variable (the deflection of the beam), and two independent variables (time, and a co-ordinate giving distance of a point along the beam). This equation can then be solved by normal methods for a beam with any set end boundary conditions.

In what follows the assumption $\sigma_y = \sigma_z = \tau_{yz} = 0$ will often be made. If the beam is visualised as being made up of long fibres parallel to the axis of X (see Fig. 5) this assumption implies that these fibres exert neither direct nor shear forces on each other in transverse directions but exert cohesive forces in the longitudinal direction only.

Further assumptions regarding the stresses or the displacements will be introduced in the solution of each problem. Strictly speaking, assumptions are justified only when they lead to a solution that satisfies the equations of equilibrium along with the boundary and compatibility conditions. But such a solution is exact and unique and here not an exact solution but a simplified one is sought, so that, in general, there will not be complete fulfilment of equilibrium or boundary or compatibility equations and the justification for assumptions can lie only

*For example, The assumption of plane stress or plane strain. This treatment is given by Timoshenko (1922) and Prescott (1942).

in the pragmatic value of the resulting solution.

It will be observed that the above set of equilibrium equations does not distinguish between the various types of vibration and contains extensional and torsional modes as well as the flexural type. For beams whose cross-sections have symmetry about Y and Z axes (see Fig. 5), it can be postulated that for bending, displacement u should be an odd function of z and an even function of y , v should be an odd function of z and of y , and w should be an even function of z and y . Under these conditions, the equations should yield solutions for flexural vibrations alone.

3.2. The Classical Equation.

Here simplification of the equilibrium equation (3.1) is carried to the extreme. The direct stress σ_x and the shear stress τ_{xz} are the only ones considered, while of the inertia forces those in the X and Y directions are taken as zero. The equations of equilibrium are thereby reduced to

$$\left.\begin{aligned} \frac{\partial \sigma_x}{\partial x} + \frac{\partial \tau_{xz}}{\partial z} &= 0 \\ \frac{\partial \tau_{xz}}{\partial x} &= \rho \frac{\partial^2 w}{\partial t^2} \end{aligned}\right\} \quad \ldots(3.4)$$

Now, if it is borne in mind that the aim is to reduce the two above equations to one containing only deflection w as dependent variable and that the above equations represent equilibrium in any very small region of the beam. Then it is apparent that (3.4) must be integrated over the cross-section of the beam.

Multiplying the first of (3.4) by $z.dydz$ and the second by $dy.dz$ and integrating over the region (R) contained by the cross-section we obtain

$$\left.\begin{aligned} \iint_R \frac{\partial \sigma_x}{\partial x} z.dydz + \iint_R \frac{\partial \tau_{xz}}{\partial z} z\,dydz &= 0 \\ \iint_R \frac{\partial \tau_{xz}}{\partial x} dydz &= \rho \iint_R \frac{\partial^2 w}{\partial t^2} dydz \end{aligned}\right\} \quad \ldots(3.5)$$

If further the assumption is made that stresses and displacements have no variation across the width of the section (Y-wise), then the above equations (3.5) can be replaced by

$$\left.\begin{aligned} \int_z \frac{\partial \sigma_x}{\partial x} b(z) z dz + \int_z \frac{\partial \tau_{xz}}{\partial z} b(z)\, z\, dz &= 0 \\ \int_z \frac{\partial \tau_{xz}}{\partial x} b(z).\, dz &= \rho \int_z \frac{\partial^2 w}{\partial t^2} b(z) dz \end{aligned}\right\} \quad \ldots(3.6)$$

where $b(z)$ represents the section width at any height z, and the symbol $\int_z$ implies integration over the total depth of the section.

The second integral of the first equation of (3.6) can be expanded by parts to give

$$z\, b(z)\, \tau_{xz}\Big|_z - \int_z \tau_{xz}\, b(z) dz - \int_z \tau_{xz}.\, z\, \frac{\partial b}{\partial z} dz \qquad \ldots(3.7)$$

and the first term is zero since the shear stress disappears at the surface of the beam. If, in addition, it is assumed that the width of the section has only small variations with height, the final term containing $\frac{\partial b}{\partial z}$ can also be discarded and the equations (3.6) now read,

$$\left.\begin{aligned} \int_z \frac{\partial \sigma_x}{\partial x} b.z.dz - \int_z \tau_{xz}.b.dz &= 0 \\ \int_z \frac{\partial \tau_{xz}}{\partial x}.b.dz &= \rho \int_z \frac{\partial^2 w}{\partial t^2} b.dz \end{aligned}\right\} \quad \ldots(3.8)$$

A reasonable form for the displacement u is now taken. If plane sections of the beam are considered to remain plane and normal to the distorted beam axis during vibration, then the X-wise displacement is a consequence of the slope of the beam axis and the co-ordinate z of a typical point. Thus, approximately,

$$u = -z \frac{\partial w}{\partial x} \qquad \ldots(3.9)$$

and hence

$$\sigma_x = E.\frac{\partial u}{\partial x} \quad ; \quad \frac{\partial \sigma_x}{\partial x} = -E.z \frac{\partial^3 w}{\partial x^3}$$

and w is assumed to be a function of (x,t) alone.

Using these displacements the first of (3.8) becomes

$$-E \frac{\partial^3 w}{\partial x^3} \int_z bz^2 dz - \int_z \tau_{xz}.b dz = 0$$

which can be differentiated with respect to x and substitution made for $\frac{\partial}{\partial x}\int_z \tau_{xz}.b.dz$ in the second equation of (3.8) giving,

$$-E \frac{\partial^4 w}{\partial x^4} \int_z b.z^2 dz = \rho \frac{\partial^2 w}{\partial t^2} \int_z b.dz$$

or

$$EI_y \frac{\partial^4 w}{\partial x^4} + \rho A \frac{\partial^2 w}{\partial t^2} = 0 \qquad \ldots(3.10)$$

the Classical equation, originally derived by Daniel Bernoulli in the eighteenth century.

Since displacements which are continuous have been chosen the equations of compatibility need not be considered; this will be true in all the following sections.

It may be observed that the assumed stress and displacement simplifications are not consistent with the set of equations (3.2) but this is typical of this approach in that the equations (3.1) and (3.2) are not regarded as requiring rigorous satisfaction but are used selectively, terms that are considered important being retained; the remainder disregarded.

3.3. The Equation including Correction for Rotatory Inertia.

Consideration of the inertia of the motion in which cross-sections of the beam rotate about their neutral axis during flexural vibration gives rise to a corrected form of equation (3.10). All the assumptions of the classical equation are included with the exception that the inertia term in the X direction is not disregarded.

The equilibrium equations are taken as

$$\left.\begin{aligned} \frac{\partial \sigma_x}{\partial x} + \frac{\partial \tau_{xz}}{\partial z} &= \rho \cdot \frac{\partial^2 u}{\partial t^2} \\ \frac{\partial \tau_{xz}}{\partial x} &= \rho \cdot \frac{\partial^2 w}{\partial t^2} \end{aligned}\right\}$$

following through the reasoning of the previous section we obtain

$$\left.\begin{aligned} \int_z \frac{\partial \sigma_x}{\partial x} b.z\,dz - \int_z \tau_{xz}.b\,dz &= \rho \int_z \frac{\partial^2 u}{\partial t^2} b.z\,dz \\ \int_z \frac{\partial \tau_{xz}}{\partial x} b.dz &= \rho \int_z \frac{\partial^2 w}{\partial t^2} b.dz \end{aligned}\right\} \ldots (3.11)$$

Assuming again the displacement functions

$$u = -z \frac{\partial w}{\partial x}$$

$$v = 0$$

$$w = w(x,t)$$

and substituting stress components calculated from these into (3.11) there results the equations,

$$-EI_y \frac{\partial^3 w}{\partial x^3} - \int_z \tau_{xz}.b\,dz = -\rho I_y \frac{\partial^3 w}{\partial x\,\partial t^2}$$

$$\int_z \frac{\partial \tau_{xz}}{\partial x} b.dz = \rho A \frac{\partial^2 w}{\partial t^2}$$

Finally τ_{xz} can be eliminated from these two equations giving the final form

$$EI_y \frac{\partial^4 w}{\partial x^4} - \rho I_y \frac{\partial^4 w}{\partial x^2 \partial t^2} + \rho A \frac{\partial^2 w}{\partial t^2} = 0 \quad \ldots(3.12)$$

This equation was originally derived independently by Bresse and Rayleigh. The middle term of (3.12) represents the correction allowing for the rotatory inertia of the cross-sections.

3.4. The Equation including Correction for Shearing Displacement of Cross Sections.

Here, the physical feature that shear forces acting are also capable of deflecting the beam independently of the action of the bending itself, is taken into account.

Let the general point on the beam axis be considered. Then at any time the slope of the axis through that point can be represented by $\partial w/\partial x$, and this quantity must be the combination of that slope at the point which would be caused by bending action alone and that which would be caused by shearing action alone. Referring to these quantities as ϕ and $\bar{\beta}$ respectively, then

$$\frac{\partial w}{\partial x} = \phi + \bar{\beta}$$

The u-motion is now assumed to be a consequence of the bending action alone and displacement components

$$\left.\begin{aligned} u &= -z\,\phi(x,t) \\ v &= 0 \\ w &= w(x,t) \end{aligned}\right\} \qquad \ldots(3.13)$$

are taken.

The simplified equations of equilibrium (3.4) are again used. Stress components σ_x and τ_{xz} can be calculated from the displacement components (3.13).

In order to make some compensation for the assumption that τ_{xz} or γ_{xz} does not vary over the depth of the cross-section a numerical factor (η) is introduced such that

$$\int_z \tau_{xz}.b.dz = \eta GA\left(\frac{\partial w}{\partial x} - \phi\right)$$

η is thus the well known shear deflection coefficient of Timoshenko.

The equilibrium equations become on substitution

$$\left.\begin{aligned} -EI_y \frac{\partial^2 \phi}{\partial x^2} - \eta\left(\frac{\partial w}{\partial x} - \phi\right)AG &= 0 \\ \eta\left(\frac{\partial^2 w}{\partial x^2} - \frac{\partial \phi}{\partial x}\right)AG &= \rho A \frac{\partial^2 w}{\partial t^2} \end{aligned}\right\}$$

from which ϕ can be eliminated to give the final equation

$$EI_y \frac{\partial^4 w}{\partial x^4} - \frac{EI_y \rho}{\eta G}.\frac{\partial^4 w}{\partial x^2 \partial t^2} + \rho A \frac{\partial^2 w}{\partial t^2} = 0 \qquad \ldots(3.14)$$

At this juncture it is very important to see the formal nature of the change in the assumed displacement forms from those of the classical theory. This

change lies in the independence of the displacements u and w in (3.13). Whereas in (3.9) the displacements are linked by the relation $u = -z\frac{\partial w}{\partial x}$, in (3.13) no such coupling exists.

Now we have arrived at the independence of u by a physical argument involving shear slope and bending slope, but strictly speaking such reasoning was not necessary. Formally, we have merely postulated the independence of the displacement u by the relation $u = -z.\phi(x,t)$ and nothing further need be said about the function $\phi(x,t)$. This approach will be used in a later section when motion in the three orthogonal directions is being considered.

3.5. <u>The Equation including Corrections for Rotatory Inertia and Shear</u>:-

In this equation the corrections of sections 3.3 and 3.4 are combined. The displacement components of equation (3.13) are assumed and are used in conjunction with the equations of equilibrium including X-wise inertia,

$$\frac{\partial \sigma_x}{\partial x} + \frac{\partial \tau_{xz}}{\partial z} = \rho \frac{\partial^2 u}{\partial t^2}$$

$$\frac{\partial \tau_{xz}}{\partial x} = \rho \frac{\partial^2 w}{\partial t^2}$$

The equations are manipulated in the manner of the preceding pages and with the same assumptions, the numerical factor η is again introduced. The equilibrium equations integrated over the cross section reduce to the pair

$$\left.\begin{aligned} EI_y \frac{\partial^2 \phi}{\partial x^2} + \eta\left(\frac{\partial w}{\partial x} - \phi\right)AG &= \rho I_y \frac{\partial^2 \phi}{\partial t^2} \\ \eta\left(\frac{\partial^2 w}{\partial x^2} - \frac{\partial \phi}{\partial x}\right)AG &= \rho A \frac{\partial^2 w}{\partial t^2} \end{aligned}\right\} \quad \ldots(3.15)$$

The ϕ-function can now be eliminated from (3.15) giving the final differential equation

$$EI_y \frac{\partial^4 w}{\partial x^4} - \left(\frac{EI_y \rho}{\eta G} + \rho I_y\right)\frac{\partial^4 w}{\partial x^2 \partial t^2} + \rho A \frac{\partial^2 w}{\partial t^2} + \frac{I_y \rho^2}{\eta G} \cdot \frac{\partial^4 w}{\partial t^4} = 0 \quad \ldots(3.16)$$

Equation (3.16) is well known as the Timoshenko equation. The second term can be seen to be the sum of the corrections obtained separately in equations (3.12) and (3.14) while the final term has not appeared before. This term in $\left(\partial^4/\partial t^4\right)$ will be shown to be of some importance, being responsible for the possibility of a second frequency spectrum, and it is instructive to consider why it should make its appearance in this equation while being absent from those previous.

Some consideration will show that the appearance of this term follows from the allowance of two degrees of freedom for the typical particle of the beam; one in the transverse direction and one axially. This implies that the axial motion (u) of the particle is independent of the transverse motion (w), and that inertia terms in both directions are taken into account.

Thus no such term arose when the rotatory inertia correction alone was made, because there the assumed motion parallel to the axis was related to the vertical

motion by the relation $u = -z \frac{\partial w}{\partial x}$, so that u was not an independent co-ordinate. Similarly, when correcting for shear displacement alone, only second order derivatives with respect to time were obtained. For, although the axial displacement of a point was not functionally related to its transverse displacement (i.e. was independent), the inertia parallel to the axis of the point was neglected.

A rough qualitative model of the effect can be constructed. If the vibrating beam is considered as a simple spring-mass system, then the effect of the shearing action of the beam is to increase its flexibility that is to reduce the effective spring contact of the linear oscillator. This can be conceived as being the introduction of a spring in series with the normal "bending flexibility" one (see Fig. 6).

The effect of the rotatory inertia correction is to add an inertia or mass to the system and this can be shown as a small mass rigidly fixed to the main mass.

Either of these corrections will have reduced the natural frequency of the system but there will still be only one degree of freedom.

If both corrections are applied simultaneously however, then as shown in Fig. 6 , there will result a coupled pair of spring mass systems with therefore two degrees of freedom. The frequency equation for the system will be a quadratic in frequency

squared which is the equivalent of the $(\partial^4/\partial t^4)$ of equation (3.16).

3.6. The Equation including the Effects of Rotatory Inertia, Shear, and the Twisting of Transverse Planes.

In the previous sections it has been assumed that under deformation, transverse planes originally normal to the neutral surface of the unstrained beam, remained plane. That is, the longitudinal displacement u has been taken as a linear function of z. This will, in general, be only a good approximation and a method of assessing the effect of twisting of the plane will now be presented. This theory is basically that of Arnold (1951)

The following displacement components are assumed

$$\left.\begin{aligned} u &= -z\,\phi(x,t) + e(x,z,t) \\ v &= 0 \\ w &= w(x,t) \end{aligned}\right\} \qquad \ldots(3.17)$$

So that,

$$\sigma_x = E\left(-z\frac{\partial \phi}{\partial x} + \frac{\partial e}{\partial x}\right)$$

$$\tau_{xz} = G\left(\frac{\partial w}{\partial x} - \phi + \frac{\partial e}{\partial z}\right)$$

The simplified equilibrium equations of section 3.5 are taken and the usual integration over the cross-section yields the following two equations

$$-EI_y\frac{\partial^2\phi}{\partial x^2} + E\int_z \frac{\partial^2 e}{\partial x^2} b\,z\,dz - GA\left(\frac{\partial w}{\partial x} - \phi\right) - G\int_z \frac{\partial e}{\partial z} b\,dz = -\rho I_y \frac{\partial^2\phi}{\partial t^2} + \rho\int_z \frac{\partial^2 e}{\partial t^2} b\,z\,dz$$

$$AG\left(\frac{\partial^2 w}{\partial x^2} - \frac{\partial \phi}{\partial x}\right) + G\int_z \frac{\partial^2 e}{\partial x\,\partial z} b\,dz = \rho A \frac{\partial^2 w}{\partial t^2} \qquad \ldots(3.18)$$

From the second of (3.18)

$$\frac{\partial \phi}{\partial x} = \frac{\partial^2 w}{\partial x^2} + \frac{1}{A}\int_z \frac{\partial^2 e}{\partial x \partial z} b\,dz - \frac{\rho}{G}\frac{\partial^2 w}{\partial t^2} \qquad \ldots(3.19)$$

while, eliminating ϕ from the equations (3.18), leads to

$$-EI_y\left[\frac{\partial^4 w}{\partial x^4} + \frac{1}{A}\int_z \frac{\partial^3 e}{\partial x^3 \partial z} b\,dz - \frac{\rho}{G}\frac{\partial^4 w}{\partial x^2 \partial t^2}\right] + E\int_z \frac{\partial^3 e}{\partial x^3} bz\,dz + \rho I_y\left[\frac{\partial^4 w}{\partial x^2 \partial t^2}\right.$$

$$\left. + \frac{1}{A}\int_z \frac{\partial^4 e}{\partial t^2 \partial x \partial z} b\,dz - \frac{\rho}{G}\frac{\partial^4 w}{\partial t^4}\right] - \rho\int_z \frac{\partial^2 e}{\partial x \partial t^2} bz\,dz = \rho A \frac{\partial^2 w}{\partial t^2} \qquad \ldots(3.20)$$

The shear coefficient η has not been introduced here because τ_{xz} is now no longer independent of z and e will be chosen so that τ_{xz} is a reasonable function.

It is now necessary to find an expression for $e(x,z,t)$ and for this purpose it is helpful to consider the problem physically. Fig. 7 shows a typical thin transverse slice from a vibrating beam. At the neutral axis the shear strain is assumed to be entirely devoted to providing shear slope, so that at this point both the shear slope of the beam and the total angle of shear are the same. At points some distance from the neutral axis it will be assumed that the slope remains the same as that on the neutral axis (so that $\bar{\beta}$ is a function of x alone) but that an additional angular distortion α_z is present such that $\gamma_z = \bar{\beta} - \alpha_z$ where γ_z is the total shear strain at height z. Furthermore, it will be assumed that the static distribution of shear strain is applicable; this

distribution is easily obtained for any cross-section by calculation or by graphical means from the equations given in books on the strength of materials.

Now it is apparent from Fig. 7 , that the displacement e is the sum of displacements of the type $\alpha_z dz$ so we can write

$$e = \int \alpha_z dz$$

$$= \int (\bar{\beta} - \gamma_z) dz \qquad \ldots(3.21)$$

$\bar{\beta}$ is the value of shear strain on the neutral axis while γ_z is the value of the shear strain at a distance z from the axis. Both these quantities are obtainable from the static shear strain distribution so that the above integral for e can readily be evaluated, graphically or otherwise.

Two constants for the cross-section will now be defined. These are readily computed when the curves of e against z are obtained by equation (3.21). They are

$$\epsilon_1 = \frac{1}{I_y \bar{\beta}} \int_z b.e.z\,dz \qquad \ldots(3.22)$$

and

$$\epsilon_2 = \frac{1}{A\bar{\beta}} \int_z b. \frac{\partial e}{\partial z} dz \qquad \ldots(3.23)$$

In the equation (3.20) there remain four terms which require expansion,

$$-\frac{EI_y}{A} \int_z \frac{\partial^4 e}{\partial x^3 \partial z} b\,dz \;\; ; \;\; E \int_z \frac{\partial^3 e}{\partial x^3} b.z\,dz \;\; ; \;\; \frac{\rho I_y}{A} \int_z \frac{\partial^4 e}{\partial x \partial z \partial t^2} b\,dz \;\; ; \;\; -\rho \int_z \frac{\partial^3 e}{\partial x \partial t^2} b.z\,dz$$

using the constants defined in (3.22) and (3.23); these terms can be written respectively

$$-EI_y\epsilon_2\frac{\partial^3\bar{\beta}}{\partial x^3}\ ;\ EI_y\epsilon_1\frac{\partial^3\bar{\beta}}{\partial x^3}\ ;\ \rho I_y\epsilon_2\frac{\partial^3\bar{\beta}}{\partial x\partial t^2}\ ;\ -\rho I_y\epsilon_1\frac{\partial^3\bar{\beta}}{\partial x\partial t^2}$$

Further, it is known that $\bar{\beta} = \left(\frac{\partial w}{\partial x} - \phi\right)$ ...(3.24)

while from (3.19),

$$\frac{\partial\phi}{\partial x} = \frac{\partial^2 w}{\partial x^2} - \frac{\rho}{(1+\epsilon_2)G}\cdot\frac{\partial^2 w}{\partial t^2} \qquad ...(3.25)$$

With the use of these relations the four terms can be written with w as dependent variable, and the final differential equation is

$$EI_y\frac{\partial^4 w}{\partial x^4} + \rho A\frac{\partial^2 w}{\partial t^2} - \frac{\partial^4 w}{\partial x^2\partial t^2}\left[\frac{EI_y\rho}{G}\left(\frac{1+\epsilon_1}{1+\epsilon_2}\right) + \rho I_y\right]$$

$$+ \frac{\rho^2 I_y}{G}\left(\frac{1+\epsilon_1}{1+\epsilon_2}\right)\frac{\partial^4 w}{\partial t^4} = 0 \qquad ...(3.26)$$

Equation (3.26) is the same as the Timoshenko equation (3.16) except that the shear constant η is replaced by the factor $\left(\frac{1+\epsilon_2}{1+\epsilon_1}\right)$.

For a rectangular section this factor can be calculated and has the value 2/3 which is the corresponding value for η obtained by normal methods for the Timoshenko equation. It is also known that 2/3 is an inferior value to the 5/6 obtained for η by strain energy considerations (or the value $\pi^2/12$; see Mindlin and Deresiewicz (1954)). Thus, this analysis, though avoiding the rather crude process of the introduction of the η constant, is unlikely to give any better results than the Timeshenko equation, and

when the η value is judiciously chosen may give inferior results to that equation.

3.7. The Equation including the Effects of Rotatory Inertia, Shear, and an Independent Lateral Motion.

A logical extension of the preceding sections is now made by allowing for the lateral motion of the beam. This motion will be chosen to be independent of the u and w motion because this independence can be expected to provide new features in the equation, after the manner of the Timoshenko equation in section 3.5. In the spirit of the remarks at the end of section 3.4, it will not be necessary to conceive the mechanism whereby v receives its independence (although it is fairly obvious that it is due to the influence of the lateral shearing stresses in much the same way as the independence of u comes from the transverse shear stress). That the displacements must, in general, be independent follows from the fact that flexural vibration is an elastic problem in three dimensions; if any of the displacements could be expressed in terms of another, the problem would reduce to one in two dimensions because one of the displacements could be eliminated from the equations.

The lateral inertia will also be considered so that the typical particle will have three degrees of freedom.

The equilibrium equations for a small element are

taken as

$$\left.\begin{aligned} \frac{\partial \sigma_x}{\partial x} + \frac{\partial \tau_{xy}}{\partial y} + \frac{\partial \tau_{xz}}{\partial z} &= \rho \frac{\partial^2 u}{\partial t^2} \\ \frac{\partial \tau_{yz}}{\partial z} + \frac{\partial \tau_{xy}}{\partial x} &= \rho \frac{\partial^2 v}{\partial t^2} \\ \frac{\partial \tau_{yz}}{\partial y} + \frac{\partial \tau_{xz}}{\partial x} &= \rho \frac{\partial^2 w}{\partial t^2} \end{aligned}\right\} \quad \ldots(3.27)$$

The first equation is now multiplied by $z\,dydz$, the second by $z/y\,dydz$, the third by $dy.dz$ and the three equations are then integrated over the region (R) of the YZ-plane occupied by the cross-section; this gives

$$\left.\begin{aligned} \iint_R \frac{\partial \sigma_x}{\partial x} z\,dydz + \iint_R \frac{\partial \tau_{xy}}{\partial y} z\,dydz + \iint_R \frac{\partial \tau_{xz}}{\partial z} z\,dydz &= \rho \iint_R \frac{\partial^2 u}{\partial t^2} z\,dydz \\ \iint_R \frac{\partial \tau_{yz}}{\partial z}.\frac{z}{y}\,dydz + \iint_R \frac{\partial \tau_{xy}}{\partial x}.\frac{z}{y}\,dydz &= \rho \iint_R \frac{\partial^2 v}{\partial t^2}.\frac{z}{y}.dydz \\ \iint_R \frac{\partial \tau_{yz}}{\partial y}\,dy.dz + \iint_R \frac{\partial \tau_{xz}}{\partial x}.\,dydz &= \rho \iint_R \frac{\partial^2 w}{\partial t^2}.\,dydz \end{aligned}\right\} \quad \ldots(3.28)$$

If the eventual displacement components which are assumed are such that none of the terms u, w, $\partial\tau_{xy}/\partial y$, $\partial\tau_{yz}/\partial y$, are functions of y; the equations (3.28) can be written,

$$\left.\begin{aligned} \int_z \frac{\partial \sigma_x}{\partial x} z\,bdz + \int_z \frac{\partial \tau_{xy}}{\partial y} z.b.dz + \int_z \frac{\partial \tau_{xz}}{\partial z} z\,bdz &= \rho \int_z \frac{\partial^2 u}{\partial t^2} z.b.dz \\ \iint_R \frac{\partial \tau_{yz}}{\partial z}.\frac{z}{y}\,dydz + \iint_R \frac{\partial \tau_{xy}}{\partial x}.\frac{z}{y}\,dydz &= \rho \iint_R \frac{\partial^2 v}{\partial t^2}.\frac{z}{y}\,dydz \\ \int_z \frac{\partial \tau_{yz}}{\partial y}\,bdz + \int_z \frac{\partial \tau_{xz}}{\partial x}.\,bdz &= \rho \int_z \frac{\partial^2 w}{\partial t^2}\,bdz \end{aligned}\right\} \quad \ldots(3.29)$$

where $b = \int dy$; the section width.

The term $\int_z \frac{\partial \tau_{xz}}{\partial z} z.b\,dz$ of the first equation of (3.29) can be dealt with in the manner of equation (3.7) so that it will be replaced by the term

$$-\int_z \tau_{xz} \cdot b\,dz \quad .$$

The first term of the second equation of (3.29) can be similarly treated and can be replaced by the term $-\iint_R \tau_{yz} \cdot \frac{1}{y}\,dy\,dz$.

It is now necessary to choose reasonable displacement functions. The axial (u) and transverse (w) components might well be taken the same as those chosen for the Timoshenko equation in section 3.5, but a function for the lateral displacement (v) will have to be invented. Some consideration suggests that a linear relationship with respect to y and z would not be unreasonable and is of the simplest possible form.

Consequently displacement components

$$\left.\begin{aligned} u &= -z.\phi(x,t) \\ v &= y.z\,f(x,t) \\ w &= w(x,t) \end{aligned}\right\} \qquad \ldots(3.30)$$

are taken.

Stress components can now be evaluated and substituted in (3.29) with the result

$$\left.\begin{aligned} -E\frac{\partial^2\phi}{\partial x^2}\int_z z^2 b\,dz + G\frac{\partial f}{\partial x}\int_z z^2 b\,dz - \eta G\left(\frac{\partial w}{\partial x} - \phi\right)\int_z b\,dz & \\ = -\rho\frac{\partial^2\phi}{\partial t^2}\int_z z^2.b\,dz & \\ -Gf\iint_R dy\,dz + G\frac{\partial^2 f}{\partial x^2}\iint_R z^2\,dy\,dz = \rho\frac{\partial^2 f}{\partial t^2}\iint_R z^2.dy\,dz & \\ Gf\int_z b\,dz + \eta G\left(\frac{\partial^2 w}{\partial x^2} - \frac{\partial\phi}{\partial x}\right)\int_z b\,dz = \rho\frac{\partial^2 w}{\partial t^2}\int_z b.dz & \end{aligned}\right\} \qquad \ldots(3.31)$$

where the shear coefficient η has again been introduced and $\phi(x,t)$, $f(x,t)$, and $w(x,t)$, have been written as ϕ , f , and w respectively.

The remaining integrals in (3.31) obviously represent the area of the cross-section (A) and the second moment of area of the cross-section about its lateral axis I_y . Thus (3.31) become,

$$\left.\begin{aligned} -EI_y\frac{\partial^2\phi}{\partial x^2} + GI_y\frac{\partial f}{\partial x} - \eta GA\left(\frac{\partial w}{\partial x} - \phi\right) &= -\rho I_y\frac{\partial^2\phi}{\partial t^2} \\ -GAf + GI_y\frac{\partial^2 f}{\partial x^2} &= \rho I_y\frac{\partial^2 f}{\partial t^2} \\ GAf + \eta GA\left(\frac{\partial^2 w}{\partial x^2} - \frac{\partial\phi}{\partial x}\right) &= \rho A\frac{\partial^2 w}{\partial t^2} \end{aligned}\right\} \quad \ldots(3.32)$$

It now remains to eliminate from the three equations (3.32), the two unknowns $\phi(x,t)$ and $f(x,t)$ and a differential equation in w as dependent variable will result.

From the third equation,

$$\frac{\partial\phi}{\partial x} = \frac{\partial^2 w}{\partial x^2} + \frac{f}{\eta} - \frac{\rho}{\eta G}\cdot\frac{\partial^2 w}{\partial t^2} \qquad \ldots(3.33)$$

This can be substituted in the first equation differentiated with respect to x , giving eventually the equation,

$$\left[GI_y\frac{\partial^2}{\partial x^2} - \frac{EI_y}{\eta}\cdot\frac{\partial^2}{\partial x^2} + GA + \frac{\rho I_y}{\eta}\cdot\frac{\partial^2}{\partial t^2}\right]f$$

$$= \left\{EI_y\frac{\partial^4 w}{\partial x^4} - \left(\frac{EI_y\rho}{\eta G} + \rho I_y\right)\frac{\partial^4 w}{\partial x^2\partial t^2} + \rho A\frac{\partial^2 w}{\partial t^2} + \frac{I_y\rho^2}{\eta G}\frac{\partial^4 w}{\partial t^4}\right\} \ldots(3.34)$$

while the second equation of (3.32) can be written,

$$\left(\frac{\partial^2}{\partial x^2} - \frac{\rho}{G}\cdot\frac{\partial^2}{\partial t^2} - \frac{A}{I_y}\right)f = 0 \qquad \ldots(3.35)$$

We now operate on both sides of equation (3.34) with

$\left(\frac{\partial^2}{\partial x^2} - \frac{\rho}{G}\cdot\frac{\partial^2}{\partial t^2} - \frac{A}{I_y}\right)$, and on both sides of (3.35) with $\left[GI_y\frac{\partial^2}{\partial x^2} - \frac{EI_y}{\eta}\cdot\frac{\partial^2}{\partial x^2} + GA + \frac{\rho I_y}{\eta}\frac{\partial^2}{\partial t^2}\right]$ and subtract, giving the final result

$$\left(\frac{\partial^2}{\partial x^2} - \frac{\rho}{G}\frac{\partial^2}{\partial t^2} - \frac{A}{I_y}\right)\left(EI_y\frac{\partial^4 w}{\partial x^4} - \left(\frac{EI_y\rho}{\eta G} + \rho I_y\right)\frac{\partial^4 w}{\partial x^2\partial t^2} + \rho A\frac{\partial^2 w}{\partial t^2} + \frac{I_y\rho^2}{\eta G}\cdot\frac{\partial^4 w}{\partial t^4}\right) = 0 \qquad \ldots(36)$$

or expanding,

$$EI_y\frac{\partial^6 w}{\partial x^6} - \frac{\partial^6 w}{\partial x^4\partial t^2}\left(\frac{EI_y\rho}{\eta G} + \rho I_y + \frac{EI_y\rho}{G}\right) + \frac{\partial^6 w}{\partial x^2\partial t^4}\left(\frac{EI_y\rho^2}{\eta G^2} + \frac{\rho^2 I_y}{G} + \frac{\rho^2 I_y}{\eta G}\right)$$

$$-EA\frac{\partial^4 w}{\partial x^4} + \frac{\partial^4 w}{\partial x^2\partial t^2}\left(2\rho A + \frac{EA\rho}{\eta G}\right) - \frac{\rho A^2}{I_y}\cdot\frac{\partial^2 w}{\partial t^2} - \frac{\partial^4 w}{\partial t^4}\left(\frac{\rho^2 A}{G} + \frac{\rho^2 A}{\eta G}\right) \qquad \ldots(3.37)$$

$$-\frac{\rho^3 I_y}{\eta G^2}\cdot\frac{\partial^6 w}{\partial t^6} = 0$$

Equation (3.37) contains the sixth order derivative with respect to time that was expected by analogy with the analysis of the Timoshenko equation. This will give rise to the possibility of three frequency spectra or three branches to the dispersion curves for flexural waves.

3.8. The Effect of Anticlastic Curvature.

The effects of anticlastic curvature can be included in the analysis of the previous section by assuming the statical deflection

$$w(x,y,z,t) = w_o(x,t) + \frac{\nu}{2}\cdot\frac{\partial\phi(x,t)}{\partial x}(z^2 - y^2) \qquad \ldots(3.38)$$

along with the u and v displacement functions of section 3.7. Here w_o is the transverse deflection of the neutral line of the beam and ν is Poisson's ratio.

Following the procedure of section 3.7 the

equilibrium equations become

$$\left.\begin{aligned} -EI_y\frac{\partial^2\phi}{\partial x^2} + GI_y\frac{\partial f}{\partial x} - \eta AG\left(\frac{\partial w_o}{\partial x} - \phi\right) - G\frac{\nu}{2}\cdot\frac{\partial^2\phi}{\partial x^2}\left(I_y - I_z\right) \\ = -\rho I_y\cdot\frac{\partial^2\phi}{\partial t^2} \\ -GAf + \nu GA\frac{\partial\phi}{\partial x} + GI_y\frac{\partial^2 f}{\partial x^2} = \rho I_y\cdot\frac{\partial^2 f}{\partial t^2} \\ GAf - \nu GA\frac{\partial\phi}{\partial x} + \eta GA\left(\frac{\partial^2 w_o}{\partial x^2} - \frac{\partial\phi}{\partial x}\right) + \frac{\nu G}{2}\cdot\frac{\partial^3\phi}{\partial x^3}\left(I_y - I_z\right) \\ = \rho A\frac{\partial^2 w_o}{\partial t^2} + \frac{\rho\nu}{2}\frac{\partial^3\phi}{\partial x\,\partial t^2}\left(I_y - I_z\right) \end{aligned}\right\} \quad \ldots(3.39)$$

I_z is the second moment of area of the cross-section about an axis in the plane of bending. The constant η has been introduced before that part of τ_{xz} which is dependent on the shear deflection because this should vary across the section independently of the other part which is due to the anticlastic curvature. Boley (1955) suggests that the value taken for η should depend on the width/depth ratio for the beam because of the effect of the other shear stresses, and finds that 5/6 is a suitable value up to width/depth ratios of 3, the value decreasing more rapidly thereafter.

The functions ϕ and f can be eliminated from equations (3.39) and after manipulation a differential equation in w_o as dependent variable is obtained. This is

$$EI_y\frac{\partial^6 w_o}{\partial x^6} - \frac{\partial^6 w_o}{\partial x^4\partial t^2}\left(\frac{EI_y\rho}{\eta G} + \rho I_y + \frac{EI_y\rho}{G} - \frac{\nu\rho}{2}\left(I_y - I_z\right)\left(1 - \tfrac{1}{\eta}\right)\right) + \frac{\partial^6 w_o}{\partial x^2\partial t^4}\left(\frac{EI_y\rho^2}{\eta G^2}\right.$$

$$\left. + \frac{\rho^2 I_y}{G} + \frac{\rho^2 I_y}{\eta G} - \frac{\nu\rho^2}{2G}\left(I_y - I_z\right)\left(1 - \tfrac{1}{\eta}\right)\right) - \frac{\partial^4 w_o}{\partial x^4}\left(EA - 2G\nu A\right) + \frac{\partial^4 w_o}{\partial x^2\partial t^2}\left(2\rho A\right.$$

$$\left. + \frac{EA\rho}{\eta G} - \rho\nu A\left(1 + \tfrac{1}{\eta}\right) - \frac{\rho\nu A}{2I_y}\left(I_y - I_z\right)\left(1 - \tfrac{1}{\eta}\right)\right) - \frac{\rho A^2}{I_y}\cdot\frac{\partial^2 w_o}{\partial t^2}$$

$$- \frac{\partial^4 w_o}{\partial t^4}\left(\frac{\rho^2 A}{G} + \frac{\rho^2 A}{\eta G}\right) - \frac{\rho^3 I_y}{\eta G^2}\cdot\frac{\partial^6 w_o}{\partial t^6} = 0 \qquad \ldots(3.40)$$

Equation (3.37) is a special case of (3.40) with $I_y = I_z$. For cross sections which have not too radical a departure from kinetic symmetry $(I_y = I_z)$, equation (3.37) will be a good approximation.

4. THE SOLUTION OF THE TIMOSHENKO EQUATION.

4.1. Derivation of the Boundary Conditions.

4.1.1. Introductory. Applying the Timoshenko theory of flexure to a beam of finite length, the displacement $w(x,t)$ must be such as to satisfy both the differential equation and the conditions obtaining at the ends of the beam.

These end conditions will, in general, be a specification as to displacement, slope, shear force or bending moment; consequently it is necessary to be able to evaluate these quantities. It will be shown how expressions for them can be obtained from the equilibrium equations. The method can then be used in similar fashion to yield end boundary conditions for the more complicated equation (3.37).

4.1.2. Shear Force in terms of Displacement.

By definition the shear force over any cross section of the beam is given by

$$Q = \int_z \tau_{xz}\, b\, dz \qquad \ldots(4.1)$$

This expression also appears in the first of the equilibrium equations (see equations (3.11) for example) from which

$$\int_z \tau_{xz}\, b\, dz = \int_z \frac{\partial \sigma_x}{\partial x}\, b z\, dz - \rho \int_z \frac{\partial^2 u}{\partial t^2}\, b z\, dz$$

If the relevant displacement components (3.13) are

substituted in the above equation, and if harmonic time variation is assumed (steady state resonance) so that the operator $\partial^2/\partial t^2$ may be replaced by $-p^2$, then

$$Q = -EI_y \frac{\partial^2 \phi}{\partial x^2} - \rho p^2 . I_y . \phi \qquad \ldots(4.2)$$

Also, from the second equilibrium equation (3.15)

$$\frac{\partial Q}{\partial x} = -\rho p^2 A w \qquad \ldots(4.3)$$

while by definition,

$$\left(\frac{\partial w}{\partial x} - \phi\right) = \frac{Q}{\eta AG} \qquad \ldots(4.4)$$

From equations (4.2), (4.3), and (4.4), the expression for shear force in terms of the displacement is obtained,

$$Q\left[1 - \frac{\rho p^2 I_y}{\eta AG}\right] = -EI_y \frac{\partial^3 w}{\partial x^3} - EI_y \frac{\rho p^2}{G}\left[\frac{1}{\eta} + \frac{G}{E}\right] \frac{\partial w}{\partial x} \qquad \ldots(4.5)$$

4.1.3. Bending Moment in Terms of Displacement.

By definition the bending moment at any cross-section of the beam is given by

$$M = \int_z \sigma_z . b . z \, dz \qquad \ldots(4.6)$$

Using the assumed displacement form for u (equation (3.13)), (4.6) becomes

$$M = \int_z -Ez^2 . \frac{\partial \phi}{\partial x} b \, dz \qquad \ldots(4.7)$$

From the second equilibrium equation (3.15), $\frac{\partial \phi}{\partial x}$ can be found in terms of w ; thus,

$$M = \int_z -Ez^2 b\left[\frac{\partial^2 w}{\partial x^2} - \frac{\rho}{\eta G}\cdot\frac{\partial^2 w}{\partial t^2}\right] dz$$

or since w is assumed independent of z the integration can be carried out and the final form, with $-p^2$ in place of $\partial^2/\partial t^2$, is

$$M = -EI_y\left[\frac{\partial^2 w}{\partial x^2} + \frac{\rho p^2}{\eta G}\cdot w\right] \qquad \ldots(4.8)$$

4.1.4. Standard End Conditions. The standard end conditions are those generally described as "pinned" "free" and "fixed". Their definitions in this case are

Pinned End:- $w = 0$; σ_x or $M = 0$

Free End :- σ_x or $M = 0$; τ_{xz} or $Q = 0$

Fixed End :- $\phi = 0$; $w = 0$

The above conditions are all contained in the equations following,

Displacement Zero $w = 0$

Bending Slope Zero $\left(\frac{EI_y}{\eta AG}\right)\frac{\partial^3 w}{\partial x^3} + \frac{\partial w}{\partial x}\left(1 + \frac{EI_y \rho p^2}{\eta^2 AG^2}\right) = 0$

Direct Stress (σ_x) or bending Moment Zero $\frac{\partial^2 w}{\partial x^2} + \frac{\rho p^2}{\eta G}\cdot w = 0$

Shear Stress (τ_{xz}) or Shear Force Zero $\frac{\partial^3 w}{\partial x^3} + \frac{\rho p^2}{G}\left[\frac{1}{\eta} + \frac{G}{E}\right]\frac{\partial w}{\partial x} = 0$

The equation for bending slope can be obtained almost direct from the equilibrium equations (3.15).

4.2. Solving the Equation.

The Timoshenko equation

$$EI_y \frac{\partial^4 w}{\partial x^4} - \left(\frac{EI_y \rho}{\eta G} + \rho I_y\right)\frac{\partial^4 w}{\partial x^2 \partial t^2} + \rho A \frac{\partial^2 w}{\partial t^2} + \frac{I_y \rho^2}{\eta G}\cdot\frac{\partial^2 w}{\partial t^4} = 0$$

can easily be solved for a beam under set end conditions when it is known that it is vibrating in a normal mode. For, under such conditions, the time variation of the displacement will be sinusoidal of frequency p (say) and the displacement can be taken in the form

$$w(x,t) = W(x).\cos pt$$

where $W(x)$ is the "shape function". Inserting this in the differential equation and making the substitutions

$$\left.\begin{aligned} \psi^2 &= \frac{p^2\rho}{E} \\ \alpha &= \frac{1}{K^2} \\ \beta &= \frac{E}{\eta G} \end{aligned}\right\} \qquad \ldots(4.9)$$

(where K is the radius of gyration of the cross-section about YY′) the ordinary differential equation for the shape function is obtained

$$\frac{d^4W}{dx^4} + \psi^2(1+\beta)\frac{d^2W}{dx^2} - \psi^2(\alpha - \psi^2\beta)W = 0 \qquad \ldots(4.10)$$

Assuming exponential solutions, equation (4.10) can be solved by normal methods giving the shape function,

$$W(x) = A_1 \sin\mu x + A_2 \cos\mu x + A_3 \sinh qx + A_4 \cosh qx \qquad \ldots(4.11)$$

where $A_1 \ldots A_4$ are coefficients to be determined from the end conditions of the beam and

$$2\mu^2 = \psi^2(1+\beta) + \sqrt{[\psi^4(1-\beta)^2 + 4\alpha\psi^2]}$$
$$2q^2 = -\psi^2(1+\beta) + \sqrt{[\psi^4(1-\beta)^2 + 4\alpha\psi^2]} \quad \Big\} \ldots(4.12)$$

The two relations

$$\mu^2 - q^2 = \psi^2(1+\beta) \quad \text{and} \quad \mu^2 q^2 = \psi^2(\alpha - \psi^2\beta) \quad \ldots(4.13)$$

can also be deduced.

From (4.12) it follows that μ^2 is always positive so from (4.13) q^2 becomes negative or q imaginary when $\psi^2 > \frac{\alpha}{\beta}$. Under this condition the last two terms of the shape function (4.11) will change from hyperbolic functions to their respective circular functions.

4.3. The Frequency Equation for Timoshenko Beam on Flexible End Supports.

The frequency equation for the symmetric modes of a beam, the ends of which are similarly elastically supported in deflection on horizontal hinges, will now be derived.

Consider a beam of total length 2ℓ with spring supports of rate λ (lbs./inch) at $x = 0$ and $x = 2\ell$, vibrating in a mode symmetric about the centre of the beam. An imaginary cut can be made through the beam at its centre, and the boundary conditions at $x = 0$ and $x = \ell$ can be considered. Using the boundary conditions at $x = 0$ and $x = 2\ell$ would be less restrictive in that the resulting frequency equation would contain both symmetric and antisymmetric frequencies whereas the boundary conditions at $x = \ell$

can be specially chosen to include only one type.

The boundary conditions can be written,

$$\left.\begin{aligned} [M]_{x=0} = 0 \quad ; \quad [Q]_{x=0} = \lambda [w]_{x=0} \\ \left[\frac{\partial w}{\partial x}\right]_{x=\ell} = 0 \quad ; \quad [Q]_{x=\ell} = 0 \end{aligned}\right\} \quad \ldots(4.14)$$

where M refers to bending moment and Q to shear force: the second pair of conditions follow by reason of the symmetry existing about $x=\ell$. Using the relations derived in section 4.1, equations (4.14) can be written in terms of the shape function $W(x)$, giving

$$\left.\begin{aligned} \left[\frac{d^2W}{dx^2}\right]_{x=0} &= -\psi^2\beta [W]_{x=0} \\ \lambda(\alpha-\beta\psi^2)[W]_{x=0} &= EA\left[-\frac{d^3W}{dx^3} - \psi^2(1+\beta)\frac{dW}{dx}\right]_{x=0} \\ \left[\frac{dW}{dx}\right]_{x=\ell} &= 0 \\ \left[\frac{d^3W}{dx^3} + \psi^2(1+\beta)\frac{dW}{dx}\right]_{x=\ell} &= 0 \end{aligned}\right\} \quad \ldots(4.15)$$

The shape function (4.11) is now substituted in (4.15) leading to four equations each containing the four constants A_1, A_2, A_3, A_4. The condition for independence of these constants, the vanishing of their determinant, is the frequency equation, which after simplification reduces to the form

$$(\alpha-\beta\psi^2)(\mu^2+q^2)\cos\mu\ell.\cosh q\ell - \left(\frac{EA}{\lambda}\right)\mu q\left\{\mu(\mu^2-\beta\psi^2)\cos\mu\ell.\sinh q\ell\right.$$

$$\left. + q(q^2+\beta\psi^2)\sin\mu\ell.\cosh q\ell.\right\} = 0 \quad \ldots(4.16)$$

The terms of (4.16) are defined in equations (4.9) and (4.12); ψ, μ and q are all functions of frequency..

4.4. Reduction to Case of Pinned-Ends and Free-Ends.

4.4.1. Pinned Ends From (4.16) the frequency equation for a beam with pinned ends vibrating in a symmetric mode can be obtained by letting the spring constant λ become very large so that only the first part of the equation remains important, and the frequency equation is consequently

$$\cos\mu l . \cosh ql = 0 \qquad \ldots(4.17)$$

However, for frequencies greater than a certain value, q^2 becomes negative. From (4.13) this "critical" frequency is given by the relation

$$\psi_c^2 = \frac{\alpha}{\beta} \qquad \ldots(4.18)$$

Let,

$$q^2 = -r^2 \qquad \ldots(4.19)$$

where r is a positive number.

Then $q = ir$ in equation (4.17) modifying the frequency equation to

$$\cos\mu l . \cos rl = 0 \qquad (\psi^2 > \psi_c^2) \qquad \ldots(4.20)$$

4.4.2 Free Ends. From equation (4.16) the frequency equation for a beam with free ends vibrating in a symmetric mode can be obtained by taking λ negligibly small, so that the second part only of the equation is of importance. Incorporating the modifications of section 4.4.1 for q^2 negative, the frequency equation can be written,

$$\mu(\mu^2 - \beta\psi^2)\cos\mu l.\sinh ql + q(q^2+\beta\psi^2)\sin\mu l.\cosh ql = 0 \quad \ldots(4.21)$$

for $\psi^2 < \frac{\alpha}{\beta}$, and

$$\mu(\mu^2-\beta\psi^2)\cos\mu l.\sin rl + r(\beta\psi^2-r^2)\sin\mu l.\cos rl = 0 \quad \ldots(4.22)$$

for $\psi^2 > \frac{\alpha}{\beta}$.

4.5. Discussion on the Frequency Equations.

4.5.1. Beam with Pinned Ends.

For values of frequency less than the value prescribed by the relation $\psi^2 = \frac{\alpha}{\beta}$ the transcendental frequency equation for a pin-ended beam is from (4.17),

$$\cos\mu l = 0$$

while for $\psi^2 > \frac{\alpha}{\beta}$ the equation becomes $\cos\mu l.\cos rl = 0$ which is satisfied if either

$$\left.\begin{aligned}\cos\mu l &= 0\\ \text{or}\qquad \cos rl &= 0\end{aligned}\right\} \quad \ldots(4.23)$$

The condition $\cos rl = 0$ then defines a second band of natural frequencies which does not begin until $\psi^2 > \frac{\alpha}{\beta}$. This second spectrum of frequencies is not evident in the classical theory and is a consequence of the consideration of the shear and rotatory inertia effects.

This can also be seen for a pin-ended beam by substituting in the differential equation (4.10) the shape function

$$W(x) = D.\sin\frac{m\pi x}{2\ell}$$

where the positive integer m is the number of half-waves along the beam. This shape function will be found to satisfy the end conditions for a pinned beam and its substitution in (4.10) will give an equation of condition for the frequency for each value of m .

This is

$$\psi^4 - \psi^2\left[\frac{\alpha}{\beta} + \left(\frac{1+\beta}{\beta}\right)\left(\frac{m\pi}{2\ell}\right)^2\right] + \frac{1}{\beta}\left(\frac{m\pi}{2\ell}\right)^4 = 0 \quad \ldots(4.24)$$

Since $\psi^2 \propto p^2$ the above equation is a quadratic in p^2 and prescribes two real values of frequency for each possible value of m . That the roots are real for possible values of β can be seen by considering the discriminant of (4.24).

This is

$$\left(\frac{\alpha}{\beta}\right)^2 + \left(\frac{1+\beta}{\beta}\right)^2\left(\frac{m\pi}{2\ell}\right)^4 + \frac{2\alpha}{\beta}\left(\frac{1+\beta}{\beta}\right)\left(\frac{m\pi}{2\ell}\right)^2 - \frac{4}{\beta}\left(\frac{m\pi}{2\ell}\right)^4$$

Considering only the terms in $\left(\frac{m\pi}{2\ell}\right)^4$ we have

$$\left(\frac{m\pi}{2\ell}\right)^4\left(\frac{1}{\beta^2} + 1 - \frac{2}{\beta}\right)$$

which is positive for all values of $\beta > 1$. Now $\beta = \frac{E}{\eta G} = \frac{2}{\eta}(1+\nu)$ so the smallest possible value for β (taking $\eta = 1$ and $\nu = 0$) will be 2; therefore "a fortiori" the discriminant will be positive, giving real values to the frequencies.

Frequency curves can be drawn from equation (4.24). The equation is reduced to a non-dimensional form by considering a frequency parameter ψl and a parameter αl^2 which is the $(l/K)^2$ ratio for the beam. Thus in non-dimensional form the roots for equation (4.24) are obtained from

$$\psi^2 l^2 = \frac{1}{2}\left\{\left[\frac{\alpha l^2}{\beta} + \left(\frac{1+\beta}{\beta}\right)\left(\frac{m\pi}{2}\right)^2\right] \pm \sqrt{\left[\frac{\alpha l^2}{\beta} + \left(\frac{1+\beta}{\beta}\right)\left(\frac{m\pi}{2}\right)^2\right]^2 - \frac{4}{\beta}\cdot\left(\frac{m\pi}{2}\right)^4}\right\} \quad \ldots (4.25)$$

Figure (8) shows curves drawn from (4.25) for a rectangular sectioned beam where the stress distribution factor η has been taken as 5/6 and Poisson's ratio ν as 0.29; these values making $\beta = 3.097$. These curves relate the frequency parameter ψl with number of half-waves along the beam (m), for different $(\frac{L}{K})$ ratios.

For each $(\frac{L}{K})$ ratio it is clear that two separate branches to the $\psi l / m$ curve exist. As the $(\frac{L}{K})$ value decreases, the separate branches approach one another; the lower branch frequency parameter increasing and the upper branch decreasing. The upper branch is particularly sensitive to $(\frac{L}{K})$ changes, values of ψl dropping from infinity for infinitely slender beams to the inclined straight line $\psi l = \frac{m\pi}{2}$ for $(\frac{L}{K})$ zero. For the lower branch, the ψl curves range from $\psi l = 0$ for $\frac{L}{K} = \infty$ to the straight line $\psi l = \frac{\pi}{2\sqrt{\beta}} \cdot m$ for $\frac{L}{K} = 0$.

It can also be noted from the curves that the upper branch natural frequencies are considerably

higher than the corresponding frequencies of the lower branch. For example the stubby beam of $\left(\frac{L}{K}\right) = 20$, has its fundamental frequencies $(m = 1)$ for the higher and lower branch in the ratio of approximately 21:1.

The second spectrum is thus essentially a high frequency effect and as such is probably not of much importance in most cases in practice. However, with problems involving very foreshortened beams, or involving impact or transient behaviour where high harmonics are of some importance, consideration of the higher branch of the curve may be necessary. This might also be the case when considering the vibration of very large structures excited by reciprocating machinery, for then the frequency of the exciting force may be above the first few harmonics of the lower spectrum and the higher spectrum frequencies may be important.

As has been previously mentioned the second branch of frequencies does not begin until the frequency exceeds that corresponding to the condition $\psi^2 = \frac{\alpha}{\beta}$. It is of interest to calculate at what proportion higher than $\psi^2 = \frac{\alpha}{\beta} = \psi_c^2$ (hereafter called the critical frequency) the first frequency of the higher branch $({}_2\psi_1)$ occurs. This can be carried out from the equation yielding the roots of the upper branch, namely $\cos r\ell = 0$. The first root of this equation will be given by $r\ell = \frac{\pi}{2}$ where

$$r^2 = \frac{1}{2}\left\{\psi^2(1+\beta) - \sqrt{\psi^4(1-\beta)^2 + 4\alpha\psi^2}\right\}$$

Substituting $r\ell = \frac{\pi}{\ell}$ or $rL = \pi$ and reducing to non-dimensional form, an equation relating the ratio $(2\psi_1/\psi_c)$ with $(\frac{L}{K})$ for different values of β can be obtained, thus,

$$\left(\frac{L}{K}\right)^{-2} = \frac{1}{2\pi^2}\left\{\left(\frac{2\psi_1}{\psi_c}\right)^2\left(\frac{1}{\beta}+1\right) - \sqrt{\left(\frac{2\psi_1}{\psi_c}\right)^4\left(\frac{1}{\beta}-1\right) + 4\left(\frac{2\psi_1}{\psi_c}\right)^2\left(\frac{1}{\beta}\right)}\right\} \quad \ldots(4.26)$$

In Figure (9) is plotted the frequency ratio $(2\psi_1/\psi_c)$ against $(\frac{L}{K})$ for values of β of 2, 3, and 10. For normal cross-sections and materials the value is generally between 3 and 4.

The point to be noted from the graph is that for $(\frac{L}{K})$ greater than about 30, the frequency of the fundamental of the second spectrum is within 5% of the critical frequency. Therefore, for most cases the second spectrum will begin close to the value

$$f_c = \frac{1}{2\pi}\sqrt{\frac{\eta G}{\rho . K^2}} \text{ cycles/sec.} \quad \ldots(4.27)$$

The reciprocal dependence of f_c on the radius of gyration emphasises again how the higher spectrum frequencies may be of importance for large beam like structures (K large) when the frequency f_c may be of the order of the frequency of exciting forces.

4.5.2. Beam with Free-Ends

The roots of the transcendental frequency equation for the free-ended beam are not so immediately apparent as those of the pin-ended beam and some consideration will need to be given to the nature of the equations both below and above the critical

frequency.

The frequency equations (4.21) and (4.22) can be re-written in non-dimensional form as

$$\psi^2 l^2 < \frac{\alpha l^2}{\beta} \qquad \tanh ql = -\frac{ql\left(q^2l^2 + \beta.\psi^2l^2\right)}{\mu l\left(\mu^2l^2 - \beta.\psi^2l^2\right)} \cdot \tan \mu l \quad \ldots(4.28)$$

$$\psi^2 l^2 > \frac{\alpha l^2}{\beta} \qquad \tan rl = -\frac{rl\left(\beta\psi^2l^2 - r^2l^2\right)}{\mu l\left(\mu^2l^2 - \beta.\psi^2l^2\right)} \tan \mu l \quad \ldots(4.29)$$

The roots of these equations are not available by inspection, as in the case of the pin-ended beam, and resort must be made to numerical or graphical methods. For this purpose, it is desirable to have plots of the parameters μl and ql versus the frequency parameter ψl. These are easily drawn up from the equations defining μl and ql (equation (4.12)), and can be constructed for various $\left(\frac{L}{K}\right)$ ratios for any chosen value of β.

A set of these curves for $\nu = 0{\cdot}29$, $\eta = \frac{5}{6}$ are shown in Figure (10). Decreasing slenderness of the beam brings the ql zero towards the origin, for each case ql becoming zero at the value $\psi_c l$ corresponding to the critical frequency: beyond this point the imaginary values of ql are plotted below the ψl axis. At large values of ψl the ql curves become asymptotic to the ql line for $\left(\frac{L}{K}\right) = 0$. The μl curves are less affected by $\left(\frac{L}{K}\right)$ changes and all become asymptotic to $\mu l = \sqrt{\beta}.\psi l$ for large values of ψl.

With the aid of these curves, various values

of ψl can be chosen and the two sides of equation (4.28) and (4.29) can be plotted separately as functions of ψl ; the intersections of the two functions will define the natural frequencies.

Now for equation (4.28) $\tanh ql$ will necessarily be between zero and (+1) , and since the coefficient

$$\frac{ql\,(q^2l^2+\beta\psi^2l^2)}{\mu l\,(\mu^2l^2-\beta\psi^2l^2)}$$

of $\tan\mu l$ is essentially positive, there will be a root to 4.28 somewhere between $\mu l=\frac{m\pi}{2}$ and $\mu l=\frac{(m+1)\pi}{2}$ where m is an odd integer. Thus within a 2π interval of μl we expect 2 roots.

For equation (4.29) it is not possible to say how many roots can be expected in general in any interval of μl , because the answer will depend on the relative periods of rl and μl within the interval. Obviously if the period of rl is very large compared with that of μl , then we can expect about the same number of roots in an interval of μl as from equation (4.28), except in regions close to $rl=\frac{m\pi}{2}$ (m odd) where an extra root may be obtained due to the sudden change in sign of $\tan rl$. However, examination of the μl & ql versus ψl curves, shows that due to the rapid increase of rl beyond ψ_c , the rl periods are of the same order as the μl periods, and generally, in each range of π of μl , there will fall an $rl=\frac{m\pi}{2}$ value, thus providing in each range of π of μl an additional root.

Thus tentatively we can say that within a

reasonable range of μl (or frequency), equation (4.29) will provide more roots than equation (4.28). The extra roots will interrupt the normal progression of roots and will belong to the second spectrum, as was found for the pin-ended beam by a less specious argument.

4.5.3. Beam with Elastic End Supports.

The previous argument for the existence of a second frequency spectrum in the free beam frequency equation, with an obvious extension to the case when the ends are elastically supported in deflection, can also be put forward by the following method.

If the frequency equation (4.16) is modified for the region $\psi^2 > \frac{\alpha}{\beta}$ it becomes

$$(\beta\psi^2-\alpha)(\mu^2-r^2)\cos\mu l.\cos rl - \left(\frac{EA}{\lambda}\right)\mu r\left\{\mu(\mu^2-\beta\psi^2)\cos\mu l.\sin rl + r(\beta\psi^2-r^2)\sin\mu l.\cos rl\right\} = 0$$

If the products of trigonometric functions are now written as sums, this equation can be reduced to the form

$$-\sin\left[(\mu l+rl)-\Phi_1\right]+\frac{F_2}{F_1}\left\{\sin\left[(\mu l-rl)+\Phi_2\right]\right\}=0 \quad \ldots (4.30)$$

where

$$F_2=\sqrt{\left(\frac{EA}{2\lambda}\mu r\left\{\mu(\mu^2-\beta\psi^2)-r(\beta\psi^2-r^2)\right\}\right)^2+\left(\frac{1}{2}(\beta\psi^2-\alpha)(\mu^2-r^2)\right)^2}$$

and

$$F_1=\sqrt{\left(\frac{EA}{2\lambda}\mu r\left\{\mu(\mu^2-\beta\psi^2)+r(\beta\psi^2-r^2)\right\}\right)^2+\left(\frac{1}{2}(\beta\psi^2-\alpha)(\mu^2-r^2)\right)^2}$$

and Φ_1 and Φ_2 are phase angles defined by,

$$\Phi_1 = \tan^{-1}\frac{\frac{1}{2}(\beta\psi^2-\alpha)(\mu^2-r^2)}{\frac{EA}{2\lambda}\mu r\left[\mu(\mu^2-\beta\psi^2)+r(\beta\psi^2-r^2)\right]} \quad ; \quad \Phi_2 = \tan^{-1}\frac{\frac{1}{2}(\beta\psi^2-\alpha)(\mu^2-r^2)}{\frac{EA}{2\lambda}\mu r\left[\mu(\mu^2-\beta\psi^2)-r(\beta\psi^2-r^2)\right]}$$

It can be seen that $F_2 \ll F_1$ always, the values depending on the spring constant λ, while Φ_1 and Φ_2 will lie between zero and $\frac{\pi}{2}$.

For pin-ends λ is made very large so that Φ_1 and Φ_2 both tend to $\frac{\pi}{2}$ and $F_2 \to F_1$ so that in the limit, the pin end frequency equation becomes

$$-\sin\left[(\mu l+rl)-\frac{\pi}{2}\right]+\sin\left[(\mu l-rl)+\frac{\pi}{2}\right]=0 \quad \ldots(4.31)$$

Equation (4.31) can also be deduced from the equation (4.20).

For free-ends λ ismade vanishingly small and the equation is

$$-\sin(\mu l+rl)+\frac{F_2}{F_1}\sin(\mu l-rl)=0 \quad \ldots(4.32)$$

in which case

$$\frac{F_2}{F_1}=\left\{\frac{\mu(\mu^2-\beta\psi^2)-r(\beta\psi^2-r^2)}{\mu(\mu^2-\beta\psi^2)+r(\beta\psi^2-r^2)}\right\}$$

Thus from (4.31), the natural frequencies for the pin-ended beam are obtained at the intersections of two sine curves of different (and continuously varying) periods, and of equal amplitudes (if considered plotted to a base of ψ for example). From (4.32), natural frequencies for the free-ended

beam are obtained by reducing by the factor $\left(\frac{F_2}{F_1}\right)$ the amplitude of the sine wave of larger period, and by shifting the relative phase of the curves. Due consideration will show that over a reasonable interval of ψ , both these operations will leave the number of intersections within the interval unaffected. But it is already known by studying (4.31) in the form of (4.20) that the number of roots is increased when $\psi^2 > \frac{\alpha}{\beta}$ thus introducing a second spectrum of frequencies, so this must also be true for (4.32) the free beam, and similarly for equation (4.30), the elastically supported beam.

From these considerations then it can be said that the free ended beam also demonstrates the double frequency spectrum that is predicted for the pin-ended beam. This is also true for the beam with elastically supported ends.

It should be noted that what has gone before has concerned only the number of frequencies and has not said anything about the shape functions accompanying these frequencies. These would need to be evaluated separately from space function expressions.

5. THE SOLUTION OF THE EQUATION WHICH INCLUDES LATERAL MOTION

5.1. Derivation of the Boundary Conditions.

5.1.1. Introductory The solution to the equation (3.37) which includes the effects of rotatory inertia, shear, and an independent lateral motion will now be considered. In this case, three quantities or end conditions must be specified for each end of the beam. The plane ends of the beam being assumed parallel to the YZ plane, the boundary conditions at these ends from equations (3.3) reduce to

$$\sigma_x = \bar{X} \quad ; \quad \tau_{xy} = \bar{Y} \quad ; \quad \tau_{xz} = \bar{Z} \qquad \ldots(5.1)$$

since the direction-cosines of the external normal on the Y and Z directions are zero.

The solution to the differential equation (3.37) will be found to have six arbitrary constants so that three conditions at either end will be needed to define them.

The equations representing the various end conditions can now be drawn up from the equilibrium equations after the manner of section 4.1.

5.1.2 Zero Lateral Shear Force Along Beam.

Firstly it can be observed that for purely z-wise bending vibrations there should be no nett lateral (Y-wise) shear force at any cross section of the beam.

This can be represented symbolically as

$$\iint_R \tau_{xy}\,dy\,dz = 0 \qquad \ldots(5.2)$$

for all relevant values of x.

Substitution of the assumed displacements (3.30) in (5.2) gives

$$\frac{\partial f(x,t)}{\partial x}\iint_R yz\,dy\,dz = 0$$

or

$$I_{yz} = 0 \qquad \ldots(5.3)$$

where I_{yz} is the product of inertia of the cross section, and since sections with symmetry about at least one axis are considered in this theory, the condition (5.3) and hence (5.2) will always be satisfied.

5.1.3. Transverse Shear Force in terms of Displacement.

By definition the shear force over any cross section of the beam is given by

$$Q = \int_z \tau_{xz}\,b\,dz \qquad \ldots(5.4)$$

which is the simplified form of $Q = \iint_R \tau_{xz}\,dy\,dz$ when it is assumed that τ_{xz} is not a function of y and that the section width b varies little with z.

The integral of (5.4) appears in the modified form of the first equilibrium equation of section 3.7 giving,

$$Q = \int_z \tau_{xz}\,b\,dz = \int_z \frac{\partial \sigma_x}{\partial x}\,bz\,dz + \int_z \frac{\partial \tau_{xy}}{\partial y}\,bz\,dz - \rho\int_z \frac{\partial^2 u}{\partial t^2}\,bz\,dz \qquad \ldots(5.5)$$

If the relevant displacement components (3.30) are substituted in (5.5) and the operator $\frac{\partial^2}{\partial t^2}$ replaced by $-p^2$ (p the circular frequency), (5.5) becomes

$$Q = -EI_y \frac{\partial^2 \phi}{\partial x^2} - \rho p^2 I_y \phi + GI_y \frac{\partial f}{\partial x} \qquad \ldots(5.6)$$

The third equilibrium equation (3.31) gives

$$\frac{\partial Q}{\partial x} = -\rho A p^2 w - GA\, f(x) \qquad \ldots(5.7)$$

while by definition

$$\left(\frac{\partial w}{\partial x} - \phi\right) = \frac{Q}{\eta AG}$$

Eliminating ϕ , (5.6) reduces to the form

$$\left.\begin{aligned} Q\left(1 - \frac{\rho p^2 I_y}{\eta AG}\right) = -EI_y \frac{\partial^3 w}{\partial x^3} - EI_y \frac{\rho p^2}{G}\left[\frac{1}{\eta} + \frac{G}{E}\right]\frac{\partial w}{\partial x} \\ + \frac{\partial f}{\partial x}\left[GI_y - \frac{EI_y}{\eta}\right] \end{aligned}\right\} \ldots(5.8)$$

To eliminate the term in $\left(\frac{\partial f}{\partial x}\right)$ from (5.8) recourse is made to the equations (3.34) and (3.35) from which can be deduced the result

$$f(x)\left[2GA - \rho p^2 I_y\left(1 - \frac{E}{\eta G} + \frac{1}{\eta}\right) - \frac{EA}{\eta}\right] = EI_y \frac{\partial^4 w}{\partial x^4}$$

$$+ \frac{\partial^2 w}{\partial x^2} p^2 \rho \frac{EI_y}{G}\left[\frac{1}{\eta} + \frac{G}{E}\right] + w\left[\frac{p^4 \rho^2 I_y}{\eta G} - p^2 \rho A\right]$$

$\ldots(5.9)$

(5.9) can be differentiated and substituted in (5.8) to give the complete expression for shear force at any point along the length of the beam.

5.1.4. Bending Moment in Terms of Displacement.

By definition the bending moment at any cross section of the beam is given by

$$M = \int_z \sigma_x . b.z\, dz \qquad \ldots(5.10)$$

Using the assumed displacement form for u (equation (3.30)), (5.10) becomes

$$M = -E \int_z \frac{\partial \phi}{\partial x} z^2 b\, dz \qquad \ldots(5.11)$$

From the final equilibrium equation (3.32) or from (3.33) directly,

$$\frac{\partial \phi}{\partial x} = \frac{\partial^2 w}{\partial x^2} + \frac{f(x)}{\eta} + \frac{\rho b^2}{\eta G} . w$$

and the expression for $f(x)$ is available from equation (5.9). Substituting these results in (5.11) gives the final result,

$$M = -EI_y \left\{ \frac{\partial^2 w}{\partial x^2} + \frac{b^2 \rho}{\eta G} . w + \frac{1/\eta}{\left\{ 2GA - \rho b^2 I_y \left(1 - \frac{E}{\eta G} + \frac{1}{\eta} \right) - \frac{EA}{\eta} \right\}} \left[EI_y \frac{\partial^4 w}{\partial x^4} \right.\right.$$

$$\left.\left. + \frac{\partial^2 w}{\partial x^2} . b^2 \rho \frac{EI_y}{G} \left(\frac{1}{\eta} + \frac{G}{E} \right) + w \left(\frac{b^4 \rho^2 I_y}{\eta G} - b^2 \rho A \right) \right] \right\} \qquad \ldots(5.12)$$

5.1.5. Lateral Shear Stress τ_{xy}.

Since this stress does not appear in the derivation of the Timoshenko equation there is no boundary condition referring to it and here we are left with a certain arbitrariness as to what should be considered suitable end conditions for τ_{xy} for each of the standard types of beam.

Apparently it is suitable for a free end to put the condition $\tau_{xy} = 0$ which should be exactly true since there are no external forces.

For pinned-ends, the end can be imagined constrained to maintain its undistorted shape so that v is zero and also so that $(\partial\tau_{xy}/\partial x)$ is zero which implies zero curvature of v at the ends. These also seem reasonable conditions for a fixed end.

5.1.6 Standard End Conditions.

The standard end conditions are thus defined as

Pinned End:- $w = 0$; σ_x or $M = 0$; $\frac{\partial \tau_{xy}}{\partial x}$ and $v = 0$

Fixed End:- $w = 0$; $\phi = 0$; $\frac{\partial \tau_{xy}}{\partial x}$ and $v = 0$

Free End:- σ_x or $M = 0$; τ_{xz} or $Q = 0$; $\tau_{xy} = 0$

The above equations are all contained in the equations following

Displacement Zero $$w = 0$$

Bending Slope Zero $$\left(\frac{EI_y}{\eta AG}\right)\frac{\partial^3 w}{\partial x^3} + \frac{\partial w}{\partial x}\left(1 + \frac{EI_y \rho b^2}{\eta^2 AG^2}\right) = 0$$

Bending Moment or σ_x Zero

$$\frac{\partial^2 w}{\partial x^2} + \frac{\rho b^2}{\eta G} w + \frac{1/\eta}{\left\{2GA - \rho b^2 I_y\left(1 - \frac{E}{\eta G} + \frac{1}{\eta}\right) - \frac{EA}{\eta}\right\}}\left[EI_y\frac{\partial^4 w}{\partial x^4} + \frac{\partial^2 w}{\partial x^2} b^2 \rho \cdot \frac{EI_y}{G}\left(\frac{1}{\eta} + \frac{G}{E}\right) + w\left(\frac{b^4 \rho^2 I_y}{\eta G} - b^2 \rho A\right)\right] = 0$$

Shear Force or τ_{xz} Zero

(if τ_{xy} zero also) $$\frac{\partial^3 w}{\partial x^3} + \frac{\rho b^2}{G}\left[\frac{1}{\eta} + \frac{G}{E}\right]\frac{\partial w}{\partial x} = 0$$

τ_{xy} Zero

$$EI_y\frac{\partial^5 w}{\partial x^5} + \frac{\partial^3 w}{\partial x^3} EI_y \frac{b^2 \rho}{G}\left[\frac{1}{\eta} + \frac{G}{E}\right] - b^2 \rho A \cdot \left[1 - \frac{b^2 \rho I_y}{\eta GA}\right]\frac{\partial w}{\partial x} = 0$$

The last equation differentiated with respect to x gives the condition for $(\partial\tau_{xy}/\partial x)$ zero.

When v is zero the latter part of the condition

for σ_x zero disappears.

5.2. Solving the Equation.

The differential equation for which a solution is sought is

$$EI_y \frac{\partial^6 w}{\partial x^6} - \frac{\partial^6 w}{\partial x^4 \partial t^2}\left(\frac{EI_y\rho}{\eta G} + \rho I_y + \frac{EI_y\rho}{G}\right) + \frac{\partial^6 w}{\partial x^2 \partial t^4}\left(\frac{EI\rho^2}{\eta G^2} + \frac{\rho^2 I_y}{G} + \frac{\rho^2 I_y}{\eta G}\right)$$

$$- EA\frac{\partial^4 w}{\partial x^4} + \frac{\partial^2 w}{\partial x^2 \partial t^2}\left(2\rho A + \frac{EA\rho}{\eta G}\right) - \frac{\rho A^2}{I_y}\cdot\frac{\partial^2 w}{\partial t^2} - \frac{\partial^4 w}{\partial t^4}\left(\frac{\rho^2 A}{G} + \frac{\rho^2 A}{\eta G}\right)$$

$$- \frac{\rho^3 I_y}{\eta G^2}\cdot\frac{\partial^6 w}{\partial t^6} = 0$$

Assuming a displacement harmonic with respect to time and of circular frequency p, the displacement can be taken in the form

$$w(x,t) = W(x).\cos pt.$$

Again making the substitutions of (4.9)

$$\left.\begin{aligned} \psi^2 &= \frac{p^2\rho}{E} \\ \alpha &= \frac{1}{k^2} \\ \beta &= \frac{E}{\eta G} \\ \delta &= \frac{E}{G} \end{aligned}\right\} \qquad \ldots(5.13)$$

and assuming exponential solutions of the type $A_i e^{\lambda x}$, and writing $\xi = \lambda^2$, the auxiliary equation for the differential equation becomes,

$$\xi^3 + \xi^2\left\{\psi^2(1+\beta+\delta) - \alpha\right\} + \xi\left\{\psi^4(\beta+\delta+\beta\delta) - \psi^2(2\alpha+\alpha\beta)\right\}$$

$$+ \left\{\psi^6\beta\delta - \psi^4(\alpha\delta+\alpha\beta) + \psi^2\alpha^2\right\} = 0 \qquad \ldots(5.14)$$

The three roots of this cubic in λ^2 will define the shape function $W(x)$. Equation (5.14) can, however, be factorised to give

$$\left[\xi - (\alpha - \psi^2\delta)\right]\left[\xi^2 + \psi^2(1+\beta)\xi - \psi^2(\alpha - \psi^2\beta)\right] = 0 \qquad \ldots(5.15)$$

The quadratic factor of (5.15) can be seen to be the auxiliary equation for the Timoshenko shape function (see equation (4.10)), which implies that two of the roots to (5.14) are the μ and q roots of the Timoshenko equation, as defined in (4.12), while the third root comes from the linear factor of (5.15).

Thus the shape function $W(x)$ can be written as follows,

$$W(x) = A_1\sin\mu x + A_2\cos\mu x + A_3\sinh qx + A_4\cosh qx + A_5\sinh cx + A_6\cosh cx$$
$$\text{for} \quad 0 < \psi^2 < \frac{\alpha}{\beta}$$

$$W(x) = A_1\sin\mu x + A_2\cos\mu x + A_3\sin rx + A_4\cos rx + A_5\sinh cx + A_6\cosh cx$$
$$\text{for} \quad \frac{\alpha}{\beta} < \psi^2 < \frac{\alpha}{\delta} \qquad \ldots(5.16)$$

$$W(x) = A_1\sin\mu x + A_2\cos\mu x + A_3\sin rx + A_4\cos rx + A_5\sin gx + A_6\cos gx$$
$$\text{for} \quad \psi^2 > \frac{\alpha}{\delta}$$

where,

$$\left.\begin{aligned} 2\mu^2 &= \psi^2(1+\beta) + \sqrt{\left[\psi^4(1-\beta)^2 + 4\alpha\psi^2\right]} \\ 2q^2 &= -\psi^2(1+\beta) + \sqrt{\left[\psi^4(1-\beta)^2 + 4\alpha\psi^2\right]} \\ 2c^2 &= 2(\alpha - \psi^2\delta) \end{aligned}\right\} \qquad \ldots(5.17)$$

and,

$$r^2 = -q^2 \qquad ; \qquad g^2 = -c^2 \qquad \ldots(5.18)$$

and it has been assumed that η is less than unity so that $\frac{\alpha}{\beta} < \frac{\alpha}{\delta}$.

5.3. Frequency Equations for Free Beam and Pin-Ended Beam.

5.3.1 Free Beam.

The symmetric modes of a free beam obeying the differential equation (3.37) will now be considered.

No generality is lost by considering resonant frequencies for which $\psi^2 > \frac{\alpha}{\delta}$, for which the shape function from (5.16) is

$$W(x) = A_1 \sin\mu x + A_2 \cos\mu x + A_3 \sin rx + A_4 \cos rx + A_5 \sin gx + A_6 \cos gx$$

If the origin of co-ordinates is taken at the centre of the beam then for symmetric modes, only even functions of x can appear in the shape function, which, rewriting the constants, will become

$$W(x) = A_1 \cos\mu x + A_2 \cos rx + A_3 \cos gx \qquad \ldots(5.19)$$

Alternatively this could have been shown by considering the central $(x=0)$ boundary conditions of zero total slope, zero transverse shear force, and zero lateral shear, which are necessary by conditions of symmetry. These lead to conditions $\left(\frac{\partial w}{\partial x}\right)_{x=0} = \left(\frac{\partial^3 w}{\partial x^3}\right)_{x=0} = \left(\frac{\partial^5 w}{\partial x^5}\right)_{x=0} = 0$ which in turn eliminate the odd functions of x from the shape function.

At $x = l$ the boundary conditions are Bending Moment Zero, Shear Force Zero, Lateral Shear Stress Zero.

From the boundary condition equations of section 5.1.6 these can be expressed in turn by,

$$\left.\begin{aligned}
&\left\{\frac{d^2W}{dx^2}+\psi^2\beta W+\Gamma\left(\frac{d^4W}{dx^4}+\psi^2(1+\beta)\frac{d^2W}{dx^2}-\psi^2(\alpha-\psi^2\beta)W\right)\right\}_{x=\ell}=0\\
&\left\{\frac{d^3W}{dx^3}+\psi^2(1+\beta)\frac{dW}{dx}\right\}_{x=\ell}=0\\
&\left\{\frac{d^5W}{dx^5}+\psi^2(1+\beta)\frac{d^3W}{dx^3}-\psi^2(\alpha-\psi^2\beta)\frac{dW}{dx}\right\}_{x=\ell}=0
\end{aligned}\right\}\quad\ldots(5.20)$$

where

$$\Gamma=\frac{1}{\eta}\left\{2\frac{\alpha}{\delta}-\psi^2\left(1-\beta+\frac{1}{\eta}\right)-\frac{\alpha}{\eta}\right\}^{-1}\qquad\ldots(5.21)$$

The shape function (equation (5.19)) is now substituted in the equations (5.20). It is evident that since μ and r have been derived from the Timoshenko equation, and since that equation appears, (multiplied by the factor Γ), in the first equation of (5.20), and (differentiated) in the third; then these two parts of (5.20) will remain non-zero for only the $\cos gx$ part of the shape function.

Thus equations (5.20) become

$$\left.\begin{aligned}
&A_1(\psi^2\beta-\mu^2)\cos\mu\ell+A_2(\psi^2\beta-r^2)\cos r\ell+A_3\Theta(g)\cos g\ell=0\\
&A_1\left[\mu^3-\mu\psi^2(1+\beta)\right]\sin\mu\ell+A_2\left[r^3-r\psi^2(1+\beta)\right]\sin r\ell\\
&\qquad\qquad+A_3\left[g^3-g\psi^2(1+\beta)\right]\sin g\ell=0\\
&A_1(0)+A_2(0)+A_3\left[-g^5+g^3\psi^2(1+\beta)+g\psi^2(\alpha-\psi^2\beta)\right]\sin g\ell=0
\end{aligned}\right\}\quad\ldots(5.22)$$

where

$$\Theta(g)=\left\{\psi^2\beta-g^2+\Gamma\left(g^4-\psi^2(1+\beta)g^2-\psi^2(\alpha-\psi^2\beta)\right)\right\}\qquad\ldots(5.23)$$

Setting the determinant of (5.22) equal to zero gives the frequency equation

$$\begin{vmatrix} (\psi^2\beta-\mu^2)\cos\mu l & (\psi^2\beta-r^2)\cos rl & \Theta(g)\cos gl \\ -\mu r^2.\sin\mu l & -r\mu^2\sin rl & [g^3-g\psi^2(1+\beta)]\sin gl \\ 0 & 0 & [-g^5+g^3\psi^2(1+\beta)+g\psi^2(\alpha-\psi^2\beta)]\sin gl \end{vmatrix} = 0 \quad \ldots(5.24)$$

where the relations between μ^2 and r^2 of equation (4.13) have been used.

The expansion of (5.24) gives the frequency equation

$$[-g^5+g^3\psi^2(1+\beta)+g\psi^2(\alpha-\psi^2\beta)]\sin gl\left\{(\psi^2\beta-\mu^2)(-r\mu^2)\sin rl.\cos\mu l + (\psi^2\beta-r^2)\mu r^2\sin\mu l.\cos rl\right\} = 0 \quad \ldots(5.25)$$

Thus, either

$$\left\{-\mu^2 r(\psi^2\beta-\mu^2)\sin rl.\cos\mu l + \mu r^2(\psi^2\beta-r^2)\sin\mu l.\cos rl\right\} = 0 \quad \ldots(5.26)$$

or

$$\sin gl = 0 \quad \ldots(5.27)$$

Equation (5.26) is the frequency equation for a free-ended Timoshenko beam (c.f. equation (4.22)), while (5.27) defines a new set of natural frequencies.

5.3.2 Pin-Ended Beam.

Again the co-ordinate origin is taken at the centre of the beam so that the shape function for symmetric modes is

$$W(x) = A_1\cos\mu x + A_2\cos rx + A_3\cos gx \quad \ldots(5.28)$$

The boundary condition equations can be obtained from

section 5.1.6. The assumption that the ends retain their shape so that v is zero simplifies the equation for bending moment as derived in 5.1.4 and the boundary equations are,

$$\left.\begin{aligned} &\text{Displacement Zero} && [W]_{x=l} = 0 \\ &\text{Bending Moment Zero} && \left[\frac{d^2W}{dx^2} + \psi^2\beta.W\right]_{x=l} = 0 \\ &\left(\frac{\partial \tau_{xy}}{\partial x}\right) \text{ Zero}, && \left[\frac{d^6W}{dx^6} + \psi^2(1+\beta)\frac{d^4W}{dx^4} - \psi^2(\alpha - \psi^2\beta)\frac{d^2W}{dx^2}\right]_{x=l} = 0 \end{aligned}\right\} \quad \ldots(5.29)$$

Substituting (5.28) in (5.29) leads to the set of equations

$$\left.\begin{aligned} &A_1\cos\mu l + A_2\cos r l + A_3\cos g l = 0 \\ &A_1(\psi^2\beta - \mu^2)\cos\mu l + A_2(\psi^2\beta - r^2)\cos r l + A_3(\psi^2\beta - g^2)\cos g l = 0 \\ &A_1(0) + A_2(0) + A_3\left[-g^6 + g^4\psi^2(1+\beta) + \psi^2 g^2(\alpha - \psi^2\beta)\right]\cos g l = 0 \end{aligned}\right\} \quad \ldots(5.30)$$

Expanding the determinant of (5.30) the frequency equation is obtained in the form

$$\left[-g^6 + g^4\psi^2(1+\beta) + \psi^2 g^2(\alpha - \psi^2\beta)\right] \times \cos g l \cos\mu l \cos r l \left[(\psi^2\beta - \mu^2) - (\psi^2\beta - r^2)\right] = 0 \quad \ldots(5.31)$$

Thus either

$$\cos\mu l = 0$$

or

$$\cos r l = 0 \quad \ldots(5.32)$$

or

$$\cos g l = 0$$

The first two equations of (5.32) define the

natural frequencies for a pinned Timoshenko beam, while the third equation defines a new spectrum of frequencies.

5.4. Notes on the Differential Equation and the Frequency Equations.

5.4.1 The Differential Equation The close relation of the differential equation (3.37) with the Timoshenko equation (3.16) is interesting and is a consequence of the assumed displacement forms. For, examining the integrated equilibrium equations (3.32) it is apparent that with $f(x,t)$ taken as zero they reduce to the equilibrium equations for the Timoshenko equation, so that one solution of system (3.32) is $f(x,t)$ (or v) $= 0$, and the Timoshenko equation. This can also be seen from the equation (3.36).

The stresses τ_{xy} and τ_{yz} are not contributed to by the displacements u or w so that a solution with zero v is possible. When either w or u contribute to τ_{xy} or τ_{yz} it will no longer be possible to have v zero. This can be seen from the set of equilibrium equations (3.39) for the case when w contributes to τ_{yz} through the medium of the anti-clastic curvature. The Timoshenko equation will therefore not be a solution to the system (3.39).

5.4.2 The "Critical" Frequencies.

There are now two "critical" frequencies. There is the one which appeared in the solution to the Timoshenko equation in section 4, defined from

$$\psi^2 = \frac{\alpha}{\beta} \qquad \ldots(5.33)$$

and there is the critical frequency for the third spectrum defined from

$$\psi^2 = \frac{\alpha}{\delta} \qquad \ldots(5.34)$$

The second spectrum begins above the frequency defined in (5.33), while the third one begins above the frequency defined in (5.34). Since $\delta = \frac{E}{G} = \eta.\beta$ and since η is generally less than unity, the second critical frequency (5.34) will be higher than the first (5.33). It does not necessarily follow that the fundamental of the third spectrum is at higher frequency than the fundamental of the second spectrum, although this will be true for most cases (see section 5.4.3).

5.4.3. The Frequency Equation for the Pin-Ended Beam.

The frequency equation in this case is

$$\cos\mu l . \cos rl . \cos gl = 0$$

The cases for $\cos\mu l$ or $\cos rl$ zero are discussed in section 4.5. The third spectrum of frequencies is defined by the final factor

$$\cos gl = 0 \qquad \ldots(5.35)$$

This is satisfied if

$$gl = \frac{m\pi}{2} \quad (m \text{ odd.}) \qquad \ldots(5.36)$$

while from (5.17) and (5.18) $g = (\psi^2\delta - \alpha)^{1/2}$ so that condition (5.36) can be reduced to the form,

$$\psi l = \sqrt{\frac{m^2\pi^2 + (L/K)^2}{8(1+\nu)}} \qquad \ldots(5.37)$$

Equation (5.37) defines the symmetric natural frequencies of the third spectrum for a given $\left(\frac{L}{K}\right)$ and Poisson's Ratio (ν) .

It is of interest to see by how much the fundamental $(m=1)$ of (5.37) exceeds the lower critical frequency (5.33).

The ratio between these frequencies is

$$\left(\frac{{}_3\psi_1}{\psi_c}\right) = \sqrt{\frac{\pi^2 + (L/K)^2}{\eta (L/K)^2}} \qquad \ldots(5.38)$$

where ${}_3\psi_1$ is the third spectrum fundamental and $\psi_c^2 = \frac{\alpha}{\beta}$. Equation (5.38) is plotted on Fig. (9) for $\eta = \frac{5}{6}$ along with the ratio $\left({}_2\psi_1/\psi_c\right)$ of section 4.5.1. It can be seen from the figure that for a β value of 3, the fundamental of the third spectrum is at higher frequency than the fundamental of the second spectrum for $\left(\frac{L}{K}\right)$ greater than 12.

The shape function for the pin-ended beam at resonance in the third spectrum can be found from the equation (5.30) relating the constants A_1 , A_2 , and A_3. Equation (5.30) shows that for $\cos\gamma l$ zero, A_1 and A_2 must be zero so that the shape function reduces to

$$W(x) = A_3 \cos\gamma l\left(\frac{x}{l}\right) \qquad \ldots(5.39)$$

It can be noted that for $\psi^2 < \frac{\alpha}{\delta}$, $\cos\gamma l$ becomes $\cosh\gamma l$ and since $\cosh\gamma l$ is always non-zero, A_3 must always be zero to satisfy the final equation of (5.30).

For resonance in either of the other two spectra

$\cos gl$ will not be zero so A_3 must be zero by (5.30) and the shapes reduce to the appropriate functions as found for the Timoshenko equation.

Thus by (5.39) the m of (5.37) defines the shape function in terms of number of half-waves along the beam's length. Fig.(11) shows the curves of ψl against m for various $(\frac{L}{K})$ values for $\eta = \frac{5}{6}$ and $\nu = 0.29$. The curves of the other Spectra are shown for comparison. Beyond a certain nodal pattern, the third spectrum frequencies appear to be lower than the corresponding second spectrum frequencies: the nodal pattern where the two curves cross becoming of higher order as the $(\frac{L}{K})$ ratio is increased.

It can also be noted that, in the range shown, the third spectrum lines converge slightly towards their respective first spectrum lines, while those of the second spectrum diverge from them.

5.4.4 The Frequency Equation for the Free-Ended beam.

The frequency equation for the free beam is given in section 5.3.1. For the Timoshenko frequencies where $\sin gl$ is not zero, A_3 must be zero by equations (5.22) and the complete Timoshenko solution both in frequency and shape function follows. This solution has been treated in section 4.

The third spectrum frequencies are defined by

$$\sin gl = 0$$

or using the definition of g from (5.17) and (5.18) this can be written

$$\psi l = \sqrt{\frac{4m^2\pi^2 + \left(\frac{L}{K}\right)^2}{8(1+\nu)}} \qquad (m = 1,2,3,\ldots) \qquad \ldots(5.40)$$

Equation (5.40) defines the symmetric natural frequencies of the third spectrum for any given $\left(\frac{L}{K}\right)$ and (ν) values.

The shape function at resonance can be obtained from equations (5.22). Expressing the constants in terms of A_1

$$W(x) = A_1\left\{\cos\mu l\left(\frac{x}{l}\right) - \left(\frac{r\sin\mu l}{\mu\sin rl}\right)\cos rl\left(\frac{x}{l}\right)\right.$$

$$\left. - \frac{\left[(\psi^2\beta - \mu^2)\cos\mu l - (\psi^2\beta - r^2)\cos rl.\frac{r\sin\mu l}{\mu\sin rl}\right]}{\Theta(g).\cos gl}\cos gl\left(\frac{x}{l}\right)\right\} \qquad \ldots(5.41)$$

where $\Theta(g)$ is defined in equation (5.23). The shape function would require to be evaluated in each case for it is not possible to predict the shape by examination of (5.41) as it stands.

When the frequency is less than the third spectrum critical frequency, $\sin gl$ becomes $\sinh cl$ and by (5.22) A_3 is necessarily zero. There is thus no gl component in the shape function except during a resonance defined by $\sin gl = 0$.

6. SOLUTION TO FREE BEAM FREQUENCY EQUATIONS

6.1. Timoshenko Free Beam.

6.1.1 General. Solutions of the frequency equation for the Timoshenko free-beam will be examined especially in the neighbourhood of the critical frequency $\psi^2 = \frac{\alpha}{\beta}$.

Different frequency curves are obtained for each pair of values of $\left(\frac{L}{K}\right)$ and β . In each case plots are made with abscissa the frequency proportional factor ψl .

For $\psi^2 l^2 < \frac{\alpha l^2}{\beta}$ the two functions $\tanh ql$ and $-k'\tan \mu l$ are plotted while for $\psi^2 l^2 > \frac{\alpha l^2}{\beta}$, $\tan rl$ and $-k'\tan \mu l$ are plotted. Where

$$k = \frac{ql\left(q^2l^2 + \beta\psi^2 l^2\right)}{\mu l\left(\mu^2 l^2 - \beta\psi^2 l^2\right)} \; ; \; k' = \frac{rl\left(\beta\psi^2 l^2 - r^2 l^2\right)}{\mu l\left(\mu^2 l^2 - \beta\psi^2 l^2\right)} \qquad \ldots(6.1)$$

6.1.2 $\left(\frac{L}{K}\right) = 20$. As a typical case, the resonances around ψ_c for $\frac{L}{K} = 20$ will be examined. Fig. 12 , shows the frequency equation curves in the neighbourhood of the critical frequency $\psi_c^2 = \frac{\alpha}{\beta}$ for $\beta = 3{\cdot}097$. The line of $-k'\tan \mu l$ can be seen to intercept $\tanh ql$ at point A not far above the value of ψl corresponding to $\mu l = 3\frac{1}{2}\pi$. At ψ_c both curves reduce to zero.

The next natural frequency is at the point B shortly above $\mu l = 4\pi$ and below $rl = \pi$. Further frequencies occur just above $\mu l = 4\frac{1}{2}\pi$ and just above $\mu l = 5\pi$. These figures show that resonances

are occurring more frequently above ψ_c than below where resonances above each $\frac{m\pi}{2}$ (m odd) of μl were the only ones encountered.

In order to plot curves of frequency against some shape criterion such as the number of nodes, the shape functions corresponding to the resonances must be evaluated.

6.1.3. Note on the Shape Functions. If the origin of the x-co-ordinate is taken at the centre of the beam and symmetric modes only are considered the shape function becomes

$$\left.\begin{aligned} W(x) &\propto \left\{ ql \sin \mu l \cosh ql \left(\frac{x}{l}\right) - \mu l \sinh ql \cos \mu l \left(\frac{x}{l}\right)\right\} \\ &\qquad \psi^2 l^2 < \frac{\alpha l^2}{\beta} \\ \text{and} \\ W(x) &\propto \left\{ rl \sin \mu l . \cos rl \left(\frac{x}{l}\right) - \mu l . \sin rl . \cos \mu l \left(\frac{x}{l}\right)\right\} \\ &\qquad \psi^2 l^2 > \frac{\alpha l^2}{\beta} \end{aligned}\right\} \qquad \ldots(6.2)$$

The shapes for each resonance need to be calculated from these equations. For the second equation the shape comprises two components of different periods; the $\cos \mu l \left(\frac{x}{l}\right)$ term providng more half waves along the length of the beam than the $\cos rl \left(\frac{x}{l}\right)$ term, since $\mu l > rl$. For any resonance for which the amplitude of the higher frequency (in terms of distance not time) component (μl) is greater than that of the lower (rl) one, the shape corresponding to the higher one will predominate. Therefore for resonances where $\mu l \sin rl > rl \sin \mu l$ the number of half waves along the semi-beam will usually correspond with the number of half waves in μl at that particular resonant

frequency. (The term "half-wave" is used loosely here to refer to any shape between adjacent nodes).

Consider for example the case treated in the previous section. Resonance A occurs just above $\mu l = 3\frac{1}{2}\pi$ and the shape function displays just over $3\frac{1}{2}$ half-waves in one half length of the beam, i.e. 8 nodes over the whole length. Similarly resonance B occurs above $\mu l = 4\pi$ and the shape function has just over 4 half-waves in one half length and there are still 8 nodes on the beam at this higher frequency.

From this example it is obvious that the frequency/shape pattern is different from that of the pin-ended beam. For the pinned beam there are two distinct spectra of frequencies corresponding to two distinct sets of roots of the frequency equation, and the first root of the higher spectrum starts at the lowest nodal shape. Two frequencies with the same number of half-waves in their shape are widely separated.

For the free-beam there are not the two distinct spectra in as much as the frequency equation cannot be divided into two separate parts either of which may be zero. However, there is the equivalent of the two spectra because of the increase in the number of frequencies above ψ_c . The extra roots have shape patterns corresponding with their neighbouring roots so that similar shapes are near to each other in frequency.

A frequency/shape curve for $\frac{L}{K} = 20$ is shown in Fig. 13 and shows the increase in the number of resonances above ψ_c .

6.1.4. $\frac{L}{K} = 30.$

Frequency curves are also drawn up for $\frac{L}{K} = 30$, $\nu = 0.32$. The roots immediately above ψ_c are illustrated in Fig. 14, and the curves follow a similar pattern to those of Fig. 12. for $\frac{L}{K} = 20$.

However, if the curves are inspected it will be seen that the ψl corresponding to $5\frac{1}{2}\pi$ of μl occurs before the ψl corresponding to $\frac{\pi}{2}$ of $r l$. Therefore the first resonance above ψ_c must necessarily fall at a value of ψl for which μl exceeds $5\frac{1}{2}\pi$. Now the resonance just below ψ_c occurs just above $\mu l = 4\frac{1}{2}\pi$ so unlike the $\frac{L}{K} = 20$ case, the first resonance above ψ_c will have a different shape from the last resonance before ψ_c. Furthermore, the figure shows that there are three roots existing in the interval $5\frac{1}{2}\pi < \mu l < 6\frac{1}{2}\pi$ i.e. there are three roots with the same number of nodes in their shape.

It was also found that the interval $7\frac{1}{2}\pi < \mu l < 8\frac{1}{2}\pi$ is entirely contained within the interval $2\frac{1}{2}\pi < r l < 3\frac{1}{2}\pi$ so that only one root occurs for which the shape function contains 15 complete half-waves on the length L of the beam.

These features are shown in the frequency/shape curve of Fig. 15. This plot can no longer exist as a set of discrete points making up a smooth curve but has steps and isolated points above ψ_c.

6.1.5. $\frac{L}{K} = 29.4$

For $\frac{L}{K} = 29.4$ and $\beta = 3.097$; $r l = \frac{\pi}{2}$ occurs at lower ψl than $\mu l = 5\frac{1}{2}\pi$ (in contradistinction to

the $\frac{L}{K} = 30$ case). The first resonance above ψ_c will therefore lie below $\mu l = 5\frac{1}{2}\pi$ and will have the same number of complete half-waves (viz. 9) as the last resonance occurring before ψ_c . Again only one resonant frequency has the 15 complete half-waves or 16 node configuration.

The resulting frequency/shape curves are shown in Fig. 16 . They are similar to those for $\frac{L}{K} = 30$ but the lowest frequency for 12 nodes has been shifted down to 10 nodes, corresponding to the shape of the highest resonance before ψ_c .

The virtually straight line which connects the resonant frequencies before ψ_c is not continued above ψ_c ; the dotted straight line drawn in to join frequencies below and above ψ_c being at an angle to the lower line.

6.2. The Influence of Elastic End Supports.

6.2.1. Effect on Resonant Frequencies.

The frequency equation (4.16) for the symmetric nodes of a beam with spring end supports can be written in non-dimensional form as

$$\left.\begin{aligned} &\psi^2 l^2 < \frac{\alpha}{\beta} l^2 \\ &\tanh ql = \frac{4(\alpha l^2 - \beta\psi^2 l^2)(\mu^2 l^2 + q^2 l^2)}{\left(\frac{EI_r}{\lambda l^3}\right)\left(\frac{L}{K}\right)^2 \mu^2 l^2 . ql\,(\mu^2 l^2 - \beta\psi^2 l^2)} - \frac{ql\,(q^2 l^2 + \beta\psi^2 l^2)}{\mu l\,(\mu^2 l^2 - \beta\psi^2 l^2)} \tan \mu l \\ &\psi^2 l^2 > \frac{\alpha}{\beta} l^2 \\ &\tan rl = \frac{4(\beta\psi^2 l^2 - \alpha l^2)(\mu^2 l^2 - r^2 l^2)}{\left(\frac{EI_r}{\lambda l^3}\right)\left(\frac{L}{K}\right)^2 \mu^2 l^2 . rl . (\mu^2 l^2 - \beta\psi^2 l^2)} - \frac{rl\,(\beta\psi^2 l^2 - r^2 l^2)}{\mu l\,(\mu^2 l^2 - \beta\psi^2 l^2)} \tan \mu l \end{aligned}\right\} \quad \ldots(6.3)$$

Without the first term on the right-hand side of (6.3), each frequency equation is the same as the free-beam equation; so the first term is a factor to be added to $-K\tan\mu l$ (or $-K'\tan\mu l$ as the case may be). (See equation (6.1)). The natural frequencies may thus be obtained from the curves for the free case, by increasing the ordinate of the $-K\tan\mu l$ curve by a factor obtainable from the equation (6.3). Inspection shows that this factor is always positive so its addition to the $-K\tan\mu l$ curve will represent a bodily lifting of this curve plus some distortion of it, due to the variation of the factor with ψl .

For a chosen $\frac{L}{K}$ value, the size of the factor depends on the ratio $(EI_y/\lambda l^3)$; a larger spring constant making for a larger factor and thus increasing further the natural frequencies as read off from the curves.

When values corresponding to the rectangular experimental beams are considered, the factor turns out to be very small. Natural frequencies above the fundamental are virtually unaffected, which justifies referring to the beams as free at the higher modes.

6.2.2. Resonant Shape Function.

The shape function at resonance for the symmetric modes of the elastically supported beam can be calculated. For $\psi^2 > \alpha/\beta$ it takes the form

$$W(x) \propto \left[\cos\mu l\left(\frac{x}{l}\right) - \left\{\frac{\left(\frac{1-\psi^2\beta/\alpha}{EI_y/\lambda l^3}\right)\cos\mu l + \mu l.r^2l^2.\sin\mu l}{\left(\frac{1-\psi^2\beta/\alpha}{EI_y/\lambda l^3}\right)\cos r l + r l.\mu^2l^2.\sin r l}\right\}\cos r l\left(\frac{x}{l}\right)\right] \quad \ldots(6.4)$$

where the origin of x is at the centre of the beam. Thus at resonance the beam will adopt a shape either with the number of nodes of $\cos\mu l$ or with the number of nodes of $\cos\nu l$, depending on whether the multiplying factor of $\cos\nu l\left(\frac{x}{l}\right)$ in (6.4), is less than or greater than unity. The magnitude of the factor will in turn depend on the values of μl and νl at resonance, and on the ratio $(EI_y/\lambda l^3)$. The relationship is complicated by the fact that μl and νl of (6.4) are dependent on the $(EI_y/\lambda l^3)$ ratio by the equation (6.3). Thus when small $(EI_y/\lambda l^3)$ values are selected, some of the roots of the frequency equation will tend to those of $\cos\mu l = 0$ others to $\cos\nu l = 0$. For the roots of the former type, the multiplying factor will be small, and for roots of the latter type it will be large.

Without undertaking lengthy calculations based on the frequency equation (6.3) and the shape equation (6.4), all that can be said about the frequency/shape characteristic for a beam with elastic end supports is that for spring supports with stiffness of an order generally associated with the term, the frequency/shape curve will be similar to that of the free-free beam. However for large stiffness ($EI_y/\lambda l^3$ small) the frequency/shape characteristic might follow the pattern for the pin-ended beam.

An interesting corollary to the above is that for some stubby beams, it may be impossible to produce effectively pinned ends. Even the elasticity of the

materials of the pin itself may be sufficient to cause the frequency/shape curves to be of the free-free type.

6.3. Mindlin's Solution of the Free Timoshenko Beam Frequency Equation.

6.3.1. Introductory Mindlin (1951) in his study of the flexural vibration of free crystal plates is led to an anisotropic version of the Timoshenko beam equation and hence to a similar frequency equation to (4.29). He presents the roots of this equation in the form of a set of curves relating a frequency factor to the $(\frac{L}{K})$ of the beam. This is very convenient since for any chosen $(\frac{L}{K})$ in the range plotted, the resonant frequencies can be read off directly. His presentation suffers from the drawback that the shape functions - with respect to number of nodes - are not included. However, it will be shown that lines can be constructed on the diagram to indicate the nodal configuration at any particular resonance; any frequency lying within the region enclosed by a given pair of lines having a certain number of nodes.

6.3.2. Method of Solution.

In the case of interest, the solutions of the equation

$$\tan rl = -\frac{rl\left(\beta\psi^2l^2 - r^2l^2\right)}{\mu l\left(\mu^2l^2 - \beta\psi^2l^2\right)}\cdot\tan\mu l \qquad \psi^2 > \psi_c^2 = \alpha/\beta \qquad \ldots(6.5)$$

are required.

Proceeding in the manner of Mindlin, the following

substitutions are made,

$$\gamma = \mu l \quad , \quad a = \frac{r}{\mu} \quad , \quad g = \frac{1}{\beta} \qquad \ldots(6.6)$$

After manipulation (6.5) then simplifies to

$$(a^2-g)\tan a\gamma = a(1-ga^2)\tan\gamma \qquad \ldots(6.7)$$

and the following relations are found for a rectangular section

$$\left(\frac{\psi_c}{\psi}\right) = \left[1 - \frac{a^2(1+g)^2}{g(1+a^2)^2}\right]^{1/2} \qquad \ldots(6.8)$$

$$\left(\frac{L}{K}\right) = \sqrt{12}.\gamma.\left(\frac{\psi_c}{\psi}\right)\sqrt{\frac{1+a^2}{3(1+g)}}. \qquad \ldots(6.9)$$

It is now required to construct on the $\left(\psi/\psi_c\ ,\ L/K\right)$ -plane, curves on which lie all the points satisfying the frequency equation (6.7) and the two relations (6.8) and (6.9).

For a given beam, g is calculated; then an a value is chosen and ψ/ψ_c can be calculated from (6.8). The roots of γ which satisfy (6.7) for these values can be substituted in (6.9) and the relevant $\frac{L}{K}$ values calculated. This procedure is repeated as often as necessary for different values of a .

The lengthy part of the computation is that involved in finding the γ -roots of the transcendental frequency equation. Recourse can be made to plotting the functions as discussed in section 6.1 : Mindlin also gives a method of solution by successive approximations.

6.3.3. The Significance of the γ-Lines.

The above calculations have been carried out for a rectangular section beam with η taken as 5/6 and ν as 0.29, for a range of $\left(\frac{L}{K}\right)$ from 10 to 50 and (Ψ/ψ_c) from 1 to 1.3. This is shown in Fig. 17 .

Crossing the frequency root lines on this figure are the dotted lines joining points which satisfy

$$\gamma = \frac{m\pi}{2} \qquad (m \text{ odd})$$

These lines are determined from the relation (6.9) between γ and $\left(\frac{L}{K}\right)$ for chosen values of (Ψ/ψ_c) .

The significance of these γ-lines is evident when the nodal configuration corresponding to any point on a resonance line is considered. It was seen earlier in section 6.1.3 that in general, the shape at resonance is mostly determined by the value of μl (or γ) at the resonant frequency. For resonances between $\mu l = 3\frac{1}{2}\pi$ and $4\frac{1}{2}\pi$ for example, there will be 4 nodes on either half-length of the beam and, more generally, for resonances between the lines of $\gamma = \frac{m\pi}{2}$ and $\gamma = \frac{(m+2)\pi}{2}$, there will be (m + 1) nodes on the length of the beam (m odd). Thus roots lying between any pair of the γ lines will display the same number of nodes.

It is interesting to check up from the diagram the calculations of section 6.1. In particular, it can be seen that at $\frac{L}{K} = 30$ three resonance lines are intersected in the band between $\gamma = \frac{13\pi}{2}$ and $\gamma = \frac{11\pi}{2}$, i.e. three frequencies are predicted with 12 nodes. When $\frac{L}{K}$ is reduced to 29.4 the first resonance above

ψ_c , is in the $(9 \rightarrow 11)\frac{\pi}{2}$ band, so having 10 nodes, and only two frequencies have 12 nodes. These features agree with the calculations of section 6.1.

Some resonance points can be found actually on the γ- lines; these are special cases. Apparently since γ is an odd multiple of $\frac{\pi}{2}$, $\tan\gamma$ must be infinite and for the frequency equation to hold, $\tan a\gamma$ must also be infinite or $a\gamma$ must be an odd multiple of $\frac{\pi}{2}$. In such cases, the shape function, which comprises the two components $\cos\gamma$ and $\cos a\gamma$, will have a node at the free ends of the beam, since both $\cos\gamma$ and $\cos a\gamma$ will be zero there.

6.4. <u>The Third Spectrum Frequency Solutions.</u>

The natural frequencies in the third spectrum for the free ended beam can be calculated (for given $\frac{L}{K}$ and ν values) from equation (5.40) where m is taken as 1, 2, 3, ... successively.

In order to plot these frequencies to a base of number of nodes, the shape function for each case has to be evaluated from equation (5.41). This equation shows that the shape is the summation of three cosine curves of different wave lengths and amplitudes. In general, therefore, the shape will be complicated, and the number of nodes on the beam will depend on the relative amplitudes of each of the component cosine curves.

For all the values calculated however, it was found that the $\cos\mu l\left(\frac{x}{l}\right)$ component was overwhelming, and

hence the number of nodes appearing in the complete shape function will equal the number contained in $\cos\mu l$; this feature was found also in section 6.1.3 for the second spectrum shape functions. Due to the complicated nature of the expression (5.41) it is not possible to say that $\cos\mu l\left(\frac{x}{l}\right)$ will always be the dominant component; each case will require evaluation on its own.

The third spectrum natural frequencies are shown in Figs. 13 , 15 , and 16 , for $\frac{L}{K}$ = 20, 30 and 29.4 respectively. The points in each case can be seen to be no longer in the smooth curve of the pin-ended case (Fig. 11). The first resonance in the third spectrum has the same number of nodes as its nearest neighbour in frequency in the first spectrum. This behaviour is very similar to that of the second spectrum for the free Timoshenko beam (section 6.1.3).

7. THE DISPERSION OF FLEXURAL WAVES.

7.1. General.

For an infinite train of sinusoidal flexural waves propagating along an infinite beam with phase velocity c', the transverse displacement can be taken in the form

$$w = D.\cos(pt - sx) \qquad \ldots(7.1)$$

where

$$\left.\begin{aligned} s &= \frac{2\pi}{\Lambda} \\ p &= \frac{2\pi c'}{\Lambda} \end{aligned}\right\} \qquad \ldots(7.2)$$

and Λ is the wavelength.

This solution (7.1) can be substituted into any of the differential equations for flexural motion and there will result an expression relating the phase velocity with the wave length.

The velocity of propagation for the energy of a wave packet of flexural vibrations, i.e. the group velocity, can be related to the phase velocity by the equation

$$c_g = c' - \Lambda.\frac{dc'}{d\Lambda}$$

The substitution of equation (7.1) into the classical equation (3.10) gives the result that infinitely short waves have an infinite group velocity which is physically impossible. The equation is thus suitable for long wavelengths only : however it does demonstrate that the velocity is dependent

on the wavelength or that there is dispersion.

The effect of the rotatory inertia correction is to give a velocity expression which does not lead to infinite group velocity for very short wavelengths; the expression, however, is still only accurate for the longer wavelengths. The subject is further discussed in Kolsky.

7.2. Propagation Velocities for the Timoshenko Equation.

Substitution of equation (7.1) into the Timoshenko equation (3.16) gives the equation

$$\left(\frac{c'}{c_o}\right)^4 - \left(\frac{c'}{c_o}\right)^2 \left\{ \eta\zeta + 1 + \frac{\eta\zeta}{4\pi^2}\cdot\left(\frac{\Lambda}{K}\right)^2 \right\} + \eta\zeta = 0 \qquad \ldots(7.3)$$

where

$$\zeta = \frac{1}{2(1+\nu)} \quad ; \quad c_o = \sqrt{\frac{E}{\rho}} . \qquad \ldots(7.4)$$

Equation (7.3) defines two branches to the dispersion curves. Previous investigations seem to have been confined to the lower of these branches, the upper one being disregarded. Volterra (1955) ignores the upper branch, feeling that it has no physical significance, this decision being partly based on a remark by Hudson (1943) which will be referred to later.

The lower branch of (7.3) is fully examined by Davies (1948) his results being quoted in Kolsky. It is shown there, that the lower branch of (7.3) is,

for a circular rod, a very good approximation to the exact solution. For infinitely short wavelengths the exact theory predicts a propagation velocity equal to the Rayleigh surface wave velocity of $0.5764\, c_o$ for $\nu = 0.29$ while the lower branch of (7.3) tends to $0.5906\, c_o$. The higher branch of (7.3) tends to c_o for very short wavelengths.

7.3. Propagation Velocities from the Equation which includes Lateral Inertia.

If the expression (7.1) is substituted in the differential equation (3.37) the following expression is obtained,

$$\left(\frac{c'}{c_o}\right)^6 - \left(\frac{c'}{c_o}\right)^4\left\{\left(1+\frac{1}{\eta}\right)\frac{\eta\zeta}{s^2K^2}+1+\eta\zeta+\zeta\right\}+\left(\frac{c'}{c_o}\right)^2\left\{\frac{\eta\zeta^2}{K^4s^4}+2\cdot\frac{\eta\zeta^2}{K^2s^2}\right.$$

$$\left.+\frac{\zeta}{s^2K^2}+\eta\zeta+\zeta+\eta\zeta^2\right\} - \left(\frac{\eta\zeta^2}{K^2s^2}+\eta\zeta^2\right) = 0 \qquad \ldots(7.5)$$

in which ζ and c_o are defined in equation (7.4).

Equation (7.5) can be factorised into,

$$\left[\left(\frac{c'}{c_o}\right)^2-\left(\frac{\zeta}{s^2K^2}+\zeta\right)\right]\left[\left(\frac{c'}{c_o}\right)^4-\left(\frac{c'}{c_o}\right)^2\left\{1+\eta\zeta+\frac{\eta\zeta}{s^2K^2}\right\}+\eta\cdot\zeta\right]=0 \qquad \ldots(7.6)$$

Thus (7.6) predicts three branches to the dispersion curve. The second bracketed expression can be seen to be the expression (7.3) so that two of the branches of (7.6) are the branches from the Timoshenko equation while the third is new and is defined by

$$\left(\frac{c'}{c_o}\right) = \left[\frac{\zeta}{4\pi^2}\left(\frac{\Lambda}{K}\right)^2+\zeta\right]^{1/2} \qquad \ldots(7.7)$$

For infinitely short wavelengths the branch (7.7) tends to $\eta^{\frac{1}{2}} c_0 = c_2$ the velocity of shear waves in the medium.

The three branches of (7.5) are shown in Fig. 18 for a circular sectioned beam of $\nu = 0.29$ where η has been taken as $9/10$.

7.4. A Note on the Exact Theory.

The problem of the propagation of flexural waves along a circular cylinder was first investigated by Pochhammer (1876). The frequency equation resulting from this exact theory was expressed in determinantal form by Bancroft (1941), and Hudson (1943) computed the flexural wave dispersion curve corresponding to the lowest branch obtained from equation (7.6) illustrated in Fig. 18 . Hudson further stated that the flexural dispersion curve consists of just one branch, but gives no reason for this statement. Of this statement, Holden (1951) says that the many branched relation between wavelength and phase velocity "is true in particular of the flexural type of mode, and in his otherwise excellent treatment of flexure, Hudson's statement to the contrary must be disregarded".

Thus, although there is no support from the exact theory for the three branches of (7.6), neither is there any definite contradiction.

8. APPARATUS.

8.1. Beam and its Supports.

Since the physical existence of higher spectra of bending frequencies was to be examined, it was necessary to choose a size of beam for which these frequencies would be experimentally available.

Theoretically it was known that the second spectrum of the Timoshenko equation would begin shortly above the critical frequency $f_c = \frac{1}{2\pi}\sqrt{\frac{\eta G}{\rho K^2}}$, so that a large radius of gyration was desirable to reduce f_c . However, a larger radius of gyration necessarily implies an increased flexural stiffness, and excitation of the vibration would become a problem if the beam were made too massive. A compromise had therefore to be made between a low value for f_c and a low value for the flexural rigidity, the decision being influenced by the maximum excitation force known to be obtainable and by the available signal amplification for the vibration pick-up (see sections 8.2 and 8.5). It was decided that a rectangular sectional beam of depth about 4" would be suitable if made from mild steel or some other material with a $\frac{G}{\rho}$ value of the same order; a rectangular cross section being amenable to theoretical treatment. A depth/width ratio of about 2 was chosen: it was feared that a lower value would make for too great rigidity while a higher value would be too near the

plane-stress case and would not allow the three-dimensional stress system to develop. The beam length was chosen to give a reasonable $\left(\frac{L}{K}\right)$ ratio about 30.

The method of supporting the ends of the beam were considered. There are practical difficulties involved in representing pinned or fixed end conditions in that as the frequency or mode of motion of the beam increases so also increases the demand for rigidity of the supports. Any elastic yielding will change the end conditions from pinned or fixed to something between these and the free case. Since the higher frequencies and modes were of most interest, it was decided not to attempt to produce pinned or fixed ends.

Free-ends can effectively be produced by suspension on long wires normal to the plane of bending, or by supporting on soft springs. The free end condition is more exactly approximated to the higher the mode of motion in which the beam is vibrating, a feature which recommends the method.

With these considerations it was decided to make the experimental beam effectively free ended and to support it at both ends on 2" x 1" x 1" rectangular blocks of hard rubber. This would provide reasonable support for the beam, which would be necessary for the type of vibrator used, while still being flexible enough to be considered as a free end condition at the hihher modes of vibration.

In the actual experimental setup the rubber

supports stood on steel plates clamped to the keyway of a large lathe-bed. Fixing of the rubber was not required as the vibrations were never sufficiently severe to give accelerations approaching 'g'.

Beams of mild steel, cast iron and cast brass were made near the size indicated above. Some early experiments were conducted with a 60" length of 3½" I section vibrated in its plane of greatest flexibility.

8.2. Vibration Exciter.

It was decided to excite the beam centrally. This it was thought would restrict the resonances to the symmetric cases, which would simplify experimental work.

Three possible methods of excitation were considered. These were excitation by rotating out-of-balance masses, magnetic excitation, and excitation by an attached moving coil.

Out-of-balance excitation was considered unsuitable because of the restricted range of frequency available and the speed squared dependence of the applied force.

Magnetic excitation is very easy to apply but suffers from the tendancy to excite higher harmonic frequencies due to its impure force output. In addition its use is generally restricted to magnetic materials. It was considered inferior to moving coil excitation for these reasons.

Moving coil excitation by a short attachment

was decided on. Virtually pure sinusoidal forces can then be applied to the beam and if desired the value of the force can be obtained by calibration. The moving coil adds a vibrating mass to the beam but if the beam is large enough this mass can be neglected.

The vibrator chosen was the smallest of a range produced by Goodmans Ltd., having a maximum force output of over 1 lb. The coil operates in the field of a permanent magnet. The vibrator was bolted onto a steel plate which was clamped to the keyway of the lathe-bed. A short 4 B.A. brass rod which screwed into the moving coil portion of the vibrator also screwed into a tapped hole in the centre of the base of the beam and was locked to the beam and the vibrator by nuts (see Fig. 3). Thus arose the necessity for lateral rigidity of the beam supports mentioned in 8.1, since any angular movement of this rod might have damaged the vibrator.

8.3. Excitation Circuit.

The moving coil of the vibration exciter was supplied with alternating current of variable frequency from an audio-frequency oscillator and a power amplifier (see Fig. 4).

A Muirhead decade oscillator (type D-650-B) was used. The output frequency was variable by a cycle at a time below 10 Kc/s, and a frequency fine adjustment varied the frequency within the range of 1 cycle/sec. Thus the frequency could be increased very

gradually so that resonant frequencies could be accurately obtained, and very sharp resonances which might be missed with a coarser frequency alteration would be noticed.

The output from the oscillator passed through a power amplifier and thence via a transformer, an ammeter and an on/off switch to the vibrator. The ammeter was used at the lower frequencies to indicate when the maximum safe current for the vibrator was being approached.

The output from the power amplifier was monitored on a small Phillip's oscilloscope (type GM 5655) which showed any distortion of the outcoming wave from the amplifier. Such distortion would be harmful to the amplifier and might affect the vibrator to excite higher harmonics.

8.4. Vibration Pick-up.

The main requirements which were considered desirable for the method of pick-up were: (a) the arrangement should allow amplitude readings to be taken from any point of the beam so that nodal patterns could be determined, (b) the presence of the pick-up should have a negligible effect on the beam's vibration, (c) the unit should be sensitive to very small oscillations and should be able to respond up to frequencies of the order of 20 Kc/s.

Under (a) must be considered whether one pick-up unit, which could be varied in position along the beam,

or a plurality of fixed pick-ups with perhaps a selector switch, should be used. It was eventually decided that for simplicity's sake a single pick-up would be more suitable. It was further decided that in order to give a high degree of mobility to the pick-up, displacement-sensitive response was undesirable as re-setting would be required at each point.

In view of these features, the use of differential transformer, reluctance variation, capacitance variation, and strain gauge methods was felt to be unsuitable; while the requirement (c) of high sensitivity, along with the inconvenience involved, precluded the adoption of optical methods such as microscope readings.

A velocity-sensitive pick-up became available in the form of a Phillips (type G.M. 5526) moving coil instrument. This pick-up is actuated by a small movable contact pin to which the coil is attached internally, moving in the field of a permanent magnet. The contact pin is also attached internally to a buckled diaphragm to provide a reaction when the pin is held against the beam. A load of some 850 gms. is needed to start the buckling, but thereafter, by the nature of elastic instability the increase in force for change of pin displacement is negligible so that the instrument's own natural frequency is low and quite outwith the range of interest for this work. Although the pick-up was not recommended by the makers for use above 1000 cycles/sec., it was found satis-

factory in performance up to frequencies over 20 Kc/s.

The pick-up was bolted to a steel plate supported on two wooden blocks resting on the top of the lathe-bed (see Fig. 3), one to each side of the beam. The blocks and pick-up could thus be slid bodily to any desired position along the beam.

The pick-up could also be used held in the hand and this feature proved very useful when amplitude distributions were being examined.

A medical stethescope was also used for resonant frequencies in the audio-range as a rough guide to nodal pattern.

8.5. Amplification and Display of Pick-up Signal.

The output from the pick-up was led to a Phillips "amplitude measuring apparatus" (type GM 5522) which can be used for calibration of the pick-up and also can differentiate or integrate the incoming signal so that an output proportional to the acceleration or the displacement of the pick-up point can be obtained. At the high frequencies used, the acceleration-proportional output proved to give the largest signal.

The output from this apparatus was then passed through a Phillips battery operated pre-amplifier (type G.M. 4570); this could be set to give a signal amplification of either 8 or 35 times, approximately.

The amplified output was then passes into the first amplifier of a Cossor 1035 A.C. double beam

oscilloscope via a condenser in series and a parallel resistance to earth. The inclusion of these circuit elements constituted a simple high frequency pass filter which very effectively eliminated a considerable 50 cycle hum. Since the frequencies of interest were very much greater than 50 c.p.s., the filter did not interfere with the important part of the incoming signal.

The output from the first amplifier of the oscilloscope was then passed via a similar high pass filter into the second amplifier, the output of which was displayed on the oscilloscope screen.

The total amplification of the pick-up output voltage was thus very great. The maximum gains available from the two oscilloscope amplifiers were in the region of 3000 and 30 respectively, so that arranged in cascade the gain was of the order of 90,000. The pre-amplifier further increased this value so that between the "differentiating box" and the oscilloscope screen, the total amplification was of the order of 3×10^6. This enabled the very small oscillations obtaining at the higher frequencies to be displayed on the oscilloscope screen.

9. EXPERIMENTAL PROCEDURE.

9.1. The Resonant Frequencies.

The apparatus was run for about fifteen minutes prior to any experiments since the resonant frequencies were inclined to wander slightly immediately after switching on.

The pick-up was usually placed at the centre of the upper face of the beam, a position at which it should pick up the maximum amplitude of symmetric modes. If antisymmetric modes were being examined, the pick-up was placed a few inches from the centre of the beam to avoid the node there. The resonant frequencies were virtually unaffected by the position of the pick-up along the beam.

The oscillator frequency was increased from a low value and the oscilloscope trace watched for signs of a resonance, any frequency at which a maximum in the trace length occurred being considered as a resonant frequency. For frequencies below 10 Kc/s the frequency was increased by 1 cycle/sec increments and for frequencies greater than 10 Kc/s, a frequency increment of 10 cycles/sec. was made and the frequency fine adjustment control then used to sweep continuously through the 10 cycle frequency range.

When a resonance was located, the frequency was set to give maximum amplitude on the oscilloscope trace, after which the beam was examined for nodal configuration.

At the high frequencies when the beam response was low, the maximum output from the oscillator and power amplifier that was consistent with maintaining an undistorted waveform, as shown on the monitor oscilloscope, was used.

9.2. Discrimination between Types of Resonance.

It was found that all the possible modes of vibration for a bar were being excited. The anti-symmetric bending modes and the torsion modes were presumably excited by virtue of slight assymmetry in the excitation, or in the bar itself. Extensional modes would be excited because the vibrator was forcing the lateral contraction associated with longitudinal motion.

With all these different modes being excited, some method of classifying resonances was necessary. At a given resonsnce this was done by examining with the pick-up the amplitude distribution on the surfaces of the beam, motion in each of the co-ordinate directions being considered.

The following criteria were used to distinguish between the types.

Bending Mode.

On Ends:-

u-motion, Z-wise distribution - one central node.

On Flanks:-

v-motion, Z-wise distribution - one central node.

On Upper Face:-

w-motion, Y-wise distribution - virtually constant.

Extension Mode.

On Ends:-

u-motion, Z-wise distribution - maximum amplitude at centre with no nodes or possibly two nodes.

On Flanks:-

v-motion, Z-wise distribution - maximum amplitude at centre with no nodes or possibly two nodes.

On Upper Face:-

w-motion, Y-wise distribution - virtually constant.

Torsion Mode.

On Flanks:-

v-motion, Z-wise distribution - one central node.

On Upper Face:-

w-motion, Y-wise distribution - one central node.

The extension mode with two nodes in the longitudinal motion is equivalent to the extensional mode with a nodal cylinder predicted by the Pochhammer Theory for a circular rod (see Bancroft (1941)).

The above amplitude distributions were examined experimentally by exploration of the appropriate external faces of the beam with the pick-up held in

the hand. The random motion of the hand was at low frequency and did not affect the pick-up signal.

Two types of parasitic resonance were possible so that resonances had to be checked to make sure they were resonances of the beam. These two types of resonance were, contact resonance of the pick-up pin, and resonance of the beam supports or vibrator supporting plate.

The contact resonance is due to the pick-up point bouncing on the beam surface and is therefore a function of the elasticity of the materials in contact. After a resonance had been found with the normal pick-up contact pin, a short attachment was fitted over the pin. This attachment is provided with an insulated point of a plastic material and will therefore have a different contact resonance frequency from the contact pin itself. Thus, if a resonance showed both with the attachment and without, it was considered not to be a contact resonance. The only resonance which was established as contact resonance was at 3,885 cycles/sec.

Some very small resonances found with the pick-up on the beam turned out to be resonance of the plate holding the vibrator. In these cases, the motion of the plate was examined with the pick-up and was found to be much greater than the motion of the beam. No case of resonance of the plates supporting the rubber blocks at the ends of the beam was found.

Another possibility of extraneous resonance is

the extensional motion of the short driving rod from the vibrator to the beam. Considering the beam as a mass on the rod as a weightless spring, brief calculation shows that the natural frequency is well below the frequencies examined experimentally; while for the rod in extensional vibration itself, the calculated frequency is well above the experimental range.

9.3. Nodal Distribution Patterns.

Once a resonant frequency had been located and its type determined by the methods of section 9.1, the distribution of nodes in the lateral (w) motion along the top surface of the beam was examined. To do this, the pick-up was held in the hand and applied to the beam at close intervals along its length: points where the oscilloscope trace was zero were marked as nodes. The number and location of these nodes were noted.

The pick-up was thus used mainly as a null-reading instrument. It was found that with the pick-up placed on its supports the oscilloscope signal depended on the contact of the pick-up pin with the beam so that it was difficult to repeat amplitude readings. The pick-up was therefore not suitable for taking complete amplitude distribution curves, but was quite satisfactory as a null-reading device.

For some of the lower frequencies, a stethescope was used as a guide to nodal configuration but the pick-up was always used to confirm the pattern.

10. EXPERIMENTAL RESULTS.

10.1. Steel Beam.

The dimensions of the rectangular section steel beam were

Length 35.65"

Depth 4.20"

Width 1.86"

from these figures an $\frac{L}{K}$ ratio of 29.4 is obtained.

The observed resonant frequencies were classified in the manner outlined in section 9.2. The bending natural frequencies with their associated number of nodes on the beam are quoted in the table in section 10.4.

The amplitude of the resonances dropped off fairly rapidly as the 10 and 12 node configurations were approached and no bending resonances were found beyond the last one listed in the table. Extensional modeswere being excited up to frequencies in the region of 25 Kc/s.

The natural frequencies are plotted on Fig. 19 which also shows some of the extension and torsion resonances which were picked up. Other extension frequencies were found beyond the frequency range shown but these were not examined seriously, being beyond the scope of this work.

The responses of the two 10 node frequencies were of the same order of magnitude; as was also the case for the two 12 node frequencies.

10.2 Cast Iron Beam.

The dimensions of the rectangular section cast-iron beam were

Length	35.60"
Depth	4.19"
Width	1.85"

giving an $\frac{L}{K}$ ratio of 29.44.

The bending resonant frequencies are given in section 10.4 and are plotted against nodal number in Fig. 20 . The responses of the higher 10 node configuration and the 12 node configurations were poor, while the 14 node resonance was very small. This falling off in response is presumably partly a consequence of the high internal damping of cast iron.

Some of the torsion and extension frequencies picked up are also shown in Fig. 20 . These extensional frequencies marked E' had two nodes in the longitudinal motion (see section 9.2). Extensional resonances occurred very frequently in a frequency band between 16,500 c.p.s. and 20,000 c.p.s. but were not examined generally.

As in the case of the steel beam the responses of both frequencies with 10 nodes were of similar magnitude as was the case with the two 12 node frequencies.

10.3 Brass Beam.

The dimensions of the rectangular section brass beam were

Length	35.64"
Depth	4.12"
Width	1.88"

giving an $\frac{L}{K}$ ratio of 29.98.

The bending resonant frequencies are given in the table in the following section and are plotted in Fig. 21 .

The 12 node resonance at 10,588 c.p.s. and the 14 node resonances at 12,156 c.p.s. and 13,742 c.p.s. were very small: the responses of the two remaining pairs of 12 and 14 node frequencies were much larger.

In the region of the higher bending frequencies many extensional resonances occurred and several of these exhibited the two nodes in longitudinal motion mentioned above for the cast-iron beam. Some of these extensional resonances were examined for nodal pattern and these points are shown on Fig. 21 .

In this case there were one or two resonances at higher frequency than those shown in the table which appeared to be of bending type, but their nodal pattern was very difficult to establish. The pick-up trace at some points went to zero and at others showed a minimum and it was not possible to say which of these points were nodes and which were not.

A cut of .080" was taken off the upper face of the beam to reduce the depth and increase the L/K ratio slightly. The effect of this was to change the natural frequencies very slightly but the number of nodes corresponding to each resonance remained the same except for the 10 node case at 9790 c.p.s. In this case one half of the beam displayed 6 nodes, the last node being very near the end of the beam, while

the other half still had only 5 nodes, but the vibration amplitude at the end was very small. This phenomenon is presumably due to unhomogeneousness in the beam and the new L/K is obviously very near to the transition case when nodes will appear on the ends of the beam. Under these circumstances the frequency that was the second 10 node case will move across and become the first 12 node case.

10.4. Table of Observed Frequencies.

The following table includes all the observed bending resonances for the three rectangular section beams.

N refers to the total number of nodes on the beam.

	Frequency (cycles per second)		
N	Steel	Cast-iron	Brass
2	618	465	409
3	-	1232	-
4	3047	2232	1850
5	4550	3354	2770
6	6182	4573	3803
7	7858	5805	4861
8	9600	7057	5921
9	11,312	8270	6952
10	12,983	9513	8009
11	14,506	10,663	9032
10	15,650	11,405	9790
12	16,773	12,276	10,452

12	-	-	10,588
11	17,040	12,430	10,685
12	18,552	13,520	11,520
14	-	-	12,156
14	-	14,950	12,498
13	-	-	12,562
14	-	-	13,523
14	-	-	13,742

10.5. I-Section Beam.

As was mentioned in section 8.1 some early experiments were conducted with an I-section beam lying on its side and thus vibrated in its plane of greatest flexibility. The hard rubber blocks were glued to the ends of the beam and to the plates on the lathe bed, otherwise the apparatus used was the same as that for the rectangular section beams.

The beam was a 3" x 1½" standard rolled steel joist and the length of the beam between the centres of the rubber end supports was 60".

The curves of bending resonant frequencies are shown in Fig. 22 . Two spectra of frequencies were obtained. The amplitude distribution patterns were checked as being bending in each case. For the higher set of frequencies it was found generally that the maximum lateral motion on the flanks of the beam was greater than the maximum transverse motion (w) on the upper face, while for the lower set the transverse motion was always considerably greater than the lateral motion.

11. COMPARISON OF EXPERIMENT AND THEORY

11.1 Constants for the Rectangular Beams.

In order to compare the experimental results of section 10, for the rectangular sectioned beams, with the theoretical calculations of section 6; values for Poisson's ratio (ν), the density (ρ), and the elastic modulus (E) for each material have to be assumed.

The value of Poisson's ratio for steel and cast-iron has been taken as 0.29, while that for the brass has been taken as 0.32 (a value quoted by Love.). The weight densities have been taken as 0.28, 0.26, 0.32 ($lbs./in^3$) for steel, cast-iron, and brass respectively. To obtain an assessment of the elastic modulus for each metal, the following method was adopted.

The expression for the extensional natural frequencies of a circular cylinder of length L are given by the equation

$$f = \frac{m}{2L}\sqrt{\frac{E}{\rho}} \quad , \quad (m = 1,2,3,\ldots) \qquad \ldots(11.1)$$

Now, while this equation is probably not accurate for predicting the correct values of f for a rectangular section, its derivative ($\partial f/\partial m$) will presumably still be fairly close to the true value at the low modes. Thus a value of E is chosen such that when inserted along with the assumed value of ρ in equation (11.1), the resulting straight line relating

f and m is parallel to the experimental straight line obtained for the lower extension modes of the beam in question. (see Figs. 19 , 20 , 21).

This procedure gives the following values for E,

Steel, $E = 29.0 \times 10^6$ lbs./ins^2.

Cast-iron, $E = 14.4 \times 10^6$ lbs./ins^2,

Brass $E = 12.3 \times 10^6$ lbs./ins^2.

11.2 Theoretical Natural Frequencies.

The theoretical natural frequencies have already been calculated in section 6 where the results are given in terms of the frequency proportional parameter ψl . These values can readily be converted into values of frequency, by the relation

$$\psi l = \pi . f . L \sqrt{\frac{\rho}{E}} . \qquad \ldots(11.2)$$

where f is the frequency in cycles per second. Using the values for elastic modulus quoted in section 11.1, the conversion factors are,

Steel $f = 1785\ \psi l$

Cast-iron $f = 1306\ \psi l$

Brass $f = 1105\ \psi l$

The calculated frequency factors shown on Figs. 15 , 16 , are now converted by these relations and the following tables show both the calculated and the experimental values of natural frequency for each beam.

Steel Beam: The values of Fig. 16 , for $L/K = 29.4$; $\nu = 0.29$, are used. N refers to the total number

of nodes on the beam.

N	Frequency (c.p.s.) Experimental	Calculated
2	618	610
4	3047	3017
6	6182	6158
8	9600	9461
10	12,983	12,673
10	15,650	15,315
12	16,773	16,547
12 (3)	-	16,939
12 (3)	-	17,850
12	18,552	18,099

The number (3) indicates that a resonance belongs to the third spectrum.

Cast-Iron Beam: The values of Fig. 16 , for $L/K = 29.4$, $\nu = 0.29$ are again used.

N	Frequency (c.p.s.) Experimental	Calculated
2	465	450
4	2232	2208
6	4573	4507
8	7057	6923
10	9513	9275
10	11,405	11,208
12	12,276	12,109
12 (3)	-	12,396
12 (3)	-	13,063

12	13,520	13,233
14 (3)	-	14,238
14	14,950	14,539

Brass Beam: The values of Fig. 15 , for $\frac{L}{K} = 30$, and $\nu = 0.32$ are used.

	Frequency (c.p.s.)	
N	Experimental	Calculated
2	409	377
4	1850	1856
6	3803	3757
8	5921	5768
10	8009	7757
10	9790	-
12	-	9437
12	10,452	10,144
12 (3)	10,588	10,420
12 (3)	-	11,083
12	11,520	11,049
14 (3)	12,156	12,044
14	12,498	12,210
14 (3)	13,742	13,315
14	13,523	13,415

Symmetric resonances only are given in the above table because the calculated frequencies refer only to these modes. Generally the anti-symmetric frequencies are found in the mean position between two symmetric resonances.

11.3 Discussion.

It can be seen from the tables that the calculated and experimental results compare reasonably well. The error apparent for the 2 node cases can be attributed to the stiffening effect of the rubber end supports, the calculated results being for free ends. Otherwise, the maximum error in frequency is less than 3% for the steel beam and the cast-iron beam, and just over 4% for the brass beam.

A comparison of the figures in the tables for the steel and cast-iron beams is made in Figs. 23 , and 24 . The calculated values are given by the continuous curve, though it is to be understood that this curve is meaningful only at the points where it crosses integral values of N. To clarify the curves, the calculated third spectrum points are omitted because none of them were picked up experimentally. The patterns of the calculated curve and the experimental points are very similar. In all cases, the experimental frequencies are higher than those calculated. This may be due to slight error in the choice of $\frac{E}{\rho}$ or ν for the materials.

The tabulated figures for the brass beam are in some respects not so satisfactory. The first discrepancy can be seen to be that the 10 node 9790 c.p.s. experimental resonance is predicted at 9,437 c.p.s. but with 12 nodes. However, this is not really a serious error since previous calculation (section 6.) has shown that the L/K ratio of this

beam is near the transition value when the upper 10 node case will become a 12 node case due to the appearance of nodes on the ends of the beam. Slight error in the choosing of the Poisson's Ratio for example, would be sufficient to make the calculated shape have the wrong number of nodes. That the beam is near the transition L/K is made clear by the remarks at the end of section 10.3.

Also in this case three small resonances possibly corresponding to third spectrum frequencies are found experimentally. Their frequencies are near the predicted values but the 14 node 13,742 c.p.s. resonance, calculated to appear at a lower frequency than the 14 node second spectrum frequency, is actually at a higher frequency; the latter resonance being 13,523 c.p.s. The third spectrum frequencies obtained thus follow the calculated pattern for $L/K = 29.4$ more than that for $L/K = 30$. Taking this into account along with the above note on the 10 node cases, it is probable that the calculated pattern is slightly in error due to a poor choice of Poisson's ratio. However, these remarks refer only to the frequency/shape curve pattern, and do not reflect on the accuracy of frequency prediction. In Fig. 25 , the calculated values are given by the continuous curve for first and second spectrum frequencies and by the dotted curve and the isolated square points for the third spectrum.

The question arises as to why third spectrum

frequencies were obtained experimentally for the brass beam but not for the other two. In the first place it must be noted that in the brass beam these frequencies had a very poor response compared with neighbouring resonances not of the third spectrum. Now for the steel beam, the frequency of the 12 node resonances was greater than 17 Kc/s, and the response of the beam was poor even for the "ordinary" natural frequencies, so that third spectrum resonances would be too small to be observed (presuming they were of the same relative magnitude as for the brass beam). Similarly for the cast-iron beam the response at the higher resonances was poor, presumably partly because of high internal damping, and this lack of response may have been sufficient to conceal the comparatively small third spectrum frequencies.

The reason for this poor response of the third spectrum is thought to lie in the shape of the cross-section used, which was probably too small in breadth. Had the section been broader, say a 4" square section, the lateral stresses would have been better developed and the anticlastic curvature more pronounced, making the lateral inertia more important.

For the steel beam no bending frequencies with more than 12 nodes were obtained, while 14 was the maximum for the cast-iron and brass beams. Probably this is due to the limitations of the apparatus both as regards available exciting force and available pick-up sensitivity. However, the possibility of a frequency

"cut-off" due to damping cannot be excluded. Such a cut-off is predicted if internal damping of the Voigt type is assumed for the material. More powerful excitation and more sensitive pick-up equipment would be necessary to examine the question.

11.4 The I-beam Results.

The theory developed in section 3 for a beam of near-square cross section cannot be expected to apply with accuracy to the $\vdash\!\dashv$ - section of this beam for any but the lower frequencies of the first spectrum. However, the two spectra obtained experimentally are interesting, and some general remarks can be made about them.

The experimental second branch is at neither of the higher spectra frequencies that would be predicted by the theory of section 3. By that theory neither of the higher spectra can begin below the critical frequency $\psi_c^2 = \frac{\alpha}{\beta}$ which for this beam ($L/K = 185$, $K = 0.326"$) is at very much higher frequency than 1840 c.p.s. (where the experimental branch begins).

However, a comparison of the shapes of the two curves is informative. Firstly, it can be seen that the upper curve is slightly convergent on the lower one. As shown in Fig. 11 , this is also true for the theoretical third spectrum for a rectangular beam while the second spectrum curve diverges from the lowest branch. Secondly, to emphasise the above point, an idea of the velocity versus wave length, or dispersion curves, can be obtained from the observed

values by plotting the quantity $f/(N-1)$ against $(N-1)$. The former quantity is roughly proportional to the flexural wave velocity (with a slight error which decreases with larger N, due to the final nodes not being right on the ends of the beam), and the latter quantity is roughly proportional to the reciprocal of the wave-length (the proportionality being more exact for larger N). Curves relating these factors are shown in Fig. 26, and it can be seen that the two curves are approaching each other very much after the manner of the first and third branches of the dispersion curve of Fig. 18.

These two features suggest that there may be some relation between the third spectrum of frequencies and this second experimental branch for the H-beam. On reflection, this can be seen to be a reasonable possibility. For, in the shape of the beam we have what might be considered a good model to display the effects of lateral inertia. During vibration, the lateral curvature of the comparatively flexible middle portion of the beam will set up rotation of the flanges and this rotation, being about an axis parallel to the longitudinal axis, will contribute to the lateral inertia. Thus a section of this shape, obtains a relatively high lateral inertia for a moderate transverse stiffness. This feature might well be expected to enhance the importance of the third spectrum and to lower the critical frequency for this spectrum.

In a somewhat similar way a model could be devised to demonstrate the second spectrum (due to the influence of the longitudinal or rotatory inertia). In that case, a deep rectangular beam could be made, with cuts in lateral planes parallel to the YZ-plane, into both the upper and lower surfaces and at close intervals along the length. Such a beam would exhibit a relatively high rotatory inertia for a moderate transverse stiffness, and would be expected to show the second spectrum at frequencies below the ψ_c for the beam.

The experimental second branch of Fig. 22 , is of the type expected for pin-ended beams since all the nodal configurations of the lower branch are duplicated in the upper branch. This may be due to the high relative stiffness of the rubber end supports which were attached to the beam, or may be a consequence of the unusual cross-sectional shape.

12. CONCLUSION AND REMARKS.

12.1 Principal Conclusions.

12.1.1 Theoretical

(a) It has been shown that the inclusion of an independent longitudinal inertia in the derivation of an equation forflexural vibration, leads to the Timoshenko equation. This equation has been found to predict for a finite beam, different natural frequencies which have the same number of nodes.

This duplication of nodal number at resonance can occur only at frequencies greater than a certain critical frequency which is inversely proportional to the radius of the gyration of the cross-section $\left(f_c = \frac{1}{2\pi}\sqrt{\frac{\eta G}{\rho K^2}}\right)$

(b) For the Timoshenko beam with pinned-ends, the frequency equation is separable into two parts each defining a spectrum of frequencies. The second spectrum repeats the nodal patterns of the first spectrum but at higher frequency; the first resonance of the second spectrum has the same number of nodes as the fundamental of the lower spectrum.

For the Timoshenko free-beam, the frequency equation is no longer directly separable, but there is still the equivalent of two spectra of frequencies because of the increase in the number of resonances in a given range above the critical frequency. The extra frequencies have shape patterns corresponding with that of their neighbouring frequencies so that similar

shapes are close in frequency. Thus the first resonance of the second spectrum has the same number of nodes as its nearest neighbour in the first spectrum.

(c) An extension of the theory to include the effects of an independent lateral inertia has provided another differential equation which predicts yet another set of natural frequencies; a third spectrum. The displacement forms assumed for this equation are such that the solution retains, unmodified, the roots of the Timoshenko equation, while still providing an additional root.

From this extended theory, the shape function of a free beam comprises three sinusoidal functions of differing periods. The shape of the beam at resonance depends on which is the dominant component. Thus there may be five resonant frequencies with the same number of nodes (two of which are from the third spectrum), but more usually there will be four resonances (two from the third spectrum), and occasionally there will be fewer, each case having to be considered individually.

(d) The equation which includes the effect of lateral inertia gives three values for the velocity of propagation of flexural waves of given wave length, that is, it defines a three branch dispersion curve. Two of these branches are also obtainable from the Timoshenko equation. For the two higher branches, at very small wavelengths the phase velocity tends

to $\sqrt{\frac{E}{\rho}}$ in the one case, and to shear wave velocity in the other. The latter branch is the one peculiar to the equation with lateral inertia.

12.1.2. Experimental.

(a) The experimental frequencies and their correlation with the calculated frequencies have demonstrated fairly conclusively the physical existence of the second spectrum of natural frequencies for a free beam, as predicted by the theory.

(b) The experimental evidence for the third spectrum of frequencies is not so conclusive. It was detected very faintly, for only one of the three rectangular sectioned beams: as explained in the text, this may have been a result of the shape of the beam. However, this third spectrum type of frequency, which arises on account of lateral inertia effects, may be important for beams which in virtue of their cross-sectional shape, can have a high lateral inertia during bending. This feature is suggested by the ⊢⊣- beam experiments.

(c) The difference between the calculated and experimental frequencies is quite small. The method for estimating E is open to some error and Poisson's Radio ν was just guessed although it might have been estimated by comparing the slopes of the extension and torsion frequency curves. Assuming these errors in the choice of the elastic constants to be fairly small, the experiments can be said to have confirmed

the validity of the theory, at least for first and second spectrum frequencies. In all cases, the experimental frequencies were slightly greater than the corresponding calculated frequencies, presumably because of the inaccuracies in the values for the elastic constants. The rubber end supports would also tend to make the calculated frequencies somewhat smaller although the theory indicates that this effect is negligible after the first two or three harmonics.

(d) The experiments have also confirmed the physical existence of higher modes of longitudinal vibration for the rectangular bars.

12.2 Remarks.

(a) The equation which includes lateral inertia is easily solved because the assumed displacement forms are such that its solution includes the known solutions of the Timoshenko equation. It may be found from further experiments for example, that this equation having the simplest possible displacement forms, is not accurate enough, and that refinements such as anticlastic curvature or longitudinal displacement a function of lateral position ($u = \phi(x,y,z,t)$) may have to be included to provide a satisfactory solution. In that case, the more involved differential equation that will be derived (c.f. equation(3.40)) will not contain the Timoshenko equation and the solution will be more complicated.

(b) As can be seen from the figures, the plotting

of natural frequency against number of nodes on the beam, although quite satisfactory for a pin-ended beam, gives a relatively disordered array of points for a free-beam above the critical frequency. This follows because the flexural motion is propagated at three different velocities along the beam with a different wave length and amplitude associated with each. For the free beam it appears that for all resonances, the lowest velocity (and shortest wave-length) component has the largest amplitude so that the nodal shape always corresponds to this component. Thus it would not be permissable to use the number of nodes on the beam to obtain an approximation to the wavelength associated with a particular frequency (as was done in section 11.4 for the ⊢⊣ -beam results) : in order words, the higher branches of the dispersion curve cannot be drawn from frequency and nodal observations on a free-beam. Because of the practical difficulties involved in making an end effectively pinned, it follows that pulse propagation technique is probably the only satisfactory method for obtaining these dispersion curves.

(c) The existence of higher spectra of bending frequencies is probably not of much practical significance. They may possibly require consideration for accurate computations of deflection response in impact problems, particularly on foreshortened beams when the second spectrum begins at a relatively low order of vibration. The experiments showed that

the response of the beam in the second spectrum was of the same order of magnitude as neighbouring frequencies of the first spectrum.

The experiments on the ⊢⊣ -beam show that the third spectrum frequencies may be important for open-section beams where an appreciable proportion of the cross-sectional area is situated near vertical planes some distance from the longitudinal axis. Such cross-sections will exaggerate the influence of lateral inertia and third spectrum type frequencies may be important.

(d) For future investigation, a theory describing the vibration characteristics of beams of cross section of the type mentioned above, would be useful. Such a theory might be derived by an extension of the methods of section 3, that is, plausible assumptions could be made regarding the displacement functions, and these, substituted in the equations of equilibrium and integrated over the cross-section, would give a differential equation for the displacement of the beam.

Experimentally, further work is necessary to examine the third spectrum frequencies for a rectangular section. For this, a broader section than that used experimentally, and a greater available driving force would probably be required.

PRINCIPAL NOTATION

The following list defines the principal usage of the symbols indicated. In certain sections other meanings may be attached to some of the symbols but this will be made clear in the relevant portions of the text.

The symbols are arranged in approximately the order in which they appear in the text.

σ_x , σ_y , σ_z	Direct stress components
τ_{xy} , τ_{yz} , τ_{xz}	Shear stress components
E	Young's Modulus
G	Rigidity Modulus
ν	Poisson's Ratio
u, v, w	Longitudinal (X-wise), lateral (Y-wise), and transverse (Z-wise), displacement components.
X, Y, Z	Cartesian co-ordinate axes. (See Fig. 5)
x , y , z	Co-ordinates
ρ	Mass Density
t	Time
b	Section breadth (Y-wise)
I_Y	Second moment of area of cross-section about YY'.
A	Area of cross-section
$\phi(x,t)$, $\bar{\beta}(x,t)$	Functions representing bending slope and neutral axis shear slope respectively
η	Timoshenko shear coefficient.
$e(x,z,t)$	Function representing distortion of cross-sections.

ϵ_1 , ϵ_2	Constants for cross-section.
$w_o(x,t)$	Deflection of neutral line of beam.
I_z	Second moment of area of cross-section about ZZ'.
Q	Shear force over any cross-section
M	Bending moment at any cross-section.
P	Circular frequency
f	$(P/2\pi)$
$W(x)$	Shape function corresponding to $w(x,t)$.
ψ	$(P^2\rho/E)^{1/2}$; frequency proportional parameter.
K	Radius of gyration of section about YY'.
α	$(1/K^2)$
β	$(E/\eta G)$
A_i	Constants (i = 1, 2, 3, ...)
μ , q , r	Parameters defined in terms of ψ , α , β ; see equations (4.12) and (4.19).
$L = 2l$	Total length of beam
λ	Spring constant.
m	Positive integer.
ψ_c	$(\alpha/\beta)^{1/2}$; parameter defining the "critical" frequency.
f_c	$\frac{1}{2\pi}\left(\frac{\eta G}{\rho K^2}\right)^{1/2}$: "critical" frequency.
${}_2\psi_1$, ${}_3\psi_1$	Fundamental frequencies (parametric) of the second and third spectra respectively.
δ	$E/G = 2(1+\nu)$
g , c	Parameters defined by $g^2 = (\psi^2\delta - \alpha)$; $c^2 = -g^2$.

Λ	Wavelength of flexural waves
s	$(2\pi/\Lambda)$
c' , c_g	Phase velocity, group velocity, of flexural waves.
c_o	$(E/\rho)^{1/2}$
ζ	δ^{-1}
c_2	$(G/\rho)^{1/2}$
N	Integer; total number of nodes on beam.

BIBLIOGRAPHY

ANDERSON, R.A. (1954), Trans. A.S.M.E., 75, 504. "Flexural Vibrations in Uniform Beams According to the Timoshenko Theory".

ARNOLD, R.N. (1951), Proc. Inst. Mech. Engs. 165, 185 discussion on paper by Christopherson, D.G. "Effect of Shear in Transverse Impact on Beams".

BANCROFT, D. (1941), Phys. Rev., 59, 588 "The Velocity of Longitudinal Waves in Cylindrical Bars".

BOLEY, B.A. (1955), An Approximate Theory of Lateral Impact on Beams", J. Appl. Mechs. 22, 1, 69.

BRESSE, M. (1859), "Cours de Mecanique Applique" Mallet-Bachelier, Paris.

CHREE, C. (1889), Trans. Camb. Phil. Soc. 14, 250. "The Equations of an Isotropic Elastic Solid in Polar and Cylindrical Co-ordinates, their Solution and Application".

DAVIES, R.M. (1948), Phil. Trans. A, 240, 375 "A Critical Study of the Hopkinson Pressure Bar".

GOODMAN, L.E. (1954), Trans. A.S.M.E., 76, 203, discussion on paper by Anderson (1954).

HOLDEN, A.N. (1951) Bell Syst. Tech. Jou. XXX, 956 "Longitudinal Modes of Elastic Waves in Isotropic Cylinders and Slabs".

HUDSON, G.E. (1943), Phys. Rev. 63, 46, "Dispersion of Elastic Waves in Solid Circular Cylinders".

KOLSKY, H. (1953), "Stress Waves in Solids", Oxford.

LAMB, H. (1917), Proc. Roy. Soc. Lond. (A), 93, 114, "On Waves in an Elastic Plate".

LOVE, A.E.H. (1927), "Mathematical Theory of Elasticity" Cambridge.

MINDLIN, R.D. (1951), J. Appl. Phys. 22, 316, "Thickness Shear and Flexural Vibrations of Crystal Plates".

MINDLIN, R.D. and DERESIEWICZ, H. (1954), Proc. 2nd. U.S. Congr. Appl. Mech. "Timoshenko's Shear Coefficient for Flexural Vibrations of Beams".

POCHHAMMER, L. (1876), J. reine angew. Math., 81, 324, "On the Velocity of Propagation of Small Vibrations in an Isotropic Cylinder of Infinite Length". (In German).

PRESCOTT, J. (1942), Phil Mag., 33, 703, "Elastic Waves and Vibrations of Thin Rods".

RAYLEIGH, (1877), "Theory of Sound", Macmillan, London.

SUTHERLAND, J.G. and GOODMAN, L.E. (1951), Univ. of Illinois, Contract N6 ori-71, Project NR-064-183, "Vibrations of Prismatic Bars including Rotatory Inertia and Shear Corrections".

TIMOSHENKO, S. (1921), Phil. Mag., 41, 744, "On the Correction for Shear of the Differential Equation for Transverse Vibrations of Prismatic Bars".

TIMOSHENKO, S, (1922), Phil. Mag., 43, 125, "On the Transverse Vibrations of Bars of Uniform Cross-Section".

TRAILL-NASH, R.W. and COLLAR, A.R. (1953), Quart. J. Mech. and App. Math. VI, 2, 186, "The Effects of Shear Flexibility and Rotatory Inertia on the Bending Vibrations of Beams".

VOLTERRA, E. (1955), Rensselaer Polytech. Inst. Report No. 3, Troy N.Y. "On the Propagation of Flexural Waves in Elastic Rods according to the One-Dimensional Theory based on the Method of Internal Constraints".

LIST OF FIGURES

Fig. No.

ELECTRONIC EQUIPMENT

1. DECADE OSCILLATOR
2. POWER AMPLIFIER
3. MONITOR OSCILLOSCOPE
4. d/dt
5. PRE-AMPLIFIER
6. C.R. OSCILLOSCOPE

FIG. 1

General Arrangement of Beam

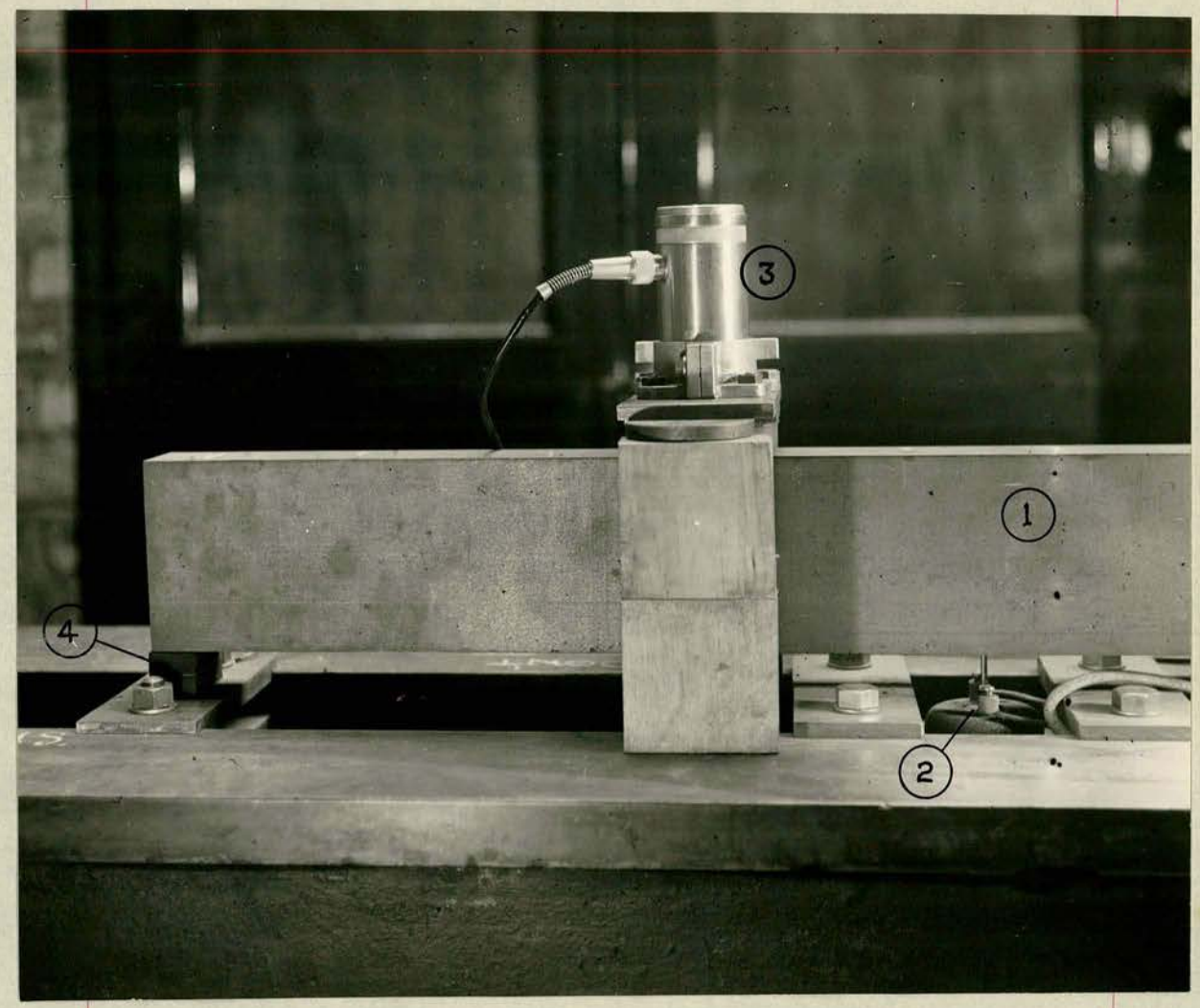

1. BEAM
2. VIBRATOR
3. PICK-UP
4. RUBBER END SUPPORT

Fig. 2

General Arrangement of Vibrator and Pick-up

1 : PICK-UP
2 : VIBRATOR
3 : PICK-UP CONTACT PIN
4 : LATHE BED
5 : SUPPORTING BLOCK

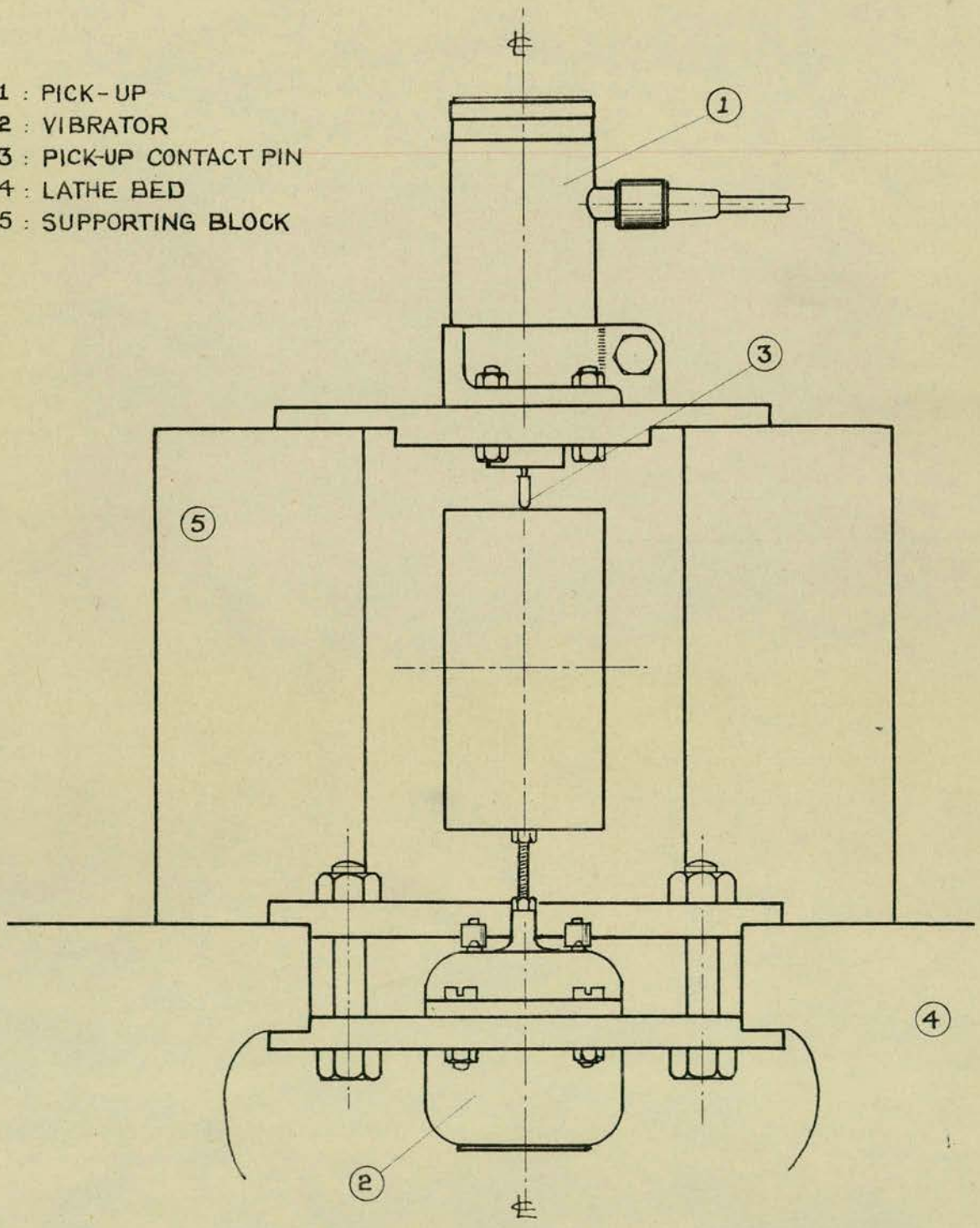

Fig. 3

Block Diagram of Circuit

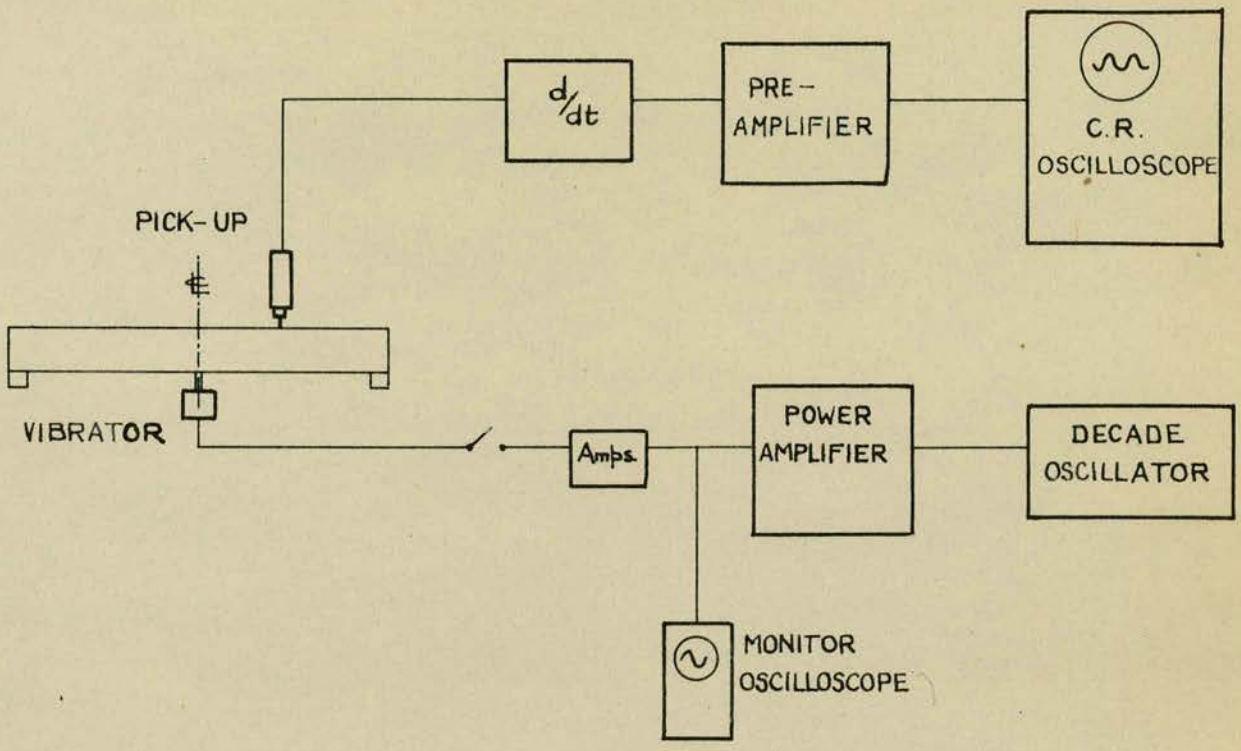

Fig. 4

End Supports and Co-ordinate Directions

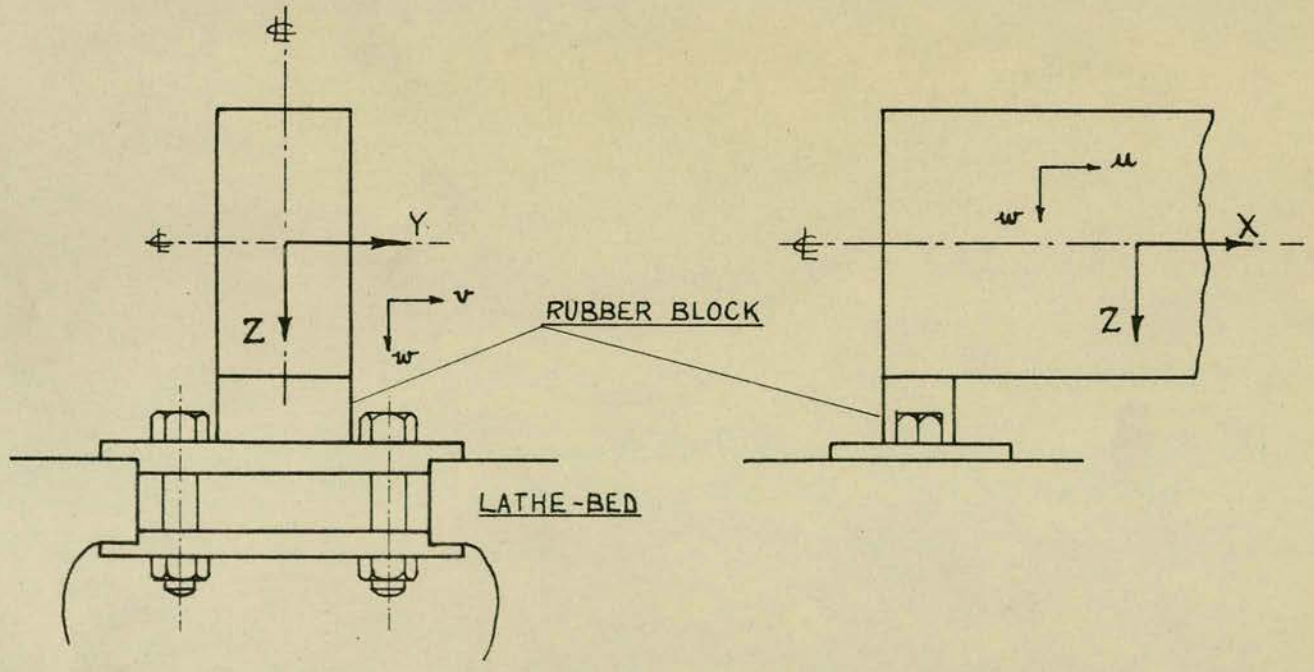

Fig. 5

Models of Rotatory Inertia and Shear Effects

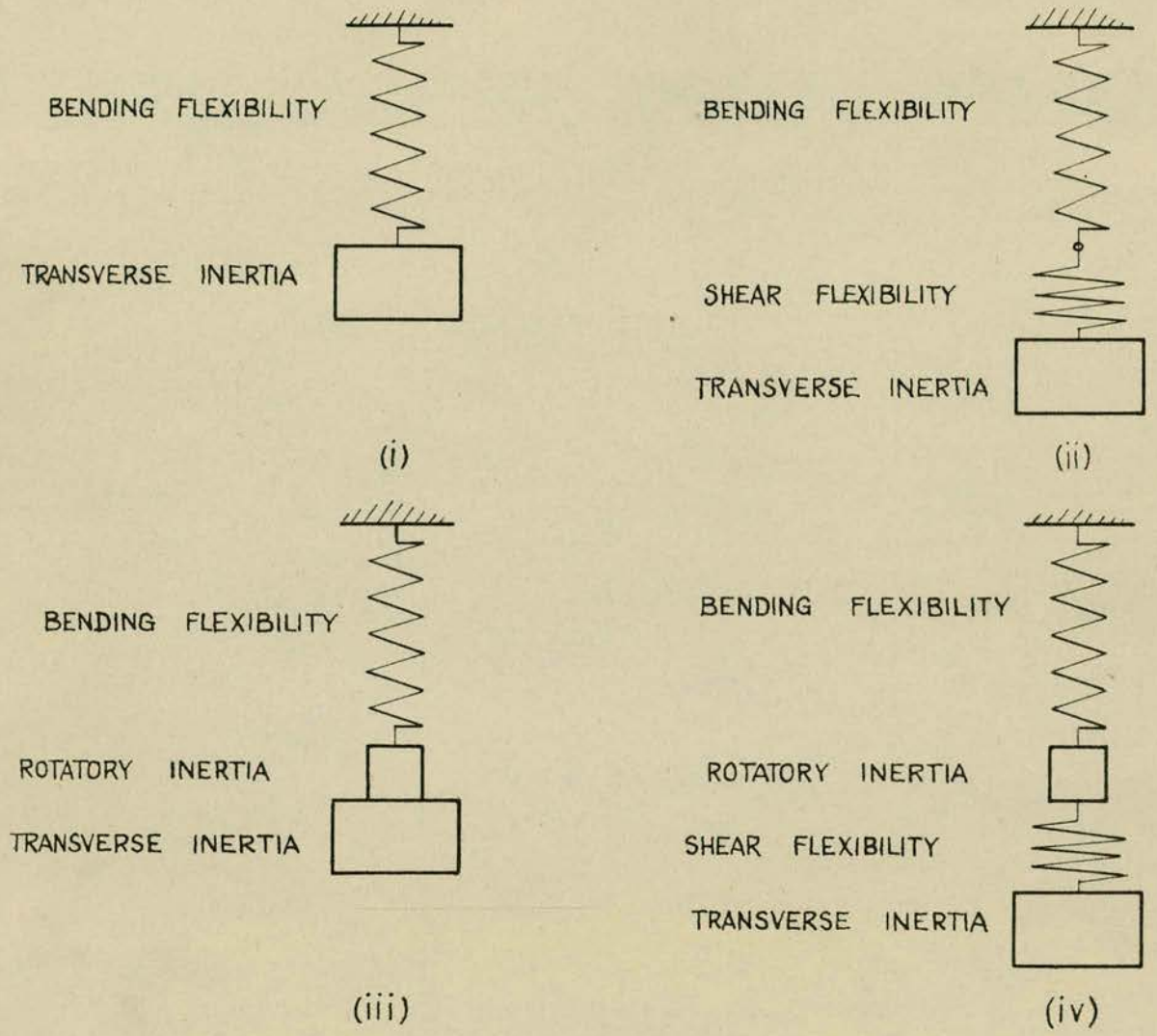

(i) MODEL FOR CLASSICAL THEORY

(ii) INTRODUCTION OF SHEAR CORRECTION

(iii) INTRODUCTION OF ROTATORY INERTIA CORRECTION

(iv) COMBINATION OF (ii) AND (iii)

Fig. 6

Twisting of Typical Transverse Planes

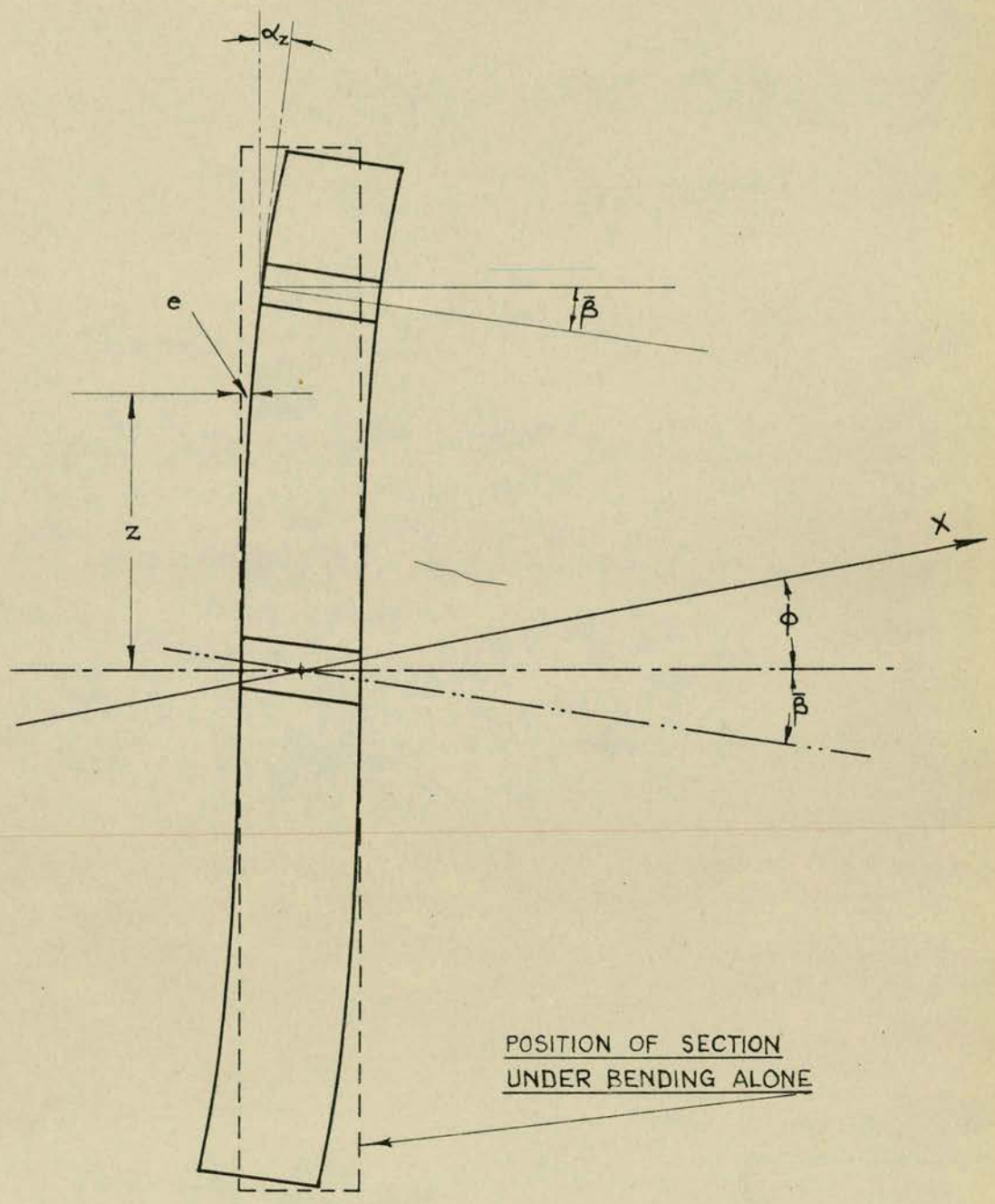

Fig. 7

RESONANT FREQUENCIES OF PIN-ENDED TIMOSHENKO BEAM

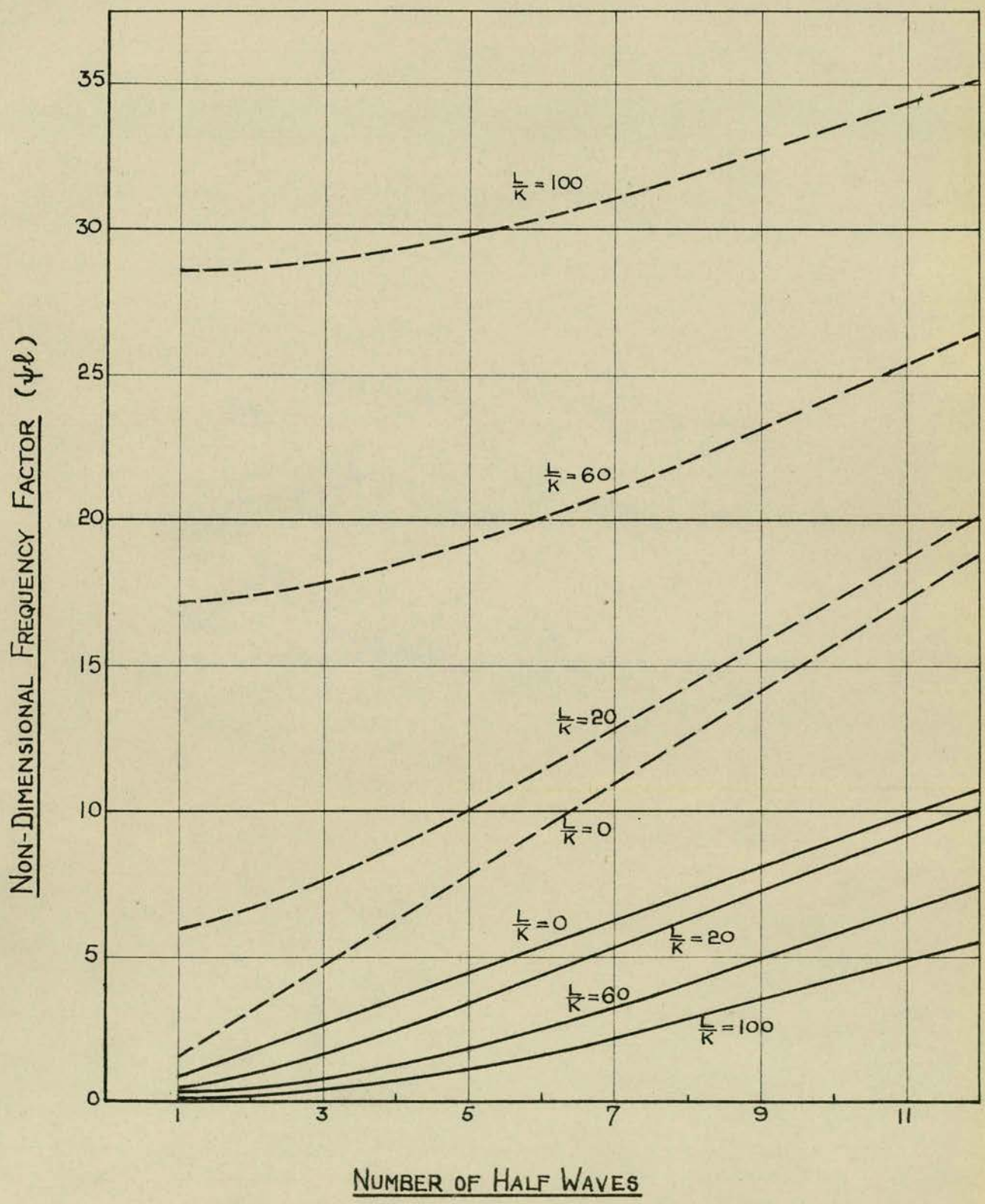

FIG. 8

Fundamental Frequencies of Higher Spectra

Pin-Ended Beam

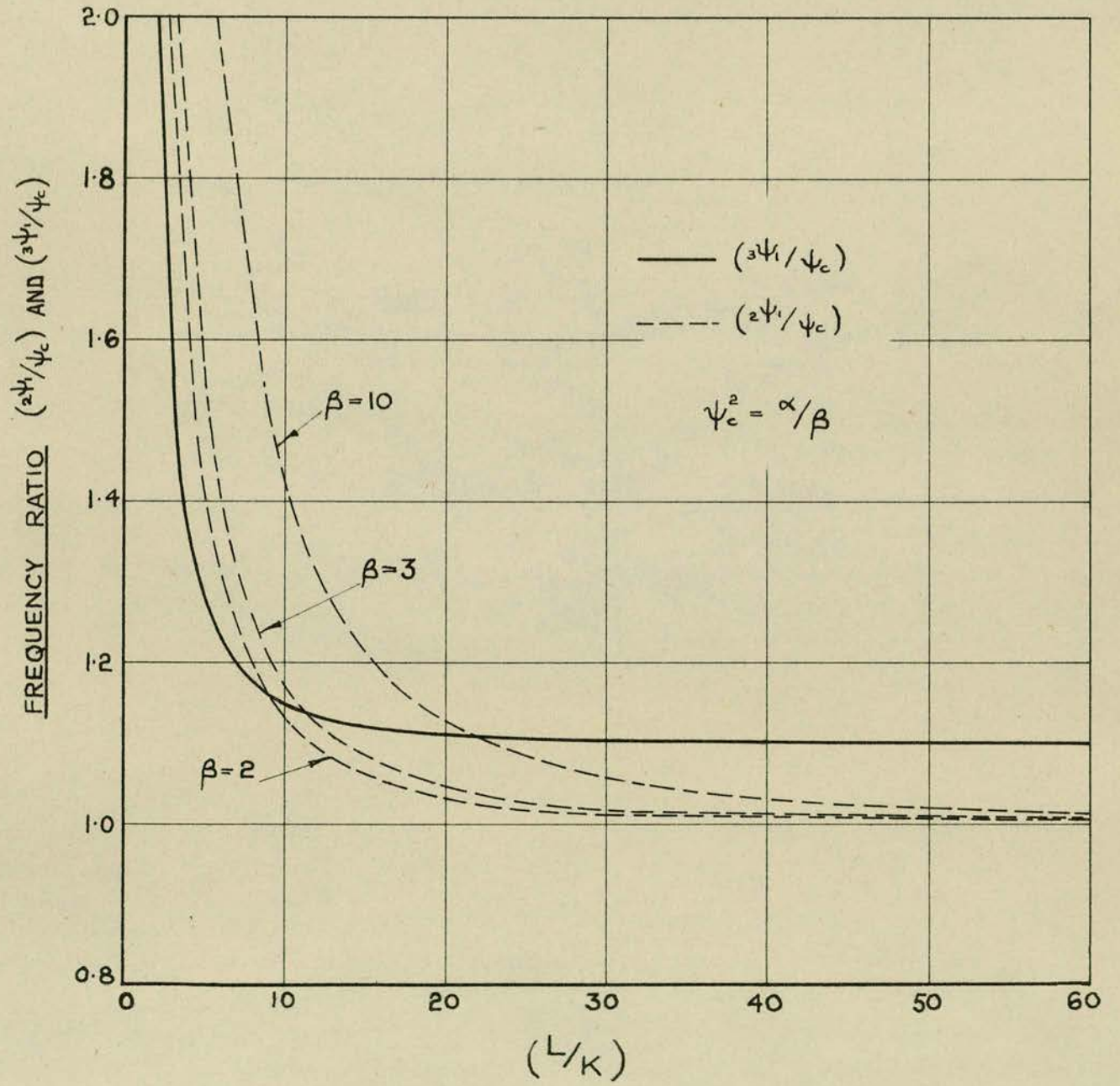

Fig. 9

VARIATION OF μl, ql WITH FREQUENCY FACTOR ψl

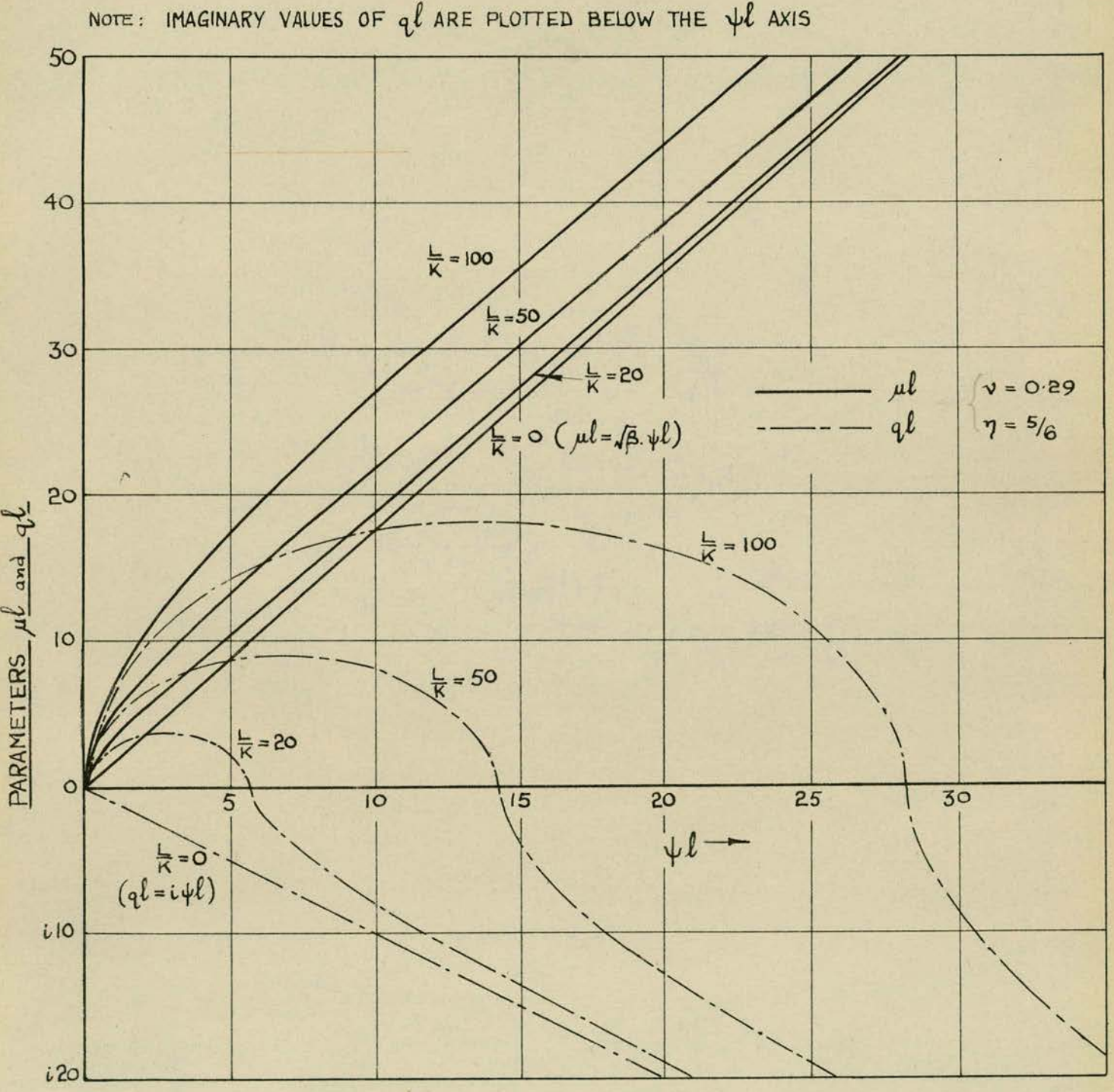

FIG. 10

THE THREE FREQUENCY SPECTRA

BEAM WITH PINNED ENDS

$\nu = 0.29 : \eta = 5/6$

I- FIRST SPECTRUM II - SECOND SPECTRUM III- THIRD SPECTRUM

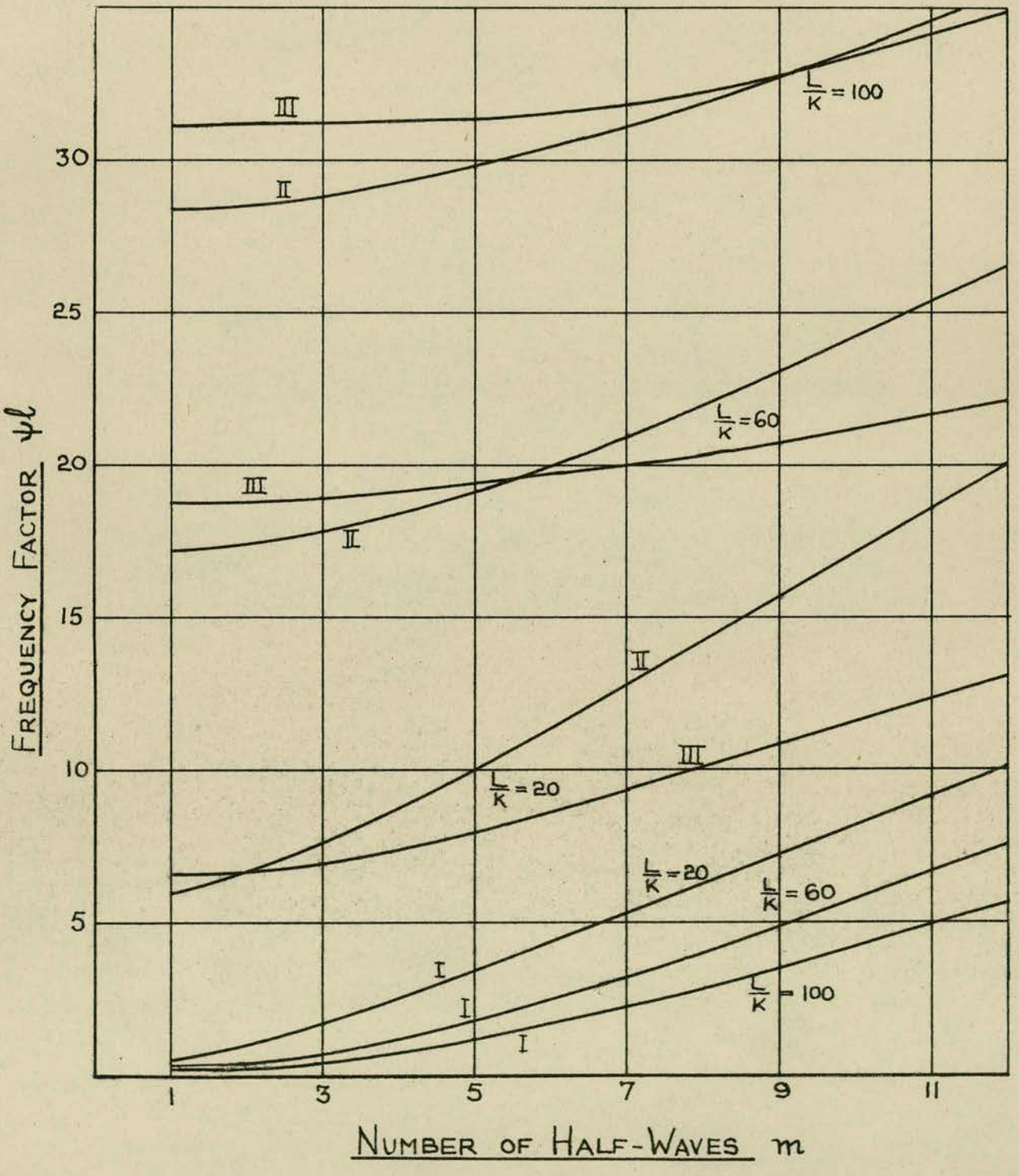

FIG. 11

Solution of Frequency Equation (4.28), Around ψ_c

$\frac{L}{K} = 20$; $\nu = 0.29$; $\eta = \frac{5}{6}$

K, K' DEFINED IN EQ^{N} (6.1)

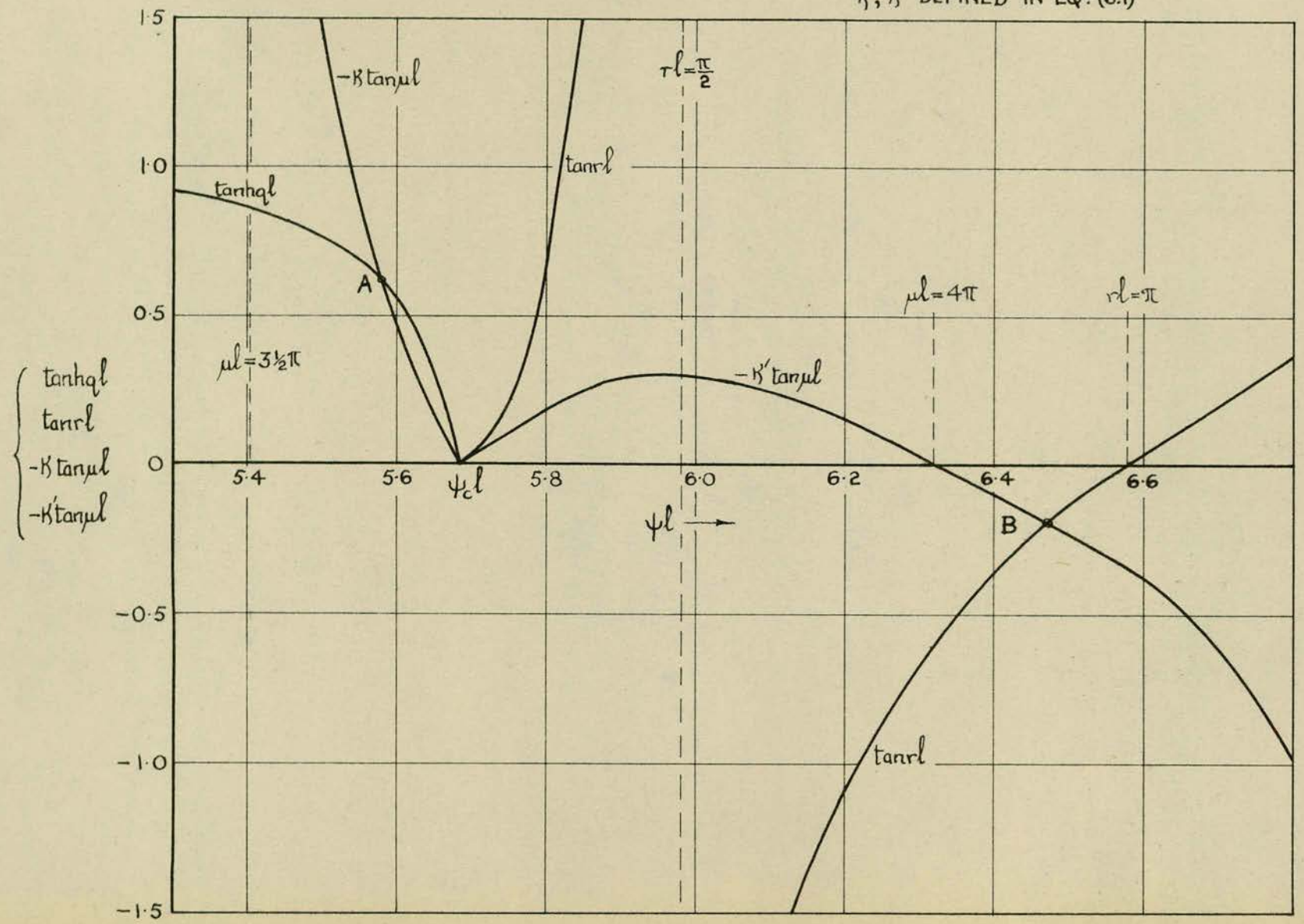

FIG. 12

THEORETICAL NATURAL FREQUENCIES

FREE-BEAM SYMMETRIC MODES

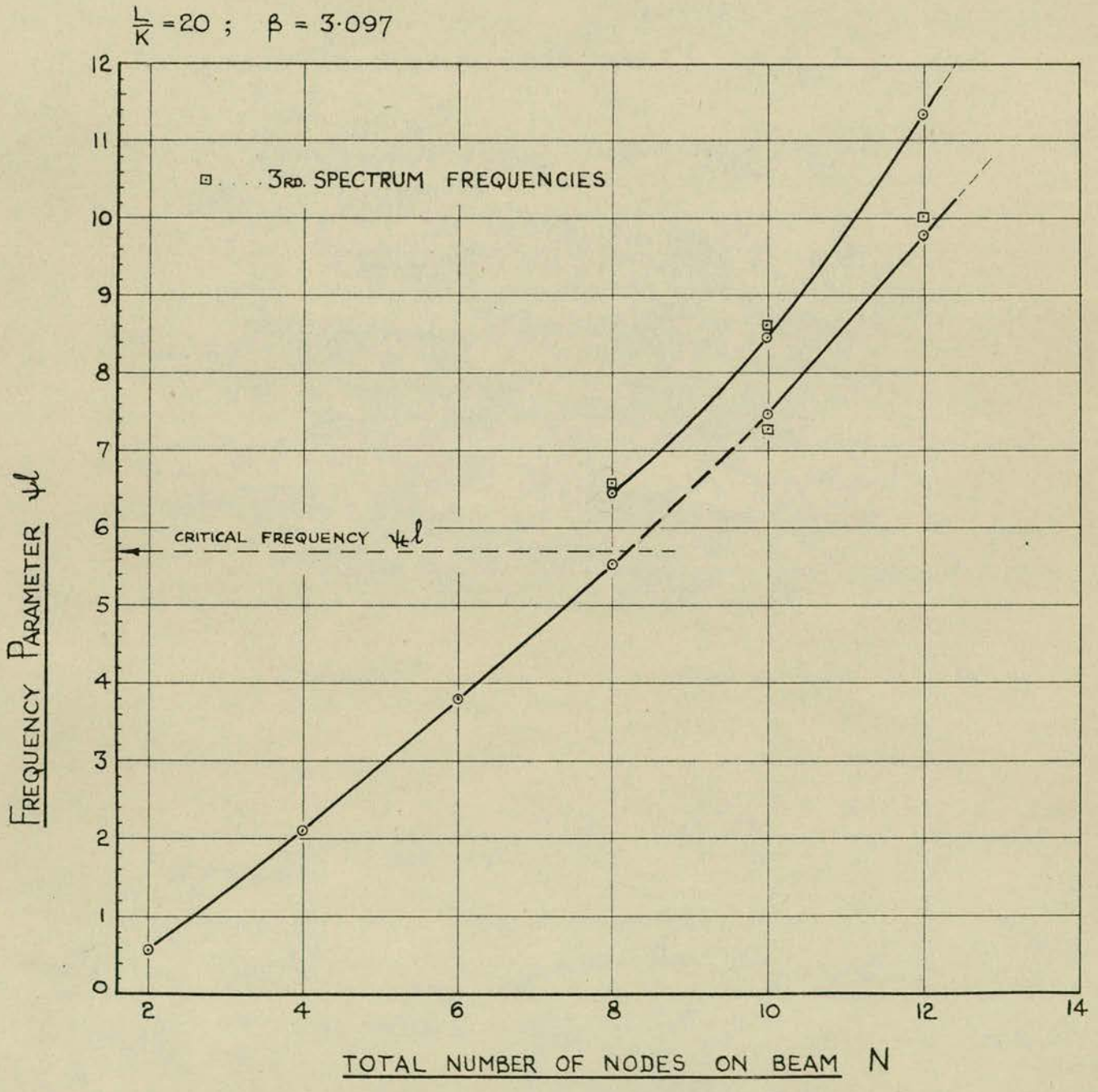

FIG. 13

Solution of Frequency Equation (4.28), near ψ_ϵ

$\frac{L}{K} = 30$; $\nu = 0.32$; $\eta = 5/6$

K, K' defined in Eqn (6.1)

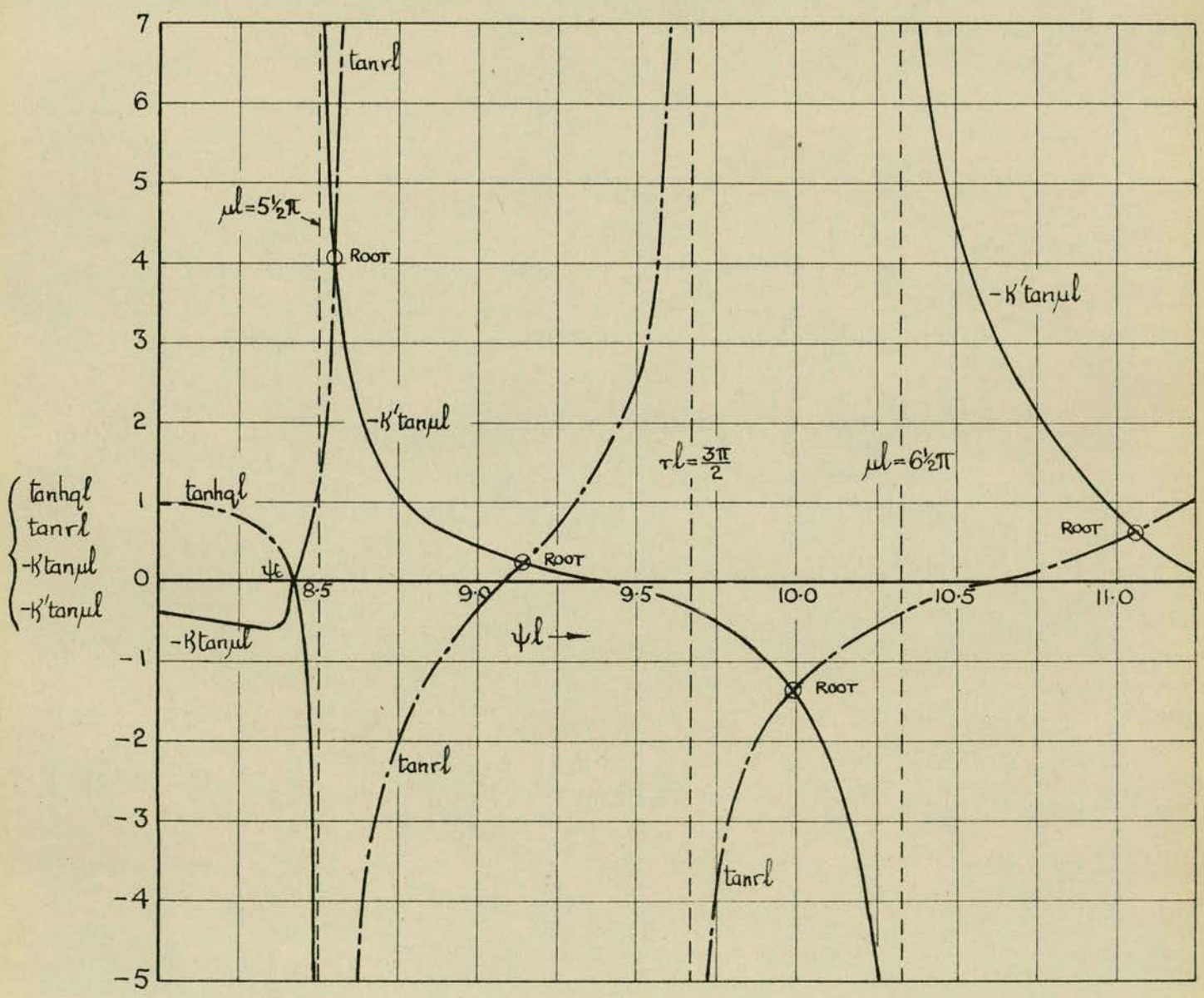

Fig. 14

THEORETICAL NATURAL FREQUENCIES

FREE-BEAM SYMMETRIC MODES

$\frac{L}{K} = 30$; $\beta = 3{\cdot}17$

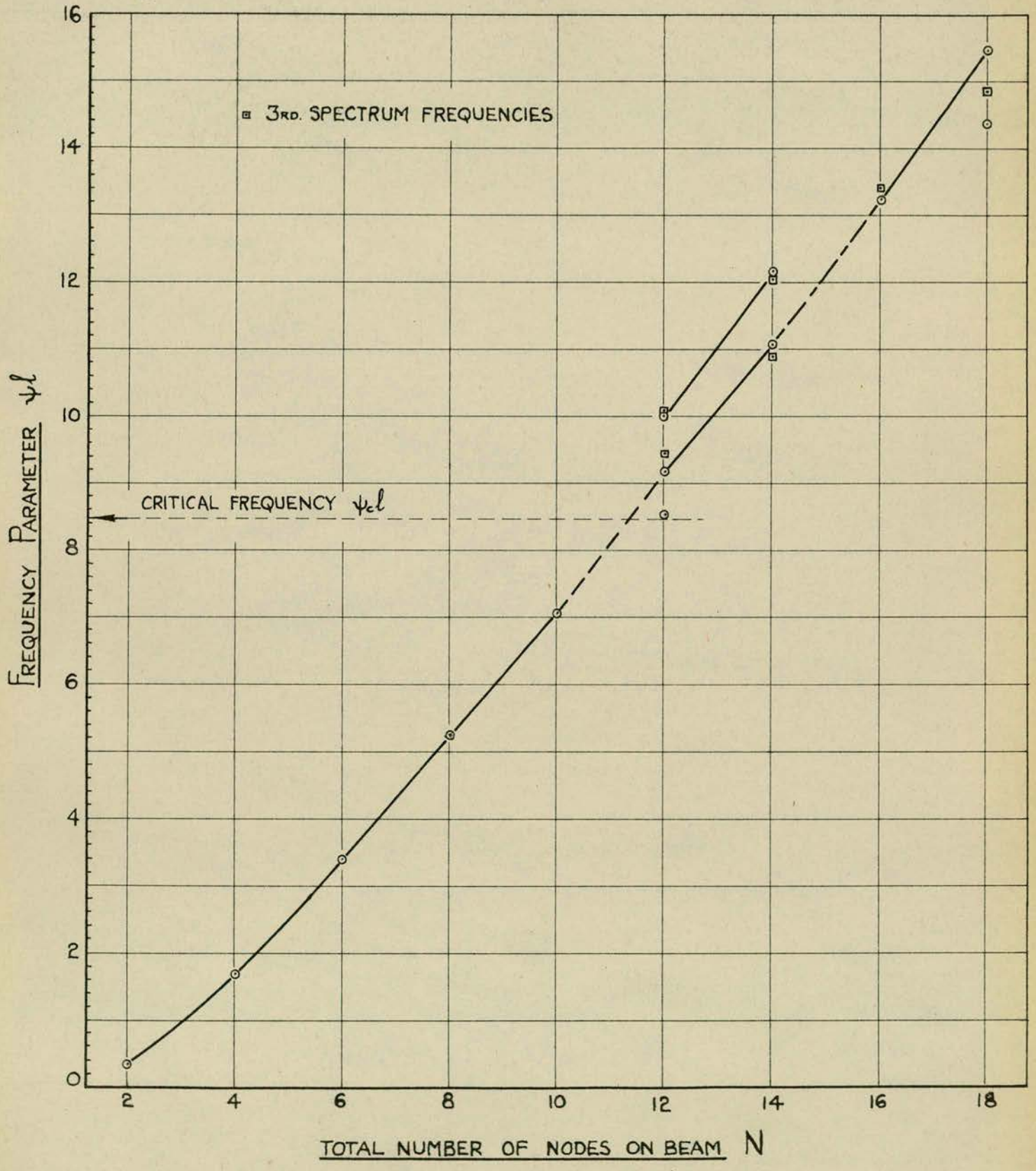

FIG. 15

THEORETICAL NATURAL FREQUENCIES

FREE-BEAM SYMMETRIC MODES

$\frac{L}{K} = 29.4$; $\beta = 3.097$

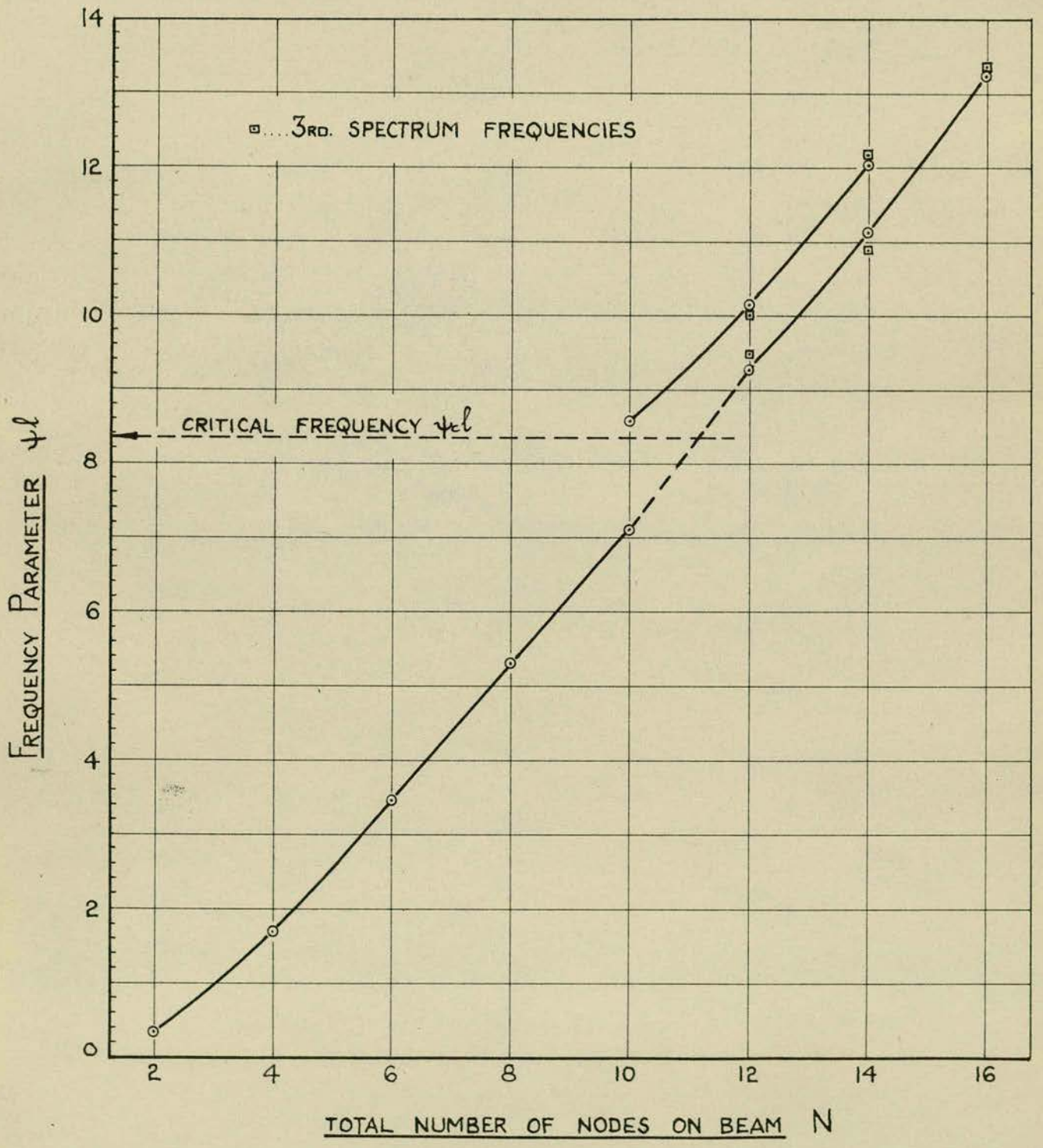

FIG. 16

Symmetric Resonances Of Free Timoshenko Beam

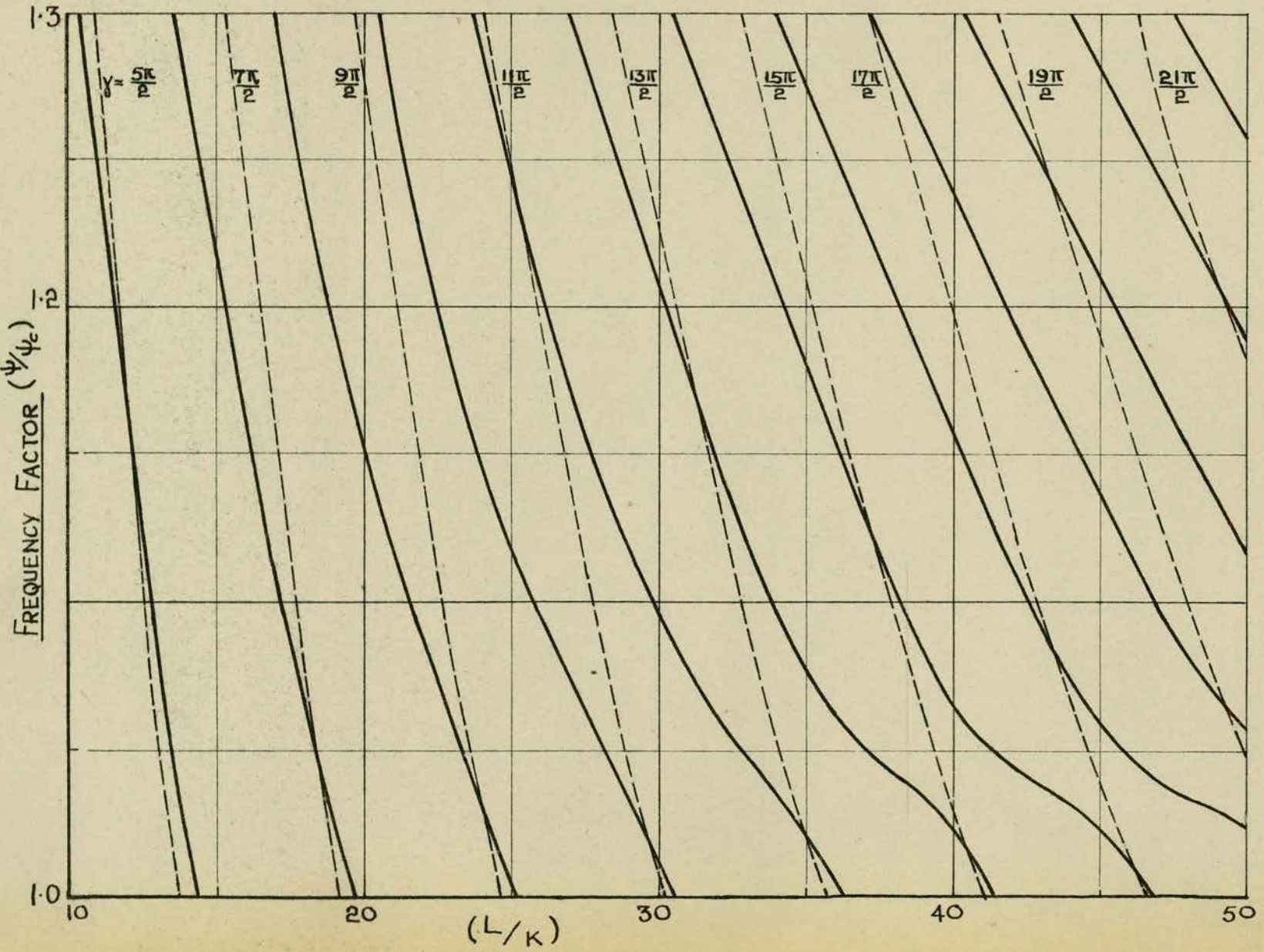

Fig. 17

DISPERSION CURVES FOR CYLINDRICAL ROD

(BY EQUATION (7.5))

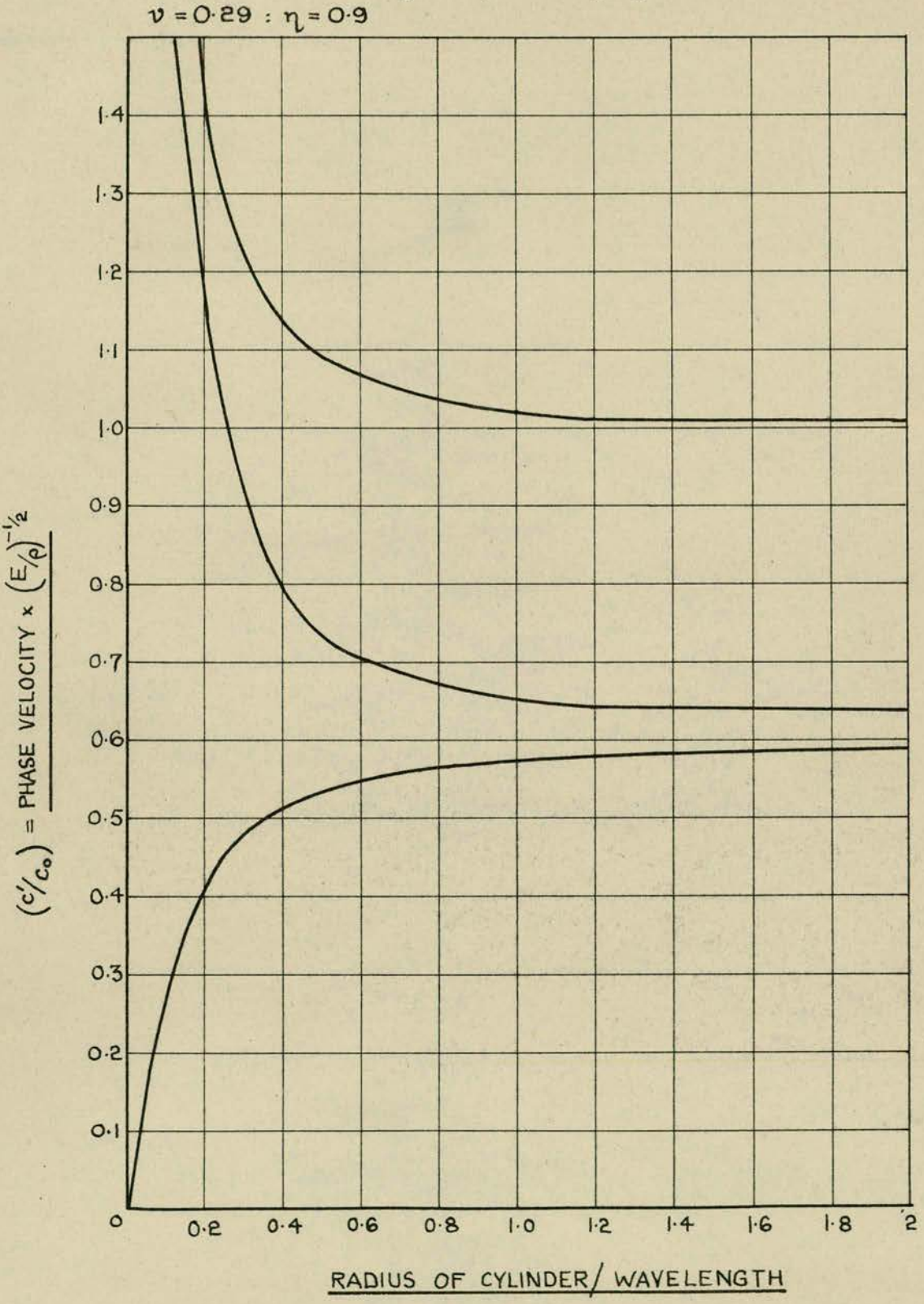

FIG. 18

Experimental Resonant Frequencies

Steel Beam

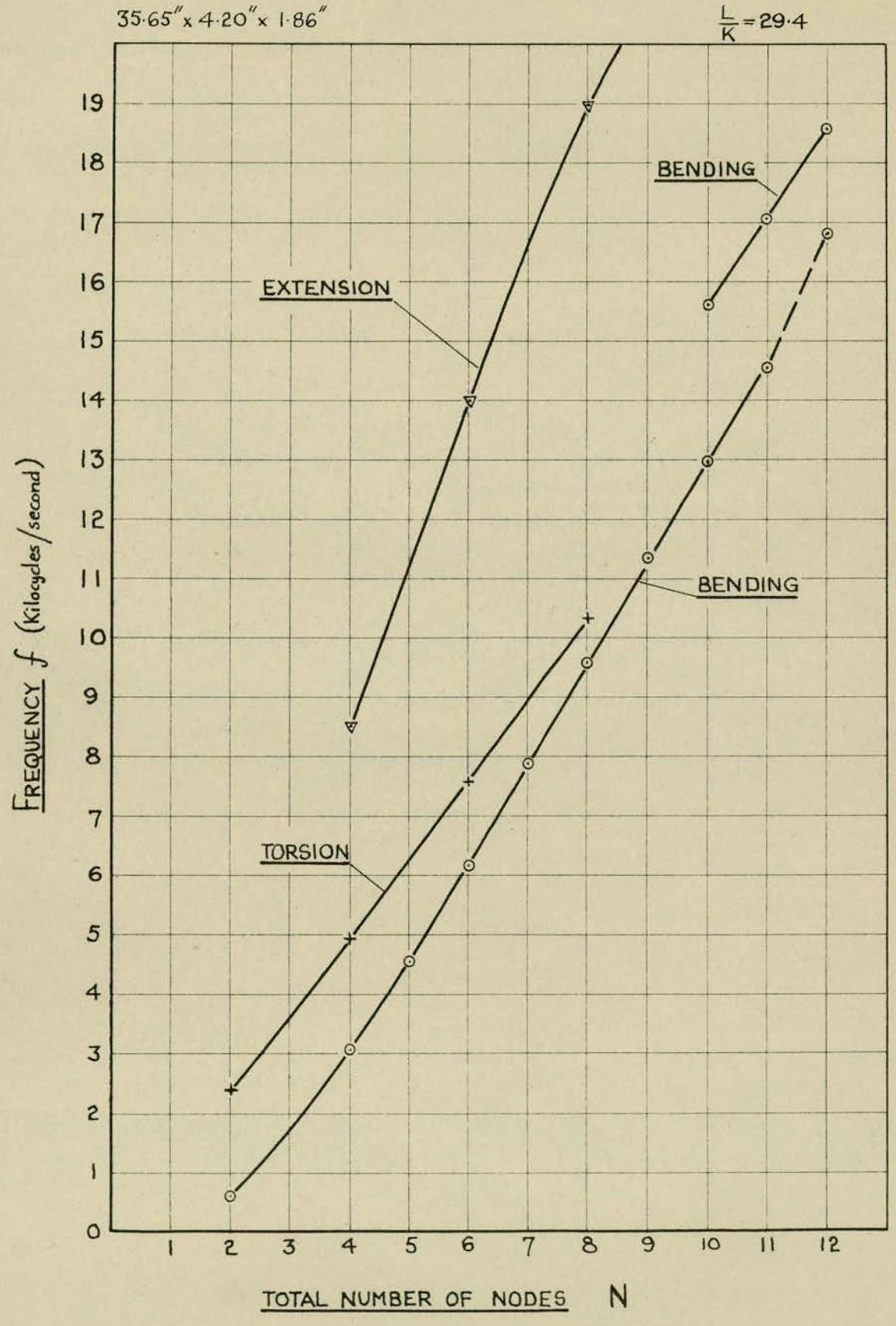

Fig. 19

Experimental Resonant Frequencies

Cast-Iron Beam

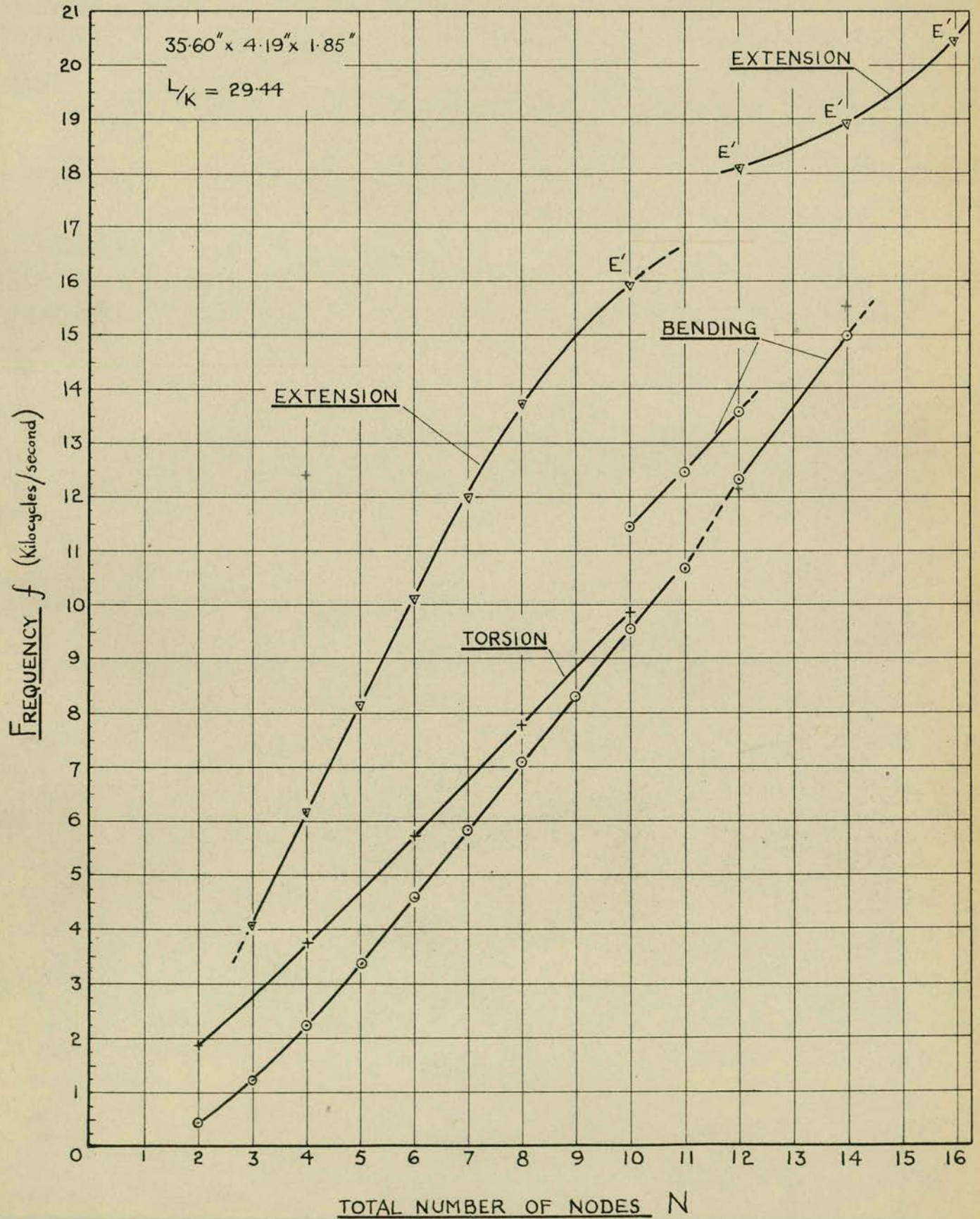

Fig. 20

Experimental Resonant Frequencies

Brass Beam

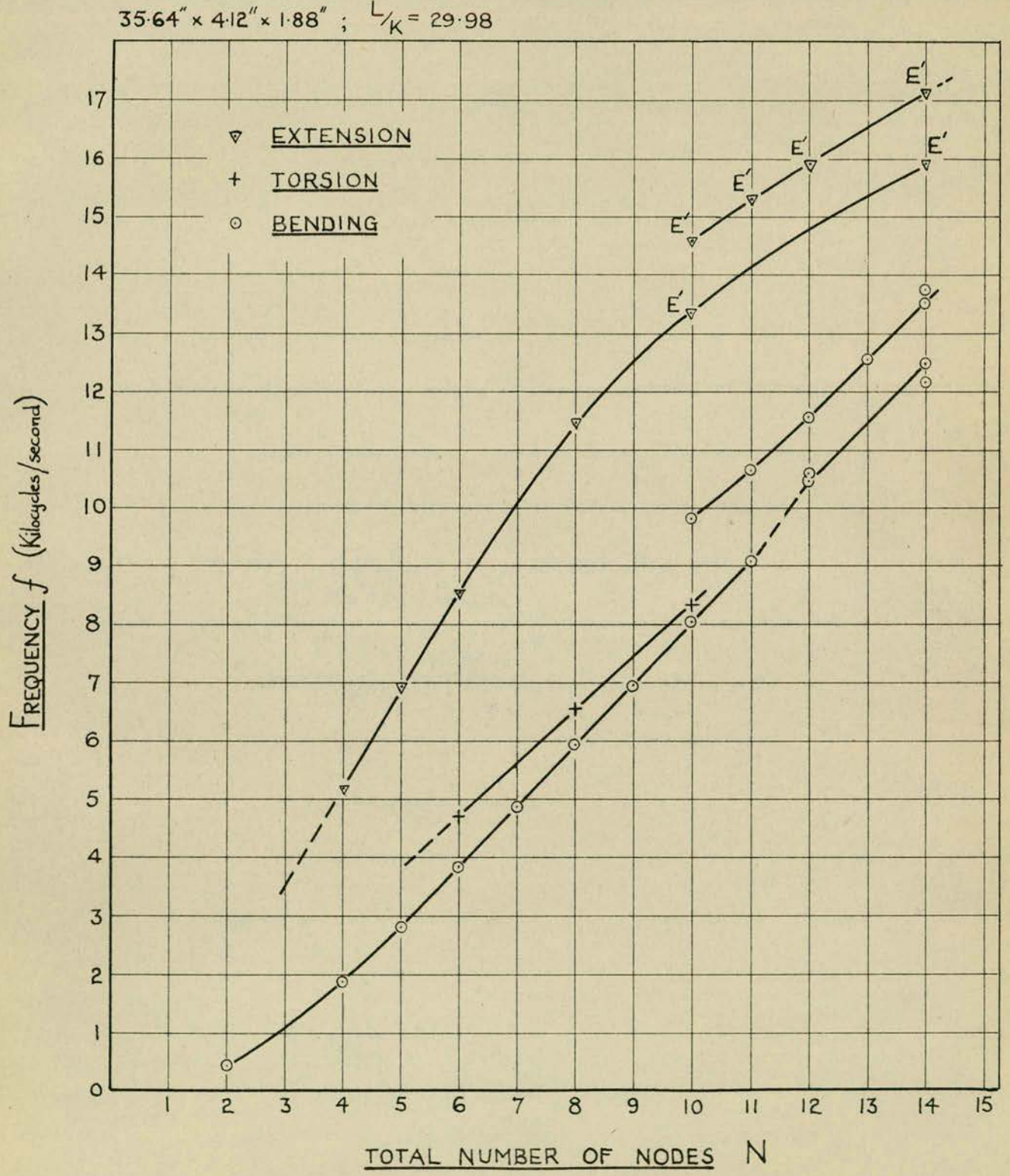

Fig. 21

EXPERIMENTAL RESONANT FREQUENCIES

FOR 3" × 1½" R.S.J. BEAM

(VIBRATED IN PLANE OF GREATEST FLEXIBILITY)

LENGTH BETWEEN ELASTIC SUPPORTS 60"

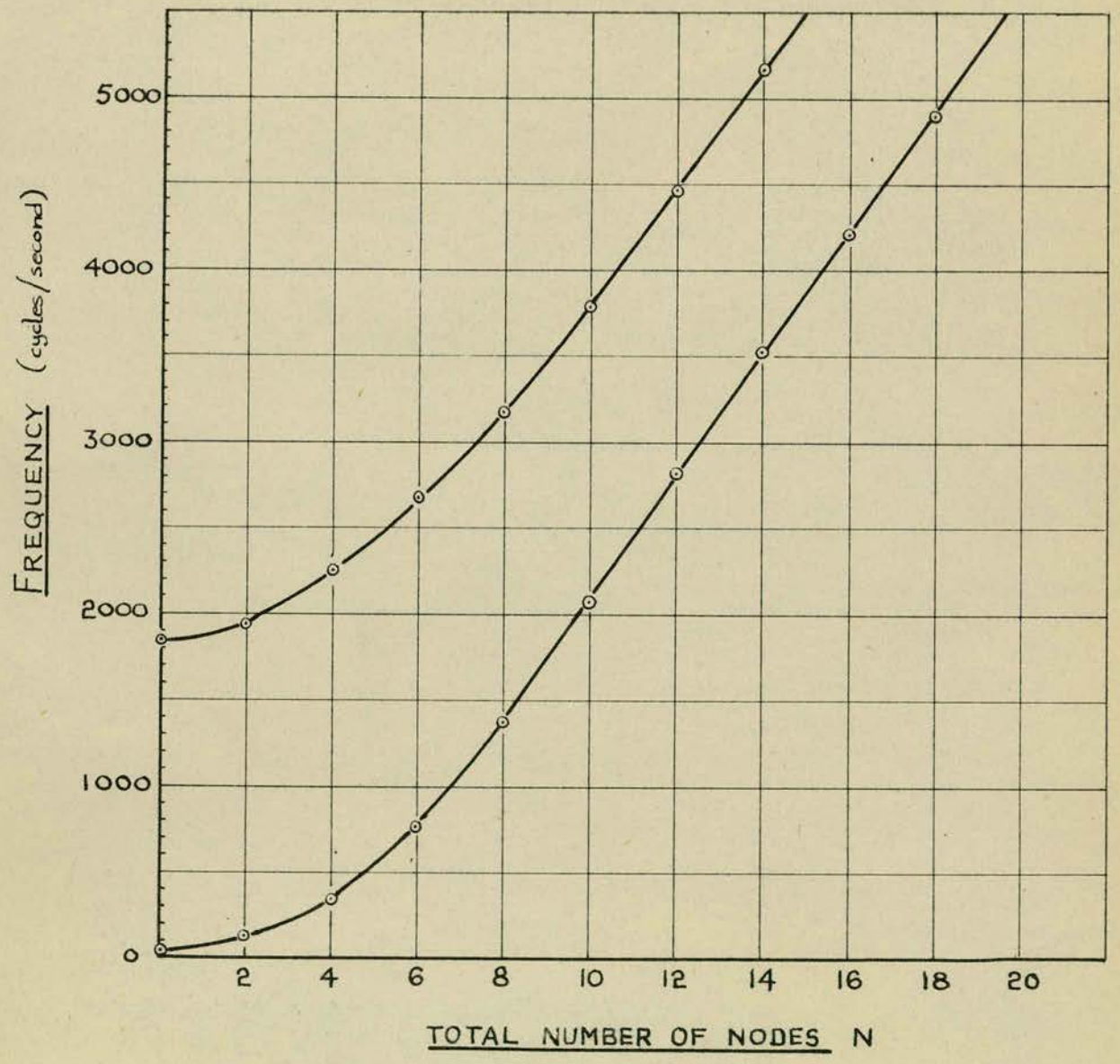

FIG. 22

Natural Frequencies of Steel Beam

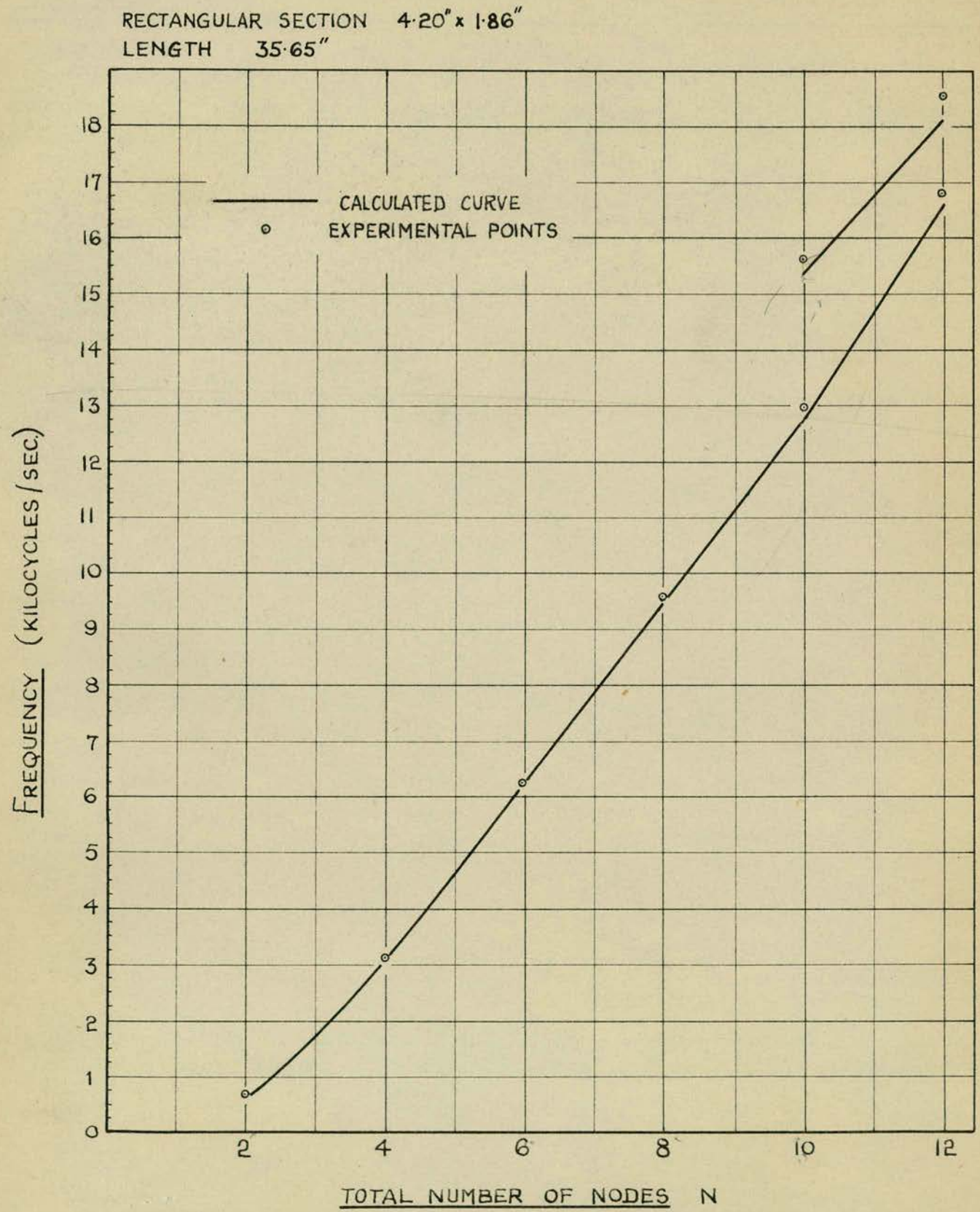

Fig. 23

Natural Frequencies of Cast-Iron Beam

(Calculation and Experiment Compared)

$\frac{L}{K} = 29{\cdot}44$

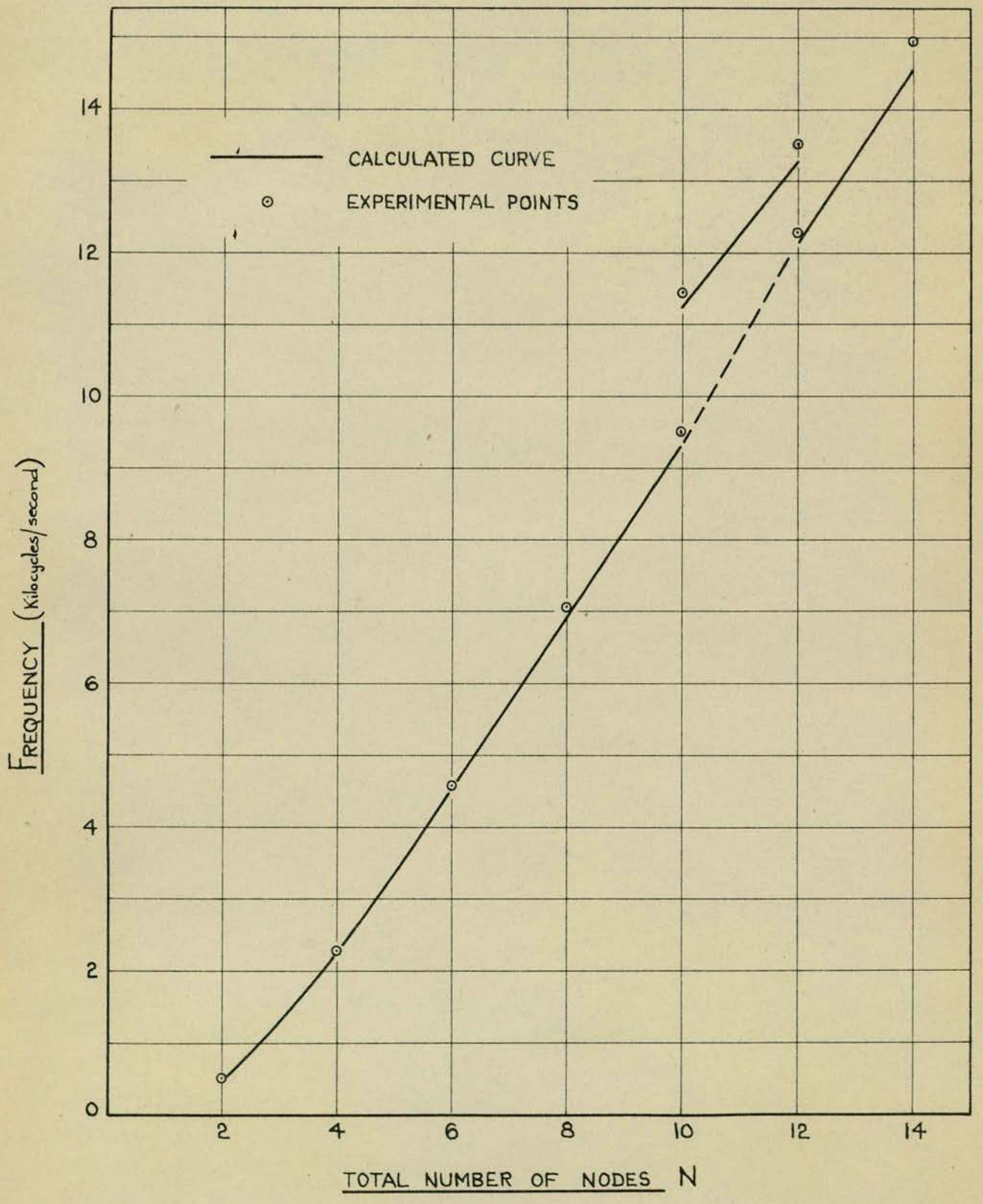

Fig. 24

Natural Frequencies of Brass Beam

(Calculation and Experiment Compared)

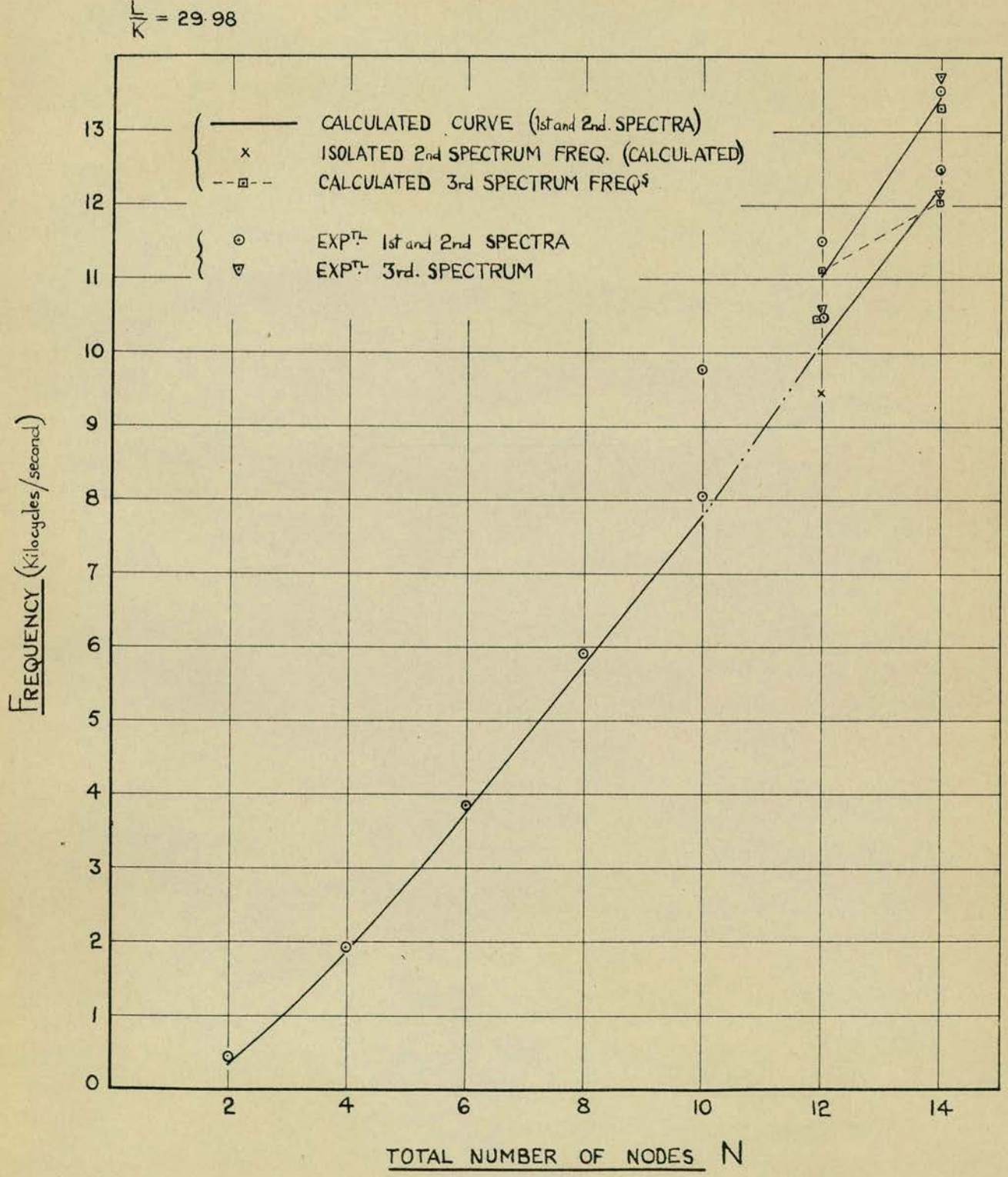

Fig. 25

The Results of Fig. 22 Replotted

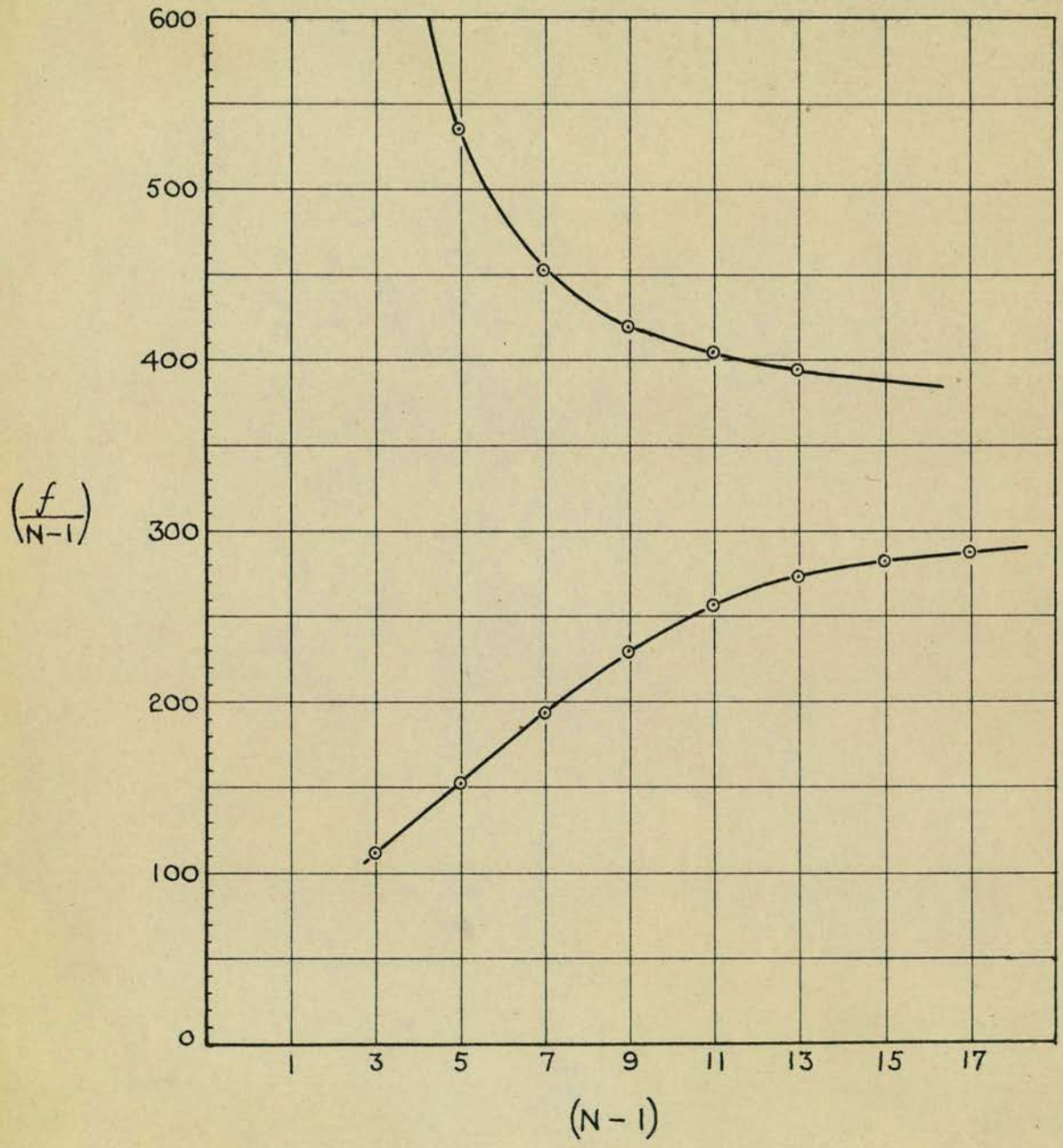

Fig. 26